COMBUSTION MEASUREMENTS IN PULVERISED COAL FLAMES

by

Karim Ahmedali Abdulla Hirji

Thesis Submitted for the Degree of

Doctor of Philosophy

in The University of London

and for the

Diploma of Membership of Imperial College

Fluids Section

Mechanical Engineering Department

Imperial College of Science and Technology

London, SW7 2BX

July 1986

To

my beloved late sister, Mumtaz.

"Good fortune is not known until it is lost"

Cervantes

Abstract

The results of an experimental study on the combustion of pulverised coal fired in a laboratory cylindrical furnace are presented. The furnace features an industrial type double concentric burner with variable secondary air swirl. Access ports are provided along the 3m length of the furnace to permit radial and axial probing of the flames.

The principal fuel studied was a United Kingdom bituminous Gedling coal. This fuel was chosen because the Gedling seam is particularly consistent so that the properties of any future deliveries would not exhibit unacceptable variations. Combustion data of Gedling coal were used as reference for comparison with those of the other fuels.

A direct water quench (shower) probe was used to extract particle-laden gas samples from the combustion space. After drying, the gas samples were analysed for CO, CO_2, O_2 and unburnt hydrocarbon species concentrations.

Time-averaged inflame temperature was measured using fine-wire thermocouples. A water-cooled probe was used to measure Nitrogen Oxides (NO_x) emission near the combustion chamber exit. Flame stability was both visually observed and monitored with an infrared flame detection system.

The results of on-axis combustion measurements for Gedling coal for two levels of excess air and two swirl numbers are presented as well as the mapping results of inflame combustion measurements for the two levels of secondary air swirl. The results facilitate physical understanding of the combustion process and provide data for the validation studies of computer prediction codes.

Flame stability was measured for a number of fuels. The influence of swirl number, the ratio of primary stream (coal and air) to secondary air axial momenta, excess air, coal feed rate and fineness of grind on flame stability were studied. It was observed that flame stability generally improved at high swirl numbers and low momenta ratio. The effect of increasing excess air on flame stability was marginal. Flame stability was enhanced with an increase in the volatile content of the fuel and with increasing fineness of grind. The stability of flames was also dependent upon the firing rate of coal.

Data on NO_x emissions of pulverised Gelding coal for various firing conditions are presented. NO_x emissions increase with increasing excess air and decrease with increasing swirl in the range of swirl numbers of practical interest. Further increase of swirl number resulted in increased NO_x emission. For momenta ratios greater than 0.16, NO_x emissions were found to be insensitive to this parameter.

ACKNOWLEDGEMENTS

First and foremost, I would like to express my gratitude to my supervisor, Dr. F.C. Lockwood, for his benign guidance and encouragement throughout the course of this work.

I am deeply indebted by the assistance of a number of my colleagues. Mr. J. Miller and Mr. I. Wright have always been available to advise and assist me on practical engineering problems. Dr. S. Godoy and Dr. H. Moneib inspired me by their unwithering attitudes. Mr. M. Ismail kindly provided the analyses of coal. Messrs. C.W. Seitz and H. Offergeld assisted me in conducting the work presented in chapter 6. Dr. R. Aguire, Dr. A. Chakravarty and Dr. M. Rizvi sacrificed time for numerous discussions on theoretical aspects of combustion. To the ones mentioned and to those I may have missed out, I sincerely thank them.

I would like to thank Mr J. Laker, Mr. G. Tindall, Mr. P. Trowell, Mr. P. Woodward (Sooty) and Mr. M. Tennison (Sweep), for their technical support. I also thank Miss C. Barron for the secretarial assistance she has provided to me. Many thanks also to the librarians, Miss E. Archer, Mrs. L. Broadbent and Miss A.R. Sage who willingly assisted me.

I am grateful to the Science and Engineering Research Council for financial support of this work under grant GR/A/8737.1.

Finally, I would like to express my gratitude to my wife, Nurjahan, for being patient and tolerant throughout the course of my studies and for speedily typing this thesis.

TABLE OF CONTENTS

ABSTRACT		Page No.	4
ACKNOWLEDGEMENTS			6
TABLE OF CONTENTS			7
LIST OF TABLES			11
LIST OF FIGURES			12
NOMENCLATURE			18
CHAPTER 1	INTRODUCTION		23
1.1	Combustion of Pulverised Coal		23
1.2	Objectives of the Present Study		24
1.3	Review of Relevant Previous Literature		24
	1.3.1 Inflame Combustion Measurements		24
	1.3.2 Flame Stability Measurements		27
	1.3.3 No_x Emission Measurements		28
	1.3.4 Computer Prediction Studies		29
1.4	Present Contribution		30
1.5	Outline of the Thesis		31
CHAPTER 2	PHENOMENOLOGICAL STUDIES PERTAINING TO FLAME STABILITY: A REVIEW		32
2.1	Introduction		32
2.2	The Aerodynamics of the Flow		32
	2.2.1 Single Phase Isodensity Swirl Flows		33
	2.2.2 Single Phase Combusting Swirl Flows		34
	2.2.3 Two-Phase Swirl Flows		35

	2.2.4 Flame Classification	37
2.3	Particle Time-Temperature History	37
2.4	Coal Characteristics	39
2.5	Propagation of Pulverised Coal Flames	39
	2.5.1 Mode of Ignition and Propagation	40
	2.5.2 Flame Lift-Off and Blow-Off	43
2.6	Summary	44
CHAPTER 3	FURNACE, INSTRUMENTATION, AND EXPERIMENTAL METHODS	46
3.1	Introduction	46
3.2	The Furnace and Ancillary Equipment	47
	3.2.1 The Combustion Chamber	47
	3.2.2 The Burner	48
	3.2.3 Igniter and Flame Detectors	48
	3.2.4 The Scrubber	48
	3.2.5 The Air Supplies to the Furnace	49
3.3	The Coal Feed System	50
	3.3.1 The Weighbridge	50
	3.3.2 The Dilute-Phase Pneumatic Conveying System	52
3.4	The Instrumentation	54
	3.4.1 Temperature	54
	3.4.2 Gas-Concentration	55
	3.4.3 NO_x Emission	56
3.5	The Fuels Tested	57
3.6	Experimental Procedures	58
	3.6.1 Furnace Operation	58
	3.6.2 Inflame Combustion Measurements	58
	3.6.3 Flame Stability	60

	3.6.4	NO_x and O_2 Emission Measurements	60
Appendix 3.A		Petrographic Analyses of Coal	71
CHAPTER 4		INFLAME COMBUSTION MEASUREMENTS	73
4.1		Introduction	73
4.2		Experimental Conditions	74
4.3		Experimental Methods and Accuracy	76
	4.3.1	Mean Temperature	76
	4.3.2	Mean Gas-Species Concentration	79
	4.3.3	Consistency of Data	81
4.4		Discussion of Results	86
	4.4.1	The Axial Data	86
	4.4.2	The Radial Data, $\lambda = 1.15$, $S_g = 0.78$	87
	4.4.3	The Radial Data, $\lambda = 1.15$, $S_g = 1.03$	90
4.5		Summary	91
CHAPTER 5		STABILITY LIMITS OF PULVERISED COAL FLAMES	111
5.1		Introduction	111
5.2		Experimental Conditions and Procedures	111
5.3		Criterion for Flame Stability	113
5.4		Presentation of the Data	114
5.5		Preliminary Results and Influence of Coal Type	116
	5.5.1	Effect of Burner Load	116
	5.5.2	Effect of Excess Air	117
	5.5.3	Effect of Fineness of Grind	118
	5.5.4	Effect of Coal Type	118
	5.5.5	Effect of Burner Geometry	120
5.6		Influence of Burner Load and Excess Air	120

5.6.1 Dependency of the Minimum Swirl Number 120

5.6.2 Dependency of the Maximum Momentum Ratio 122

5.7 Influence of Coal Microfineness and VolatilesContent123

5.7.1 Effect of Microfineness of Coal 124

5.7.2 Effect of Volatiles Content 125

5.8 Summary 126

Appendix 5.A Prediction of Dependency of Heat Radiated to Furnace Walls on Burner Load 152

CHAPTER 6 EMISSIONS OF NITROGEN OXIDES 157

6.1 Introduction 157

6.2 Experimental Conditions 158

6.3 Experimental Methods and Accuracy 158

6.4 Prediction Procedure for NO Formation 159

6.4.1 NO Formation Mechanisms 160

6.4.2 Modelling of Fuel NO Formation 162

6.5 Discussion of Results 164

6.5.1 The Influence of Swirl Number, S_s 164

6.5.2 The Influence of Excess Air 166

6.5.3 The Influence of Primary Stream to Secondary Air Axial Momentum Ratio, R_m 167

6.6 Summary 168

CHAPTER 7 CLOSURE 173

7.1 Conclusions 173

7.2 Recommendations for Future Work 175

REFERENCES 177

LIST OF TABLES

Table	Contents	Page No.
3.1	Analyses of test coals.	61
3.2	Particle size distribution of test fuels.	62
3.3.	Petrographic analyses of test fuels.	63
4.1	Run Conditions: Inflame Measurements.	93
5.1	Run Conditions: Flame stability, test series CT.	128
5.2	Run Conditions: Flame stability, test series BL.	129
5.3	Run Conditions: Flame stability, test series MS.	129
6.1	Run Conditions: NO_x emission measurements.	169

LIST OF FIGURES

Figure	Caption	Page No
2.1	Schematic of various industrial flame types (after Bortz (1983)).	45
3.1	Schematic of furnace.	64
3.2	Details of furnace roof and burner.	65
3.3 (a)	Details of scrubber: original version.	66
(b)	Details of scrubber: modified version.	66
3.4 (a)	Schematic of coal feed system: original version.	67
(b)	Schematic of coal feed system: modified version.	67
3.5	Schematic of temperature measurement system.	68
3.6	Schematic of gas sampling system.	69
3.7	Schematic of NO_x emission sampling system.	70
4.1 (a)	Influence of thermocouple diameter on radiation correction (Vel = 1 m/s, ϵ_t = 0.3, T_{wall} = 1200K).	94
(b)	Influence of velocity on radiation correction (ϵ_t = 0.3, T_{wall} = 1200K, 2r = 200μm).	94
(c)	Influence of wall temperature on radiation correction (Vel = 1 m/s, ϵ_t = 0.3, 2r = 200μm).	94
4.2	Consistency of gas-species concentration data. Radial profile, flame S7L, X/D_s = 7.45.	95
(a)	Flow symmetrical.	
(b)	Flow asymmetrical.	

Figure	Caption	Page No
4.3	On-axis gas-species concentration profiles. Effect of swirl (15% excess air).	96
(a)	S_S = 0.78	
(b)	S_S = 1.03	
4.4	On-axis gas-species concentration profiles. Effect of excess air (S_S = 1.03).	97
(a)	15% excess air	
(b)	25% excess air	
4.5	On-axis temperature profiles.	98
4.6	Radial gas-species concentration profiles. Flame S6L, 15% excess air, S_S = 0.78.	
(a)	X/D_S = 2.09	99
(b)	X/D_S = 7.45	100
(c)	X/D_S = 12.80	101
(d)	X/D_S = 18.16	102
(e)	X/D_S = 23.52	103
(f)	X/D_S = 28.88	104
4.7	Radial unburnt hydrocarbon profiles. Flame S6L, 15% excess air, S_S = 0.78.	105
(a)	X/D_S = 2.09	
(b)	X/D_S = 7.45	
(c)	X/D_S = 12.80	

Figure	Caption	Page No
4.8	Radial temperature profiles. Flame S6L, 15% excess air, S_s = 0.78.	106
(a)	X/D_s = 2.21	
(b)	X/D_s = 3.64	
(c)	X/D_s = 5.07	
(d)	X/D_s = 9.00	
(e)	X/D_s = 14.36	
4.9	Radial gas-species concentration profiles. Flame S7L, 15% excess air, S_s = 1.03.	
(a)	X/D_s = 2.09	107
(b)	X/D_s = 7.45	108
(c)	X/D_s = 12.80	109
4.10	Radial unburnt hydrocarbon profiles. Flame S7L, 15% excess air, S_s = 1.03.	110
(a)	X/D_s = 2.09	
(b)	X/D_s = 7.45	
(c)	X/D_s = 12.80	
5.1	Stability performance of United Kingdom Grimethorpe (1) coal.	
(a)	m_c = 11.6 kg/hr, 30% excess air	130
(b)	m_c = 8.0 kg/hr, 30% excess air	130
(c)	m_c = 8.0 kg/hr, 23% excess air	131

Figure	Caption	Page No
5.2	Stability performance of United Kingdom Grimethorpe (2) coal.	
(a)	m_c = 11.6 kg/hr, 30% excess air	131
(b)	m_c = 8.0 kg/hr, 30% excess air	132
(c)	m_c = 8.0 kg/hr, 23% excess air	132
5.3	Stability performance of South African (A) coal.	
(a)	m_c = 13.3 kg/hr, 30% excess air	133
(b)	m_c = 9.2 kg/hr, 30% excess air	133
(c)	m_c = 9.2 kg/hr, 23% excess air	134
5.4	Stability performance of South African (B) coal.	
(a)	m_c = 24.8 kg/hr, 30% excess air	134
(b)	m_c = 24.8 kg/hr, 23% excess air	135
(c)	m_c = 17.1 kg/hr, 23% excess air	135
5.5	Stability performance of South African (B) coal. 31mm I.D. primary tube.	
(a)	m_c = 24.8 kg/hr, 30% excess air	136
(b)	m_c = 17.1 kg/hr, 23% excess air	136
5.6	Stability performance of United Kingdom Gedling coal, 15% excess air.	
(a)	m_c = 8.0 kg/hr	137
(b)	m_c = 12.0 kg/hr	137
(c)	m_c = 16.0 kg/hr	138
(d)	m_c = 20.0 kg/hr	138
(e)	m_c = 24.0 kg/hr	139

Figure	Caption	Page No
5.7	Stability performance of United Kingdom Gedling coal, 25% excess air.	
(a)	m_c = 8.0 kg/hr	140
(b)	m_c = 12.0 kg/hr	140
(c)	m_c = 16.0 kg/hr	141
(d)	m_c = 20.0 kg/hr	142
(e)	m_c = 24.0 kg/hr	143
5.8	Influence of burner load on minimum swirl number for stable flame. United Kingdom Gedling coal.	144
(a)	$S_{s,min}$ vs m_c	
(b)	$S_{t,min}$ vs m_c	
(c)	$S_{t,min}'$ vs m_c	
5.9	Influence of burner load on maximum momentum ratio, $R_{m,max}$, for stable flame. United Kingdom Gedling coal.	145
5.10	Predicted influence of burner load on ratio of radiation heat loss to furnace walls to flame zone heat release.	145
5.11	Stability performance of United Kingdom Gedling-microfine coal, 15% excess air.	
(a)	m_c = 12.2 kg/hr	146
(b)	m_c = 16.3 kg/hr	147
(c)	m_c = 20.4 kg/hr	148
5.12	Influence of burner load on minimum secondary air swirl number, $S_{s,min}$ for stable flame. Normally ground and microfine Gedling coal, 15% excess air.	149

Figure	Caption	Page No
5.13	Influence of burner load on maximum momentum ratio, $R_{m,max}$, for stable flame. Normally ground and microfine Gedling coal,15% excess air.	149
5.14(a)	Stability performance of low-volatile char (BLVG). m_c = 14.0 kg/hr, 15% excess air, 31mm I.D. primary tube.	150
(b)	Comparison of stability performance of low-volatile char with normally ground Gedling coal. Gross input heating value 100kW, 15% excess air. Low volatile char - 31mm I.D. primary tube. Gedling coal - 22mm I.D. primary tube.	150
5.15	On-axis gas species concentration profiles. Gross input heating value 100kW, 15% excess air. Low-volatile char: S_s = 1.45, R_m= 0.116, 31mm I.D., primary tube. Gedling coal : S_s = 1.03, R_m= 0.231, 22mm I.D. primary tube.	151
6.1	Reaction scheme for the fate of fuel nitrogen.	160
6.2	Effect of swirl on emission of NO_x.	170
6.3	Predicted near field flow patterns for S_s = 0.77 and S_s = 1.27.	171
6.4	Effect of excess air on emission of NO_x.	172
6.5	Influence of momentum ratio, R_m, on emission of NO_x.	172

NOMENCLATURE

A	pre-exponential factor in Arrhenius expression
A_E	specific particle surface area (m^2/gm)
A_g	surface area of flame zone
A_w	surface area of furnace walls
C	constant
C_{fixed}	mass fraction of fixed carbon content in coal
C_p	specific heat at constant pressure
C_{ult}	mass fraction of elemental carbon content in coal
C_{vol}	mass fraction of volatile carbon content in coal
d	particle diameter at $t = 0$
d_p, d_s	particle diameter
D_c	binary $O_2 - N_2$ diffusion coefficient
D_o	binary $O_2 - N_2$ diffusion coefficient at reference temperature T_o and pressure P_o.
$D_{p,i}$	inside diameter of primary tube (central burner gun)
$D_{p,o}$	outside diameter of primary tube (central burner gun)
D_s	diameter of secondary air tube (burner throat)
E	activation energy
F_{O2}	molar fraction of oxygen
G_θ	axial flux of angular momentum
G_{ax}	axial flux of linear momentum (excluding pressure term)
h	heat transfer coefficient
H_c	net calorific value of char
H_{H2o}	mass fraction of hydrogen in moisture per kg coal
H_{ult}	mass fraction of elemental hydrogen in coal
H_v	net calorific value of volatiles

NOMENCLATURE

H_{vol}	mass fraction of hydrogen in volatiles per kg coal
k	thermal conductivity
K	rate constant, equilibrium constant
K_{CH}	chemical reaction rate coefficient
K_o	pre-exponential factor in Arrhenius expression
K_T	overall reaction rate coefficient
L	length of half span of thermocouple supports, length of quarl divergent surface
m_c, m_F	coal mass flow rate
$m_{c,p}$	coal loading in primary stream, $m_{c,p} = m_c/(m_c + m_p)$
m_g	net gas mass flow out of the flame zone
$m_{n,c}$	mass fraction of nitrogen in coal
m_p	primary air mass flow rate
m_s	secondary air mass flow rate
M	molecular weight
M_p	fraction burnout of char particle
Nu	Nusselt number
O_{H2O}	mass fraction of oxygen in moisture per kg coal
O_{ult}	mass fraction of elemental oxygen in coal
O_{vol}	mass fraction of oxygen in volatiles per kg coal
P	pressure
P_o	pressure at reference condition
P_{NO}	nitrogen partial pressure (in atmospheres)
Pr	Prandtl number
q_p	heat release rate due to combustion of char particles
q_{rel}	heat release rate due to combustion of coal($\equiv q_v + q_p$)
q_{rad}	radiation heat loss to furnace walls

NOMENCLATURE

q_v	heat release due to combustion of volatiles
r	radial coordinate, radius of thermocouple bead.
R	universal gas constant
R_m	ratio of axial momentum of primary stream (coal plus air) to that of secondary air, $R_m = (m_c + m_p)\, V_p/(m_s V_s)$
$R_{m,max}$	maximum measured value of momentum ratio R_m for stable flame
Re_p	Reynolds number of primary jet, $Re_p = V_p D_{p,i}/\nu_p$
Re_s	Reynolds number of secondary air jet, $Re_s = V_s(D_s - D_{p,o})/\nu_s$
R_H	ratio of heat loss to walls by radiation to heat release, q_{rad}/q_{rel}
S_m	rate of mass entering the gas phase from coal due to pyrolysis and char burnout, per unit volume
S_s	secondary air swirl number, $S_s = 2G_\theta/G_{ax}\, D_s$
$S_{c,crit}$	minimum measured value of swirl number, S_s, for stable flame for a given value of R_m.
$S_{s,min}$	minimum measured value of swirl number, S_s, for stable flame
S_t	total swirl number, $S_t = S_s/(1 + R_m)$
$S_{t,min}$	minimum measured value of total swirl number, S_t, for stable flame
S_t'	modified total swirl number (excludes coal axial momentum), $S_t' = S_s/(1 + R_m(1 - m_{c,p}))$
$S_t'min$	minimum measured value of modified total swirl number, S_t', for stable flame.
t	time
t_b	burning time of particle

NOMENCLATURE

T	temperature
T_g	gas temperature, flame zone temperature
T_o	reference temperature, combustion air inlet temperature
T_p	particle temperature
T_s	temperature of thermocouple supports
T_t	thermocouple temperature
T_w, T_{wall}	furnace wall temperature
V	mass fraction of volatiles released at time t per unit mass of coal.
V^*	ultimate ($t \rightarrow \infty$) mass fraction release of volatiles per unit mass of coal.
V	volume
Vel	gas velocity
V_p	primary air axial velocity at burner exit
V_s	secondary air axial velocity at burner exit
$w_{1,2..5}$	rate of reactions 1,2,..5 (refer to Fig. 6.1)
w_{HCN}	rate of formation of HCN
w_{NH2}	rate of formation of NH_2
w_{NO}	rate of formation of NO
W	tangential velocity
x	lengthwise distance from thermocouple junction
X	axial distance from burner throat

NOMENCLATURE

GREEK SYMBOLS

α	quarl half angle
Δ	flame zone temperature minus gas temperature leaving flame zone
ϵ_g	flame emissivity
ϵ_t	thermocouple junction emissivity
λ	excess air factor, $\lambda = (A/F)/A/F)_{stoich}$
μ_f	fluid viscosity
ν_p	kinematic viscosity of primary air
ν_s	kinematic viscosity of secondary air
ρ_c	density of coal particles
ρ_p	density of particles, density of primary air
ρ_s	density of secondary air
σ	Stefan-Boltzmann constant
τ	characteristic time
τ_p	response or relaxation time of particle, $\tau_p = (d_p)^2\rho_p/18\mu_f$ for Stoke's flow
τ_g	fluid particle residence time
Φ	mechanism factor

SUBSCRIPTS

p	primary air
s	secondary air

CHAPTER 1

INTRODUCTION

1.1. Combustion of Pulverised Coal

The origin of pulverised fuel (pf) firing dates back almost two centuries. The first commercial use of pulverised coal fuel was in cement furnaces some 120 years ago, Essenhigh (1961). The success of pf in the cement industry was later to be emulated by its use for power-generation. The latest figures published by the Electricity Council (1984-85) show that about 80% of the electricity generated in the United Kingdom is due to pf firing and the total cost of that coal is about £4000 million per annum.

The characteristics of the combustion of pulverised coal are qualitatively understood but are not known well enough for quantitative prediction of performance parameters for a novel set of constraints. These constraints defined by Macek (1978) are:

(i) adaption to major changes of coal quality, and

(ii)environmental protection requirements.

The first of the above constraints requires that low quality coals be fired with adequate flame stability and efficiency, and minimum ash-fouling. Environmental constraints demand that coal be burned with high efficiency and a minimum of pollutant emission. The essential techniques of combustion process modification are the control of fuel-oxidant mixing, and of flame temperature, Beer (1986). These procedures can be used to ensure that the chemical and thermal environments of reacting coal particles in the flame favour flame stability, reduced pollutant emission, and slagging- and fouling-free combustion. The use of these techniques in design and operation requires that the fundamentals of coal combustion process

be well understood.

1.2. Objectives of the Present Study

The objectives of the present study are to obtain fundamental combustion data by means of inflame measurements,to explore flame stability and to determine the influence of operating parameters on NO_x emissions. The results of these studies will enable better physical understanding of the combustion of pulverised coal and the data will be useful for the validation of the computer prediction procedures.

1.3. Review of Relevant Previous Literature

The review is mainly devoted to the experimental work on turbulent pulverised coal combustion. Section 1.3.1. reviews the literature on inflame combustion measurements. The experimental research on flame stability is reviewed in section 1.3.2. Fundamental studies pertaining to flame stability are reviewed in chapter 2. The literature on the NO_x emissions is reviewed in section 1.3.3. Lastly, in section 1.3.4., some results of computer prediction studies are reviewed.

1.3.1 Inflame Combustion Measurements

Most of the experimental work on industrial scale pulverised coal combustion emanates from the International Flame Research Foundation (IFRF). Their work has been published mainly in the Journal of the Institute of Fuel and has been reviewed by Field et al (1967) and Gill (1975). However, the more relevant ones are briefly reviewed here.

Hubbard (1960) reported the results of the first pulverised coal experiments conducted at IFRF on the furnace 1.5m x 1.5m cross-section and 10m long. His main conclusion was that the rate controlling process is the physical mixing of air and fuel. His results show that 95% of the volatiles had evolved in 50 ms and that burnout of char residue took 350 ms. Loison and Kissel (1962) observed that the released volatiles burnt to CO due to insufficient mixing and that the flame length increased when lean coals (low-volatile) were fired. Beer (1962) reviewed the work conducted that far at IFRF.

The effects of fineness of grind and recirculation on the combustion of anthracite coal were evaluated by Beer (1964). He observed that the rate of combustion increased when finer coal was fired and that the heat transfer to the incoming fuel jet upstream of the flame was mainly by the recirculation of hot products. Chedaille and Hemsath (1965) evaluated from on-axis combustion measurements the influences of burner type, coal fineness and input conditions on the combustion of pulverised coal. One of their important observations was that the appearance of a visible flame front corresponded to a temperature of 300°C with the high volatile coal and 750°C with the anthracite. Horn et al (1966) reported a good agreement of the measured axial temperatures in a pulverised coal fired superheater with those theoretically calculated. Hein and Leuckel (1969) studied the effect of swirl on pulverised coal flames. They observed a critical swirl intensity beyond which the bituminous coal flames ignited stably within the burner quarl, and that the critical swirl was lower in the case of a divergent burner.

The above reported references provide mainly results of axial

measurements only, with the emphasis on heat transfer and particle burnout characteristics of pulverised coal flames. The first comprehensive radial and axial combustion data (including NO_x) from IFRF on the No.1 furnace which is 2m x 2m cross section x 6.25m long, are due to Michel and Payne (1980) for cement kiln type flames. Their measurements indicate that mixing is the rate determining mechanism for the overall combustion process. Large asymmetries of the radial temperature profiles were observed in their data. Most recent combustion data emerging from the IFRF relate to the characterisation of NO_x formation, for example, those of Phelan and Bortz (1984). Their findings are reviewed in section 1.3.3.

Data from the other sources are rare. Baker et al (1969) presented preliminary results from the BCURA 1m diameter x 6m long furnace. They highlight the problems of reproducibility and symmetry of pulverised coal flames. Thurgood et al (1980) presented experimental data for a burner with zero swirl. They observed enhanced mixing rates for an increase in the secondary air velocity. Hassan et al (1985) presented a preliminary set of data obtained in the present furnace for a United Kingdom Grimethorpe coal. Their data were obtained for a swirl number of unity and 24% excess air. The data are presently being used for the validation of computer prediction codes, Lockwood (1986).

Most of the available experimental data have been obtained either in small furnaces or on the axis only or from three-dimensional furnaces. It must be noted that the IFRF No.1 furnace has a square cross-section and is horizontally orientated. Only a few sets of data from large axisymmetrical furnaces are presently available.

1.3.2. Flame Stability Measurements

The study of the stability of gaseous-fuel flames usually prelude those of coal firing. The initial work on gas flames dealt with the characterisation of inner recirculation zone (IRZ), Syred et al (1970). In a series of experiments at IFRF, Leuckel and Fricker (1976) classified two flame types, those with, and those without the IRZ. Their work was continued by Wu and Fricker (1976) who studied the influence of the furnace geometry, and Fricker and Leuckel (1976) who studied the effects of swirl and burner mouth geometry on flame stability. They reported enhanced flame stability when a divergent burner nozzle was employed and that the main effect of swirl was to promote the mixing of fuel and air.

Domkundwar et al (1979) observed increased blow-off limits with increasing quarl half angles in the range of 0° to 25°. Kimoto et al (1981) experimented with a rather small unconfined double concentric burner with zero swirl. Their results show that the mixing rate decreased with increasing ratio of the axial momentum of the central jet to that of the annular jet. Rawe and Kremer (1981) observed that the flame was stabilized at the boundary of the reverse-flow zone, and that stability increased with increasing swirl strength. Beyler and Gouldin (1981) observed that the flame stabilized upstream of the IRZ and suggest that the convective transport in the recirculating zone is unimportant to the stabilization process. Claypole and Syred (1982) suggest that the flame stabilization is achieved by the formation of well-stirred regions in which hot active species and isothermal fresh reactants become intimately mixed.

Beer and Chigier (1969) observed that the application of swirl to the primary air had little effect upon the stability of pulverised coal

flames. Wolanski and Wojcicki (1974) observed in a 0.07m x 0.07m cross section combustor that the most dominant parameter controlling flame stability is the rate of release of the volatiles. Wroblewska et al (1976) correlated in isothermal flow the mass of recirculating flow with the swirl number and the ratio of the axial momentum of the primary air to that of the secondary air. They used the isothermal mixing data to predict the performance of a full-scale coal burner and observed an optimum value of the recirculating mass flow for flame stability of low-calorific value coals. Cogoli et al (1977) observed in a laminar-flow reactor improved flame stability of more porous chars.

Burner stability data provide extremities of flame conditions and as such are useful for the evaluation of computer prediction procedures. Published stability data for turbulent pulverised coal flames are scarce.

1.3.3. NO_x Emission Measurements

Published literature of NO_x emission measurements from large-scale pulverised coal burners are not numerous presumably because the results are effectively trade secrets of the burner manufacturers. Heap et al (1972) report the dependency of NO emissions on the swirl number, the proportion of primary air, and the burner geometry. They observed that the NO emission depended on the swirl number but that the dependency varied with the proportion of the primary air. The review by Morrison (1980) includes the performance results of various burners and of the influence of operating conditions.

Michel and Payne (1980) provide inflame NO_x data for long cement-kiln type flames. They observed a good correspondence between CO and HCN

peak positions, indicating that the fuel-N was very rapidly converted to HCN. Chen et al (1982) report the dependence of coal rank on NO_x. They observed decreased NO_x with decreasing coal rank. Asay et al (1983) observed reduced NO emissions for decreasing coal moisture level. Phelan and Flament (1983) and Phelan and Bortz (1984) studied on the IFRF No. 1 furnace, the influences of coal-type, swirl, excess-air, furnace temperature, turndown ratio and staging the combustion. They observed increased NO_x emission with increasing swirl number and that increasing the gas residence time in the primary (fuel-rich) zone resulted in lower NO_x emission. The dependency of the extent of staging the combustion on NO_x emission was sensitive to coal type. Okazaki et al (1984) observed in a 0.14m internal diameter furnace increased emissions with decreasing particle size and increasing volatiles content in the coal. Sadakata et al (1984) observed in a 0.3m internal diameter furnace that NO_x emissions increased as the primary air velocity was increased.

1.3.4. Computer Prediction Studies

In common with the experimental research, gas-firing studies usually precede those of firing pulverised coal. One of the typical studies is by Gosman et al (1978). They demonstrated the ability of the computations to predict reasonably well the experimental results of three different flame types. Their prediction procedure was later extended for coal fired furnaces, Lockwood et al (1980). A review of pulverised coal combustion modelling procedures has been provided by Smoot (1981). Presser et al (1982) reported that reducing the overall flow momentum increased flame stability. A procedure for NO formation prediction has been suggested by Smith et al (1982). Their procedure

was used by Hill et al (1984) to predict NO_x emissions obtained from different furnaces.

The earlier predictions by Lockwood et al (1980) were extended to include the effect of swirl, Lockwood et al (1984) and Rizvi (1985). Their procedures were validated against experimental data obtained from a 0.8m diameter furnace. A reduction in the radiation heat transfer due to increased ash content in the coal was recently predicted by Lockwood et al (1986). Currently the prediction procedures are being extended to predict the performance of full-scale power generating boilers, Abbas and Lockwood (1986).

The computation procedures have been demonstrated to predict reasonably well certain experimental data. Their universal application has been limited by the dearth of accurate experimental data for the complete validation of such procedures.

1.4. PRESENT CONTRIBUTION

Inflame axial gas-species concentration and temperature profiles are presented for a United Kingdom Gedling coal for two swirl numbers and two levels of excess air. Inflame radial gas-species concentration and temperature profiles are also presented for swirl numbers, S_s = 0.78 and S_s = 1.03. Flame stability data are provided in terms of the swirl number and the ratio of the primary stream (coal plus air) to secondary air axial momenta, R_m, for various coal types, burner loads, excess air levels, fineness of grinds and for two sizes of the central burner gun. The data of the emissions of nitrogen oxides (NO_x) for varying swirl number, excess air and the momentum ratio, R_m, are presented for the Gedling coal.Finally a prediction model for the formation of NO is proposed.

1.5. OUTLINE OF THE THESIS

The remaining part of the thesis is divided into six chapters. Chapter 2 reviews the fundamental studies pertaining to flame stability. The review covers the near burner aerodynamics of swirling turbulent diffusion flames, the effects of particle heating rates and temperature on devolatilisation and the stability dependency of the coal type and condition. The mechanisms of ignition and blow-off of flames are also reviewed in this chapter.

Chapter 3 is concerned with the description of the furnace and the instrumentation used. The difficulties encountered with the coal feed system are mentioned in section 3.3. The analyses of the coals are provided and the experimental procedures are described in this chapter.

Chapter 4 presents the inflame combustion data. The radiation and conduction errors associated with the measurement of temperature are discussed and estimated. The repeatability of the data is discussed in detail in section 4.3.3. The experimental data are physically interpreted and discussed in section 4.4.

Chapter 5 deals with the measured flame stability limits of pulverised coal flames. Preliminary results are presented in section 5.2. The burner load-dependent data are discussed in section 5.3. The stability limits of microfine Gedling coal and a low-volatile char are also presented in this chapter.

Chapter 6 concerns the emissions of nitrogen oxides, NO_x.

Experimental data are presented to evaluate the effects of the swirl number, S_g, excess air and the momentum ratio, R_m. A prediction procedure for the formation of NO is also presented in this chapter.

Chapter 7 summarises the thesis content providing conclusions and recommendations for further research.

CHAPTER 2

PHENOMENOLOGICAL STUDIES PERTAINING TO FLAME STABILITY: A REVIEW

2.1 Introduction

This review concerns the fundamental studies relevant to the stabilization of pulverised coal flames. Detailed fundamental information on the combustion of pulverised coal may be obtained from Field et al (1967), Essenhigh (1981), Howard (1981) and Smoot and Smith (1985). Most of the experimental work relating to the stabilization of pulverised coal flames concerns experiments on single particles or in laminar flow reactors. Gas and particle sampling, and flow measurements near the burner region of large turbulent flames is very difficult and data are virtually non-existent.

The fundamental factors that influence the stability of swirling turbulent diffusion flames are discussed in sections 2.2. to 2.4. A review of the mechanisms of the initiation, propagation and extinction of pulverised coal flames is presented in section 2.5. A summary of this review is provided in section 2.6.

2.2. The Aerodynamics of the Flow

In most gas diffusion flames, the process that limits the rate of combustion is the mixing of fuel and oxygen to a molecular level. In pulverised coal flames, the near field aerodynamics of flow will also influence the rate of heating and the eventual combustion of particles. For flows through a turbulent diffusion swirl burner with little or no swirl no inner recirculation zone (IRZ) is formed,(Beer and Chigier (1972)). As the swirl is further increased, vortex breakdown occurs, Escudier and Keller (1983), which heralds the

formation of an inner recirculation zone.

The IRZ plays an important role in flame stabilization by providing a hot flow of recirculated combustion products and a reduced velocity region where a flame may be stabilized, Gupta et al (1984). The heat supplied from the hot recirculating products to the incoming stream of fuel plus air may be regarded as a form of preheat, Essenhigh (1963). Turbulent diffusion (mixing) is also enhanced near the boundary of the reverse flow region due to the large velocity gradients existing there, Afrosimova (1967), Syred and Beer (1972). The strength and configuration of an IRZ depends on the swirl number, S_g, the ratio of the primary stream to secondary air axial momenta ratio, R_m, and the geometries of the burner and the combustion chamber, Syred and Beer (1974), Hagiwara and Bortz (1984).

2.2.1. Single Phase Isodensity Swirl Flows

Most of the measurements of swirling recirculating flows have been conducted under isodensity conditions, Altgeld et al (1983), Dixon et al (1983) and Rao et al (1983). Altgeld et al (1983) provide LDA measurements of the three components of mean velocities and their intensity in a 0.1m diameter cylindrical combustor for two burner configurations. They observed for a burner geometry without a central baffle, subcritical (reverse flows, refer to section 4.3.3.) flows due to the exit-area contraction of the chamber. Under identical input conditions, this behaviour was not observed in a reacting flow. Dixon et al (1983) provide data for the present type of burner in an unconfined air model. They show different flow profiles depending on the intensity of swirl, and show that the recirculated mass flow decreases with increasing momentum ratio, R_m. Rao et al (1983)

provide experimental data and their prediction for various swirl numbers. They show that there exists an optimum swirl beyond which the size of the recirculation zone decreases with a further increase in swirl.

2.2.2. Single Phase Combusting Swirl Flows

Due to the large density gradients, especially in the near-burner region, a reacting flow cannot be simulated in isothermal models, Chedaille et al (1966). Very few flow measurements have been conducted in combusting flows. Afrosimova (1967) conducted flow measurements in a 0.8m diameter furnace fired with town gas. His results indicate that combustion reduces the amount of recirculating products and the size of the recirculation zones, and also changes the pattern of their distribution when compared with isothermal flows. The results of Syred et al (1970) are in agreement with those of Afrosimova (1967), and indicate that the maximum recirculated mass flow was 80% of the central (primary) jet mass flow rate under isothermal flow and reduced to 70% under combusting flows.

The measurements of Baker et al (1974) indicate that larger regions of recirculation are formed with combustion. More recent results of Claypole and Syred (1982) for a single nozzle geometry burner firing natural gas with no confinement indicate that only 5% of the total flow is recirculated (swirl number = 1.26). The inconsistency of the characteristics of combusting recirculating flows are evident. These may be due to the different geometries of the swirl-burner and the confinement ratio. As a result of combustion a large expansion of axial flow near the burner will take place. This will reduce the effective swirl number and therefore a reduction in the size and

strength of the recirculating zone should be expected.

The precessing vortex cores (PVC's) observed in cold flow will be largely damped for the axial fuel injection burner presently used, and for excess air levels < 30%, Syred and Beer (1972). Another consequence of combustion is the increased velocity fluctuations due to the greater velocity gradients, Baker et al (1974). A significant difference in the flow characteristic must therefore be allowed for in the presence of combustion. A similar remark was also made by Escudier and Keller (1985) who analysed the data of Altgeld et al (1983).

2.2.3. Two-Phase Swirl Flows

When firing pulverised coal, the trajectories of particles and their interaction with the fluid flow must also be taken into account. Due to the difficulty of reliable measurements in such flows no experimental data are presently available for a particle laden jet surrounded by swirling air for the typical coal mass loading of 0.3 to 1.0, neither under combustion nor under isothermal flows. The velocity field for an isothermal 2-phase non-swirling turbulent flow of air and solids in a round jet was measured with LDA by Modarress et al (1982, 1984). Their results show the following effects of the dispersed phase on the development of the jet as compared to a single phase turbulent jet:

1. The expansion rate of a two-phase jet is smaller than that of a single-phase jet; this rate decreases as the initial mass loading is increased.

2. The centerline velocity decay of both phases in a 2-phase turbulent jet is smaller than that of a single-phase turbulent jet.

3. The radial diffusion rate of the dispersed phase is smaller than that of the gas phase.

4. The mean slip velocity between the two phases increases with increasing particle diameter and decreases with increase in the initial mass loading.

5. The normalized velocity fluctuations are reduced with increase in the intial mass loading.

6. The normalised Reynolds shear stress for a two-phase turbulent jet is smaller than that of single-phase turbulent jet.

The dearth of experimental data on the near burner field flow aerodynamics is due to the difficulties involved in the measurement of such flows. Conventional pitot-tube and hot-wire anemometry methods are rendered ineffective even for the isothermal measurements of swirling turbulent particle-laden jets.

The only reliable method for spatial measurements of 2-phase flow is by means of optical instrumentation. An example is the optical system developed by Tichenor et al (1984) which combines an image-plane coded-aperture method of particle sizing with ratio pyrometry and transit time measurement methods for temperature and velocity measurements respectively. Currently Hardalupas et al (1986) are developing a lasser-doppler system for velocity measurements of isothermal gas-solid flows in a small-scale swirl burner. However, these optical methods have not been tested for either reacting or isothermal flows in a large-scale furnace firing poly-disperse, non-spherical pulverised coal.

2.2.4. Flame Classification

From the observation of various industrial flames, the IFRF have classified three main types of flames, Bortz (1983), which are illustrated in Fig. 2.1. These flame types enable the qualitative classification of flame aerodynamics from their visual observation even if the flow properties are not measured. These flame types illustrate broadly whether an IRZ is present or not and also indicate roughly the trajectories that the particles would follow and hence their residence time in the near burner region. Thus visual flame observation provides valuable insight to the flame aerodynamics.

2.3. PARTICLE TIME-TEMPERATURE HISTORY

The incoming particles will be heated by radition from the flame and the refractory quarl and walls (if any) and by mixing with the hot recirculating combustion products. Beer (1962) estimated from his experimental data that near the burner region, up to 70% of the heat received by the particles was due to recirculation. This is in agreement with the predictions of Rizvi (1985). The rate and extent of particle heating will therefore depend on the aerodynamics of the burner-furnace system and the input flow conditions. Increased preheat of combustion will augment the rate of particle heating whereas an excessive amount of diluents for example nitrogen in air will tend to reduce the particle temperature. The use of finer particles (see also section 2.4) will also enhance the particle heating rates.

The rate of particle heating, the final temperature attained and the residence time of particles at that temperature have a dominant influence on the rate of coal devolatilization. Jungten and Van Heek

(1968) reported that an increase in the rate of heating shifted the release of some volatiles towards higher temperatures. Anthony et al (1974) have shown that the volatiles yield increased with temperature but that the release was insensitive to the heating rate or the duration at the final temperature. Seeker et al (1978) and Solomon and Colket (1978) report increased yield of volatiles with increasing temperature. Suuberg et al (1978) provide time-resolved data of volatiles yield. They observed that the rate and yield of various volatiles depended on the species and that the evolution of volatiles exhibited a two-step dependency on temperature similar to that observed by Kobayashi et al (1976). Kobayashi et al (1976) observed also that the devolatilisation rate and yield at a given residence time increased with increasing temperature. Recent experimental data of Jamaluddin et al (1986) show increased volatiles yield with increasing heating rate and temperature. Jost et al (1984) reported that, as would be expected, finer particles devolatilised much faster than the larger ones.

The time scale for devolatilisation and their combustion in pulverised coal flames is altogether of the order of a few tens of milliseconds whereas the combustion of char requires several hundered milliseconds, Essenhigh (1957), Hubbard (1960), Smoot and Smith (1985). Because devolatilisation begins at lower temperatures (700K) than that for the beginning of the combustion of char (1300K) Essenhigh (1976), it is essentially a near-burner phenomenon and as such bears much relevance to the process of flame stabilization for boiler-type burners. For this reason the combustion of the solid particles or char is not extensively discussed here. Useful literature on this subject includes those by Field et al (1967),

Froberg and Essenhigh (1978), Essenhigh (1981), Mitchell and McLean (1982), and Smith (1982).

2.4. COAL CHARACTERISTICS

The intrinsic property of coal that has a major influence on flame stability is the volatiles content. The higher the volatiles content the larger the proportion of gaseous phase combustion which proceeds at a much faster rate than that of solid particles, see section 2.3. For particles of a given size, the rate of devolatilisation will depend on the thermo-physical behaviour of the coal, Wendt (1980). High volatile content and low moisture and ash contents are desirable for flame stability, Wall (1985). For coals which contain small amounts of volatiles, for example chars, improved flame stability was observed for particles which were more porous, Cogoli et al (1977). The stability of pulverised coal flames must be expected to improve strongly with finer particles. Finer particles will follow the gas flow more readily, absorb heat faster and they will also augment the rate of diffusion of oxygen to its surface, Vulis (1961).

2.5. PROPAGATION OF PULVERISED COAL FLAMES

When coal enters a combustion chamber it may, depending on the various factors discussed above (refer to sections 2.2. - 2.4), ignite. The mode of ignition may be heterogeneous or homogeneous, the deciding factor is in the main the particle size of the coal. Once the fuel has been ignited reaction may propagate. The rate of propagation will depend mainly on the stoichiometry (hence mixing) and the system heat loss (or the fluid temperature). If the rate of propagation is slow compared to the incoming velocity of the

reactants, the flame will recede from the burner and may eventually blow off.

All the reported experimental research on the subject matter of this section emanates either from studies on single particles or in laminar flow reactors. Verification of these findings in large turbulent flames is hampered by the lack of experimental data at the near burner region.

2.5.1. Mode of Ignition and Propagation

It has traditionally been assumed for example Faraday and Lyell (1845), that complete devolatilisation of a particle occurs before the combustion of the residual char begins, and that the volatiles are assumed to burn rapidly compared with the burning time of the char, Field et al (1967). However, on the basis of combustion studies in a plug-flow reactor, Howard and Essenhigh (1965, 1966 (a), 1966 (b)), suggested that for particles larger than a critical diameter some combustion at the particle surface takes place before devolatilisation becomes appreciable. This is followed by the release of volatiles which emerge at such a rate that they prevent oxygen from reaching the particle surface. The particle combustion is inhibited until the rapid devolatilisation ended. For particles smaller than the critical diameter, or for low devolatilisation rates, both heterogeneous and gas-phase volatiles combustion proceed simultaneously. Howard and Essenhigh (1966 (b)) calculated the critical diameter to be 65μm. Suuberg et al (1978) estimated the critical diameter to be 40μm.

Theoretical analysis of Bandyophadyay and Bhaduri (1972) and Annamalai and Durbetaki (1977) are in general agreement with the

hypothesis of Howard and Essenhigh (1966 (b)) but indicate that the ignition behaviour will also depend on the volatiles content and the ambient oxygen concentration. The hypothesis of heterogeneous ignition was further tried experimentally in a jet stirred reactor with heating rate of 10^6 °C/sec by Goldberg and Essenhigh (1978). They reported that the initial mass loss of coal depended on the stoichiometry and under fuel-rich conditions was due mainly to devolatilisation. However, they suggested that the mechanism of ignition was the same as that of Howard and Essenhigh (1966 (b)) who experimented at a lower heating rate of 10^4 °C/sec. The contradicting observation (initial devolatilisation rather than heterogeneous ignition) was due to the 2 orders of magnitude smaller time scale required to achieve the same temperature, a time scale of about 0.2 ms, which was too small to resolve the data.

Seeker et al (1978) postulated from their experimental observations that for small particles (number mean diameter < 10μm), ignition was due to heterogeneous combustion whilst for larger particles, ignition was due to homogeneous reactions. Time resolved shadowgraphs of burning coal particles (mass mean diameter 65μm), McLean et al (1981) show clearly that the particles were shielded from oxygen by the envelope of the released volatiles so that combustion was initiated by ignition of volatiles. Similar observations were also made by Hertzberg et al (1982) and by Timothy et al (1982).

More recent experiments in small drop-tube furnaces of Chen et al (1984) and Tognotti et al (1985) exhibit ignition temperatures of coal and char particles as low as 700K. Their results are in agreement with the theory based on heterogeneous ignition. Computer predictions by Musara et al (1986) of devolatilising coal particles

indicate that ignition of particles smaller than 20μm was due to heterogeneous combustion whereas for larger particles homogeneous volatiles combustion was more important. The results of single particle ignition experiments are probably not directly applicable to the ignition of dust clouds due to the "cooperative" mechanism, Cassel and Liebman (1959). They observed a decrease in the ignition temperature with increasing dust concentration, the decrease being steeper for finer particles.

Theoretical studies of flame propagation by thermal radiation by Essenhigh and Csaba (1963) which is an extension of the original work by Nusselt (1924), show that increased preheat of reactants increased the rate of flame propagation. This is of particular relevance to enclosed jet flames with recirculation of combustion products which preheat the incoming reactant streams. Smoot et al (1976) proposed a mathematical model in which the combustion was limited by the devolatilisation rate, the diffusion of volatiles to the surroundings and the diffusion of oxygen to the particle surface. Their predictions indicate that in the near-burner region a gas phase diffusion flame was formed by volatiles generated downstream of flame.

In the review of flame propagation by Essenhigh (1976), the heterogeneous and homogeneous ignition temperatures of 1000°C and 350°C respectively are reported. It was emphasised though that the mode of ignition depended strongly on the particle size (see also Hattori (1956)), and on the reactor or flame system and the equipment scale.

2.5.2. Flame Liftoff and Blowoff

When the rate of flame propagation is less than the velocity of the incoming reactant jets, the flame detaches from the burner and stabilizes at some distance downstream. As the velocity of the jet is increased further the flame blows out. Broadly, two theories of flame liftoff exist for gaseous turbulent jet diffusion flames. One that suggests that a lifted flame is stabilized in a zone where combustion is controlled by premixing, Chakravarty et al (1984), Eickhoff and Leuckel (1984). The other concept is based on the assumption that within the stabilization region, a turbulent flame can be viewed as an ensemble of unsteady laminar diffusion flamelets. Peters and Williams (1983), Broadwell et al (1984).

The blowoff limit of swirl stabilised flames may be modelled either by the method of Longwell et al (1953) or that of Zukoski and Marble (1955). Longwell et al (1953) used the theory of well-stirred reactors to deduce a maximum mass loading rate for a fixed reactor volume and pressure. If the mass loading exceeds this limit, blow out occurs. Zukoski and Marble (1955) stipulate that for bluff-body stabilizers the contact time of combustible along the length of the recirculation zone equals to ignition time for the gases at the blow-off condition. These theories may be used to model the blow-off conditions for pulverised coal flames, by similar means to their applications for spray flames, Altenkirch and Mellor (1974), Plee and Mellor (1979). The difficulty in using the above methods in pulverised coal flames is that the ignition mechanism is still not well understood. Furthermore, the near-burner particle combustion behaviour and flow field in turbulent pulverised coal flames have not been reliably characterised. The lack of such experimental data

renders modelling of any near-burner phenomenon meaningless.

2.6 SUMMARY

The review presented in this chapter has been kept very brief and in itself is a summary of the findings. The most important deduction one can make from the review is that experimental verification of the various hypotheses of flame stabilization in large swirling turbulent diffusion flames is still lacking.

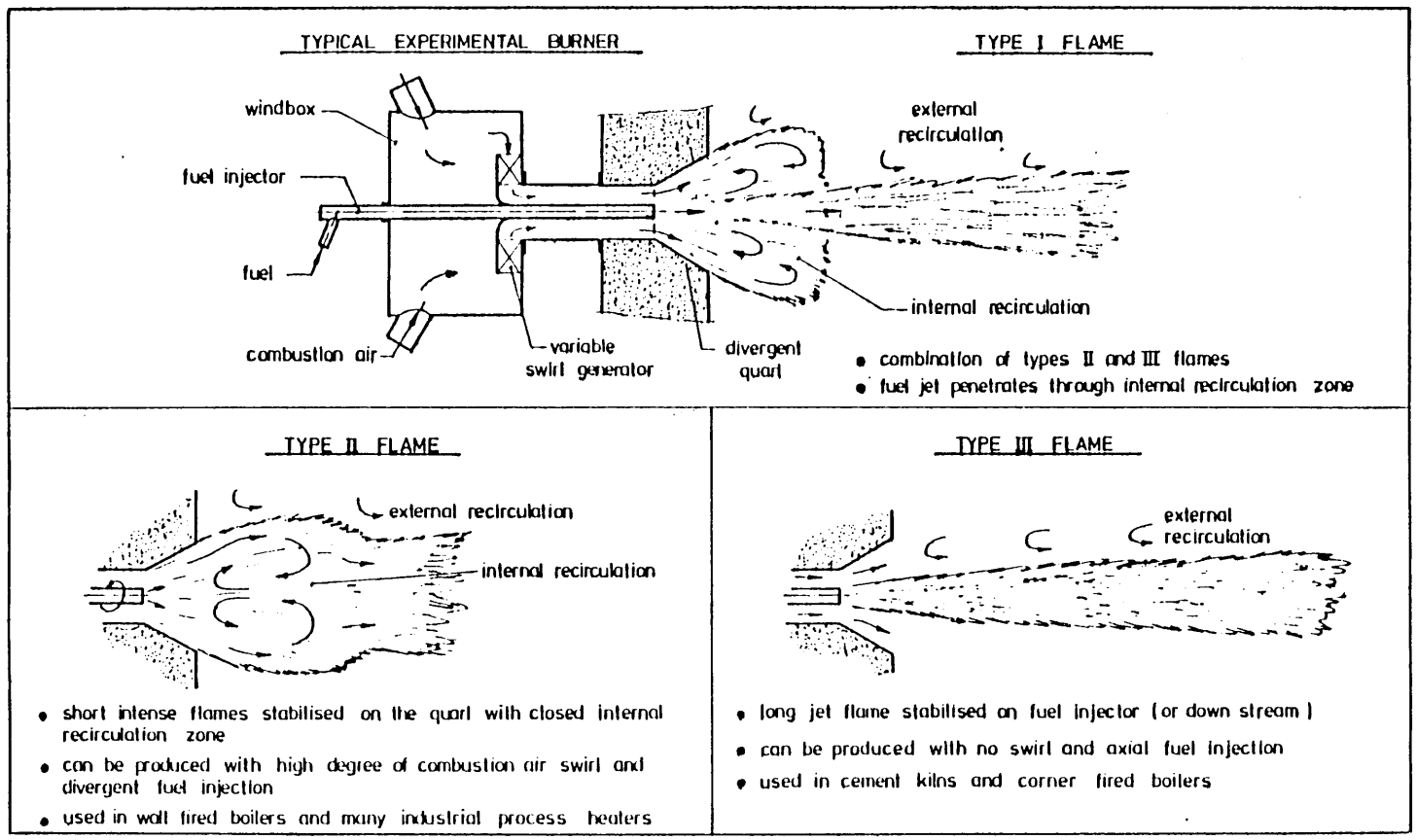


Fig. 2.1 Schematic of various industrial flame types (after Bortz (1983)).

CHAPTER 3

FURNACE, INSTRUMENTATION AND EXPERIMENTAL METHODS

3.1. Introduction

Pulverised coal-fired experimental furnaces are constructed for the study of the following:

(a) ash fouling and slagging,

(b) overall combustion efficiency and emissions,

(c) the detailed flame behaviour and pollutant formation,

and

(d) the combustion of a single particle or of a few particles.

The majority of the existing experimental furnaces are designed to study ash slagging properties, Higgins and Morley (1985). Ash slagging and the consequent down-time for maintenance constitutes a major financial drain in power station boilers.

Due to financial and time constraints, commercial research interest in burner performance results in their preference of constructing furnaces suitable for category (b) above.

The experimental study of the combustion of a single particle or of a few particles permits the quantification of descrete phenomenon, for example devolatilization. However the data can not be directly applied in burner flames with certainity. Particles tend not to burn as individual flamelets, Wendt (1980).

The furnace used for the present study is large enough to emulate the combustion behaviour, for example heat flux to the walls, in industrial boilers, see Hassan et al (1985). The design of the burner is that typically used in power stations for wall-fired boilers. The main practical advantage of this furnace is that inflame measurements

are possible, a daunting task if the same were to be conducted in large boilers.

Since the flow is axisymmetric, the validation of prediction code is much easier than a fully three dimensional combustor. The data and validated computational procedures may be used for the better understanding of the combustion process leading to better design of full-scale boilers.

Detailed account of the furnace, the instrumentation and the ancillary equipment is given by Hassan (1983). Sections 3.2 to 3.4. are limited to a summary of the salient features and to the recent modifications. The analyses of the tested fuels are presented in section 3.5 and the experimental procedures are described in section 3.6.

3.2. The Furnace and Ancillary Equipment

3.2.1. The Combustion Chamber

The combustion chamber, see Fig.3.1, is cylindrical, vertically orientated and down-fired to facilitate ash collection. Fluid flow in this simple geometry is axisymmetric which renders itself comparatively easier to predict. The internal diameter of the working section is 0.6m and it is 3m long. It is constructed in 10 separate segments each 0.3m long. The top 1.5m of the working section,its roof and the burner quarl are refractory lined. The lower half of the furnace is water cooled. The cooling water flow rate for each segment can be controlled and measured. The water temperatures at inlet and outlet may also be measured so that a heat balance may be computed. Two diametrically opposed ports for viewing and probing are provided in the first nine segments. An explosion vent is installed in the

tenth segment, see Fig. 3.1.

3.2.2. The Burner

The geometry depicts a power-station wall-fired burner. Coal and primary air exit through the central pipe and the secondary air through the annulus. An IFRF variable swirl generator provides swirling motion of the secondary air stream in the range of swirl numbers, S_s = 0 to 1.45 for the geometry shown in Fig. 3.2. The same geometry was employed for all the experiments except where specified for a few tests, whereby a central burner gun of 31.0 mm internal diameter was employed.

3.2.3. Igniter and Flame Detectors

The incoming fuel is initially ignited by a natural gas-air premixed flame provided by a P44 pulse energy torch igniter system developed by Industrial Automation Systems Ltd (IAS). Once a flame is established, the igniter is withdrawn from the furnace.

An infra-red Fireye 48PT2 together with D41 control unit is used to detect flames. This controller disables the fuel supply in the event of a flame failure. In addition to this, an independent flame detection system (CEA Controls Ltd) was used for the observations of the flame stability experiments. This composed a "Digiscan" control unit and an I.R. 800 viewing head.

3.2.4. The Scrubber

The original scrubber, see Fig.3.3.(a) was modified (Fig 3.3 (b)) to eliminate the requirement of day to day maintenance. The swirl vanes on the cone were removed. A smaller cone was constructed with a

longer skirt. The efficiency of the modified design in separating the water and ash particles from the gas was much the same. The finer ash particles which were entrained by the exhaust gas settled in the first pipe bend. A water shower and a slot were installed in the pipe. The pipe was easily cleared of the accumulated slurry without removing the scrubber from the furnace. Another ring of showers was installed at the base of the scrubber unit. This proved useful when firing a very high ash content coal. Water and ash slurry discharged from the bottom of the scrubber was drained through a large sediment tank instead of the weir tank arrangement previously used, Hassan (1983), so that longer maintenance-free firing runs were possible.

3.2.5. The Air Supplies to the Furnace

Secondary air was supplied by a 7.5kW forced draught fan, type Mc-Alldays, Peacock Co. Ltd. The quantity supplied was measured with an orifice plate installed at the inlet of the fan. The calibration of the orifice meter was checked by measuring with a pitot-static tube the air exhausted from the furnace which was otherwise sealed. The agreement between the two measurements was within $\pm$ 1% of the total flow. The secondary air was heated by a 21kW electric heater (ex Electron Co. Ltd, Croydon, England).

Oil and moisture free primary air was supplied by a dedicated air compressor (model Hydrovane 43, Hydrovane Ltd, Redditch, Worcs, England). The flow rate of air was measured with a rotameter. A U-tube mercury manometer was installed at the inlet of the rotameter. The indicated air flow rate was corrected for pressure. The rotameter measurement was checked by pitot-static measurement in the primary air supply pipe. The agreement was within $\pm$ 1% of the total flow. The

primary air tube was wrapped with two separate heating tapes (type GW, 850W each, Hot Foils Ltd) to provide the necessary preheat.

3.3 The Coal Feed System

The present coal feed system is illustrated in Fig. 3.4 (b). Coal was transported from a feed hopper by a variable speed auger into a vibrating chute. It then entered a pneumatic conveying system in which it was transported by the primary air to the burner. The feed system upstream of the pneumatic conveyor was mounted on a balance-beam weighbridge. Analogue signals from a load cell were fed to a microprocessor. The microprocessor metered the mean coal feed rate by evaluating the mass loss from the wieghbridge during a 30 second time interval. The coal feed rate was compared to that required and the rotation of the auger was appropriately adjusted by a built in proportional controller. When the amount of coal in the feed hopper was less than a preset minimum, a membrane valve was activated so that coal was fed by gravity from the storage hopper into the feed hopper.

3.3.1. The Weighbridge

During a systematic evaluation of the system, several problems were identified. These were associated with the refill and the weight measurement processes, and also with the flow properties of different coals.

During a refill process, coal from the storage hopper dropped directly into the feed hopper, see Fig. 3.4 (a). The impulse momentarily resulted in increased coal feed rate to the burner. This of course induced combustion transients, for example, an increase in

temperature. It also resulted in an increased loading in the pneumatic conveyor. It was vital that the coal feed rate be maintained constant even during the refill processes. This was achieved by inserting a cone, see Fig. 3.4 (b), in the feed hopper. The cone also helped to eliminate the problem of "plug-flow", Elliot (1981). Furthermore, the stroke of the membrane valve was also reduced in order to reduce the amount of coal ejected per opening of the valve.

Load cells permit extremely accurate measurements of weight. However, the application of these in dynamic situations such as the present continuous feed weighbridge requires very careful consideration. Any misalignment of the line of applied force, vibrations, and of course friction in the system may render a load cell technique useless. Indeed, much development time was spent in order to obtain precise and reliable weight measurements. After gaining confidence in the load signals, a precision weighing balance (Oertling type HB63) was mounted externally and used to compare the feed rate with that provided with the coal weighbridge. The constant of proportionality (kg coal/volt), a variable factor in the microprocessor software was adjusted so that there was agreement between the feed rate evaluated from these two systems.

Flow properties of solid particles are influenced by the type of product, its bulk density, the particle size distribution and also the weather, Lowry (1963). The "motor-speed" constant in the microprocessor software which regulates the nominal rotational speed of the auger feeder had to be appropriately adjusted whenever a different coal was used. During the warmer periods, an extreme condition was experienced whereby the coal "arched", Elliot (1981),

in the feed hopper resulting in no flow of coal. The arch had to be mechanically broken. The problem was however cured by injecting very low flow rate (500 cc/hour NTP) of nitrogen at the throat of the hopper. This aerates the otherwise deaerated coal due to the warm conditions.

The linkage between the weighbridge and the pneumatic conveyor was previously provided by a vibrating cascade arrangement. Since this was not mounted on the weighbridge and the coal feed rate was found to be uniform on existing from the vibrating chute, the cascade assembly was replaced with a cylindrical perspex chamber, Fig. 3.4 (b).

The present feed system provided coal flow rates accurate to within $\pm$3% of its mean value.

3.3.2. The Dilute-Phase Pneumatic Conveying System

Preliminary coal firing trials indicated unacceptable combustion instabilities. The cause was traced to coarse fluctuations of coal feed rate at the burner resulting from coal settling in the horizontal length of the primary tube which was periodically re-entrained by the primary air stream. This phenomenon also resulted in back pressure at the injector body which in turn affected the weighbridge load signals. It was clear therefore that the pneumatic conveyor had to be redesigned. A good grounding to the subject of gas-solid transport is provided by Klinzing (1981).

Two interlinked features of the pneumatic coal conveying system were considered the most important. Firstly the pressure drop in the conveyor pipe and secondly the "roping" and the subsequent settling or drifting of coal particles in the horizontal pipe runs. The

pioneering experimental work by Patterson (1959) and subsequent works of Bowers and Wright (1978), Cook and Hurworth (1980) and Mills (1980) amongst many identify the conveying velocity, the air to coal ratio (ACR), the particle size distribution, the coal type, the pipe diameter, and the pipe configuration to be important design consideration. Since the ACR, the particle size distribution and the coal type were already selected for the experimental programme, and the major part of the pipe configuration could not be altered for physical reasons, attention was concentrated on the pipe diameter and the conveying velocity.

It was observed that the worst stretch of piping as far as drifting of coal is concerned was the 3m long horizontal pipe initially 26mm internal diameter (I.D.). This pipe followed a vertical downward-flow pipe immediately after the injector body. For normal operating conditions, the superficial air velocity in the pipe was approximately 13 m/s. The diameter of the pipe was reduced to 22mm ID in order to increase the velocity to 18 m/s. The remaining of the pipe, which consist mainly of vertical pipe runs was left unchanged (26mm I.D.).

As a consequence of the changes in the pipe sizes, the injector had to be modified to provide for the additional pressure drop in the conveyor. The design of the injector had to meet the requirement that there should not be any secondary entrainment. The injector-coal feed chute linkage could not be sealed because the suction would induce load on the weighbridge. The injector was reduced in diameter so that more pressure could be supplied for the transport of coal. The injector was mounted so that it could swivel about its axis. Adjustments of the injector to blow air towards the pipe wall

permitted the excess energy, if any,to be dissipated by friction so that the pressure upstream of the injector was atmospheric.

The present system operates satisfactorily for coals nominally 70Wt% to 80Wt% under 75μm. For microfine coal (80 Wt% less than 40μm), coatings of the particles were observed even on vertical pipewalls. A similar behaviour was also observed by Yang et al (1980) when transporting very fine nuclear powders. This behaviour is believed to be due to increased cohesiveness associated with small particles. The coal feed system had to be modified so that the length of the pneumatic conveying pipe could be shortened. The complete system is described by Ismail (1986).

3.4. The Instrumentation

3.4.1. Temperature

Time averaged temperature was measured with 40μm diameter platinum/platinum-13% rhodium fine wire thermocouple, see Fig. 3.5. Basically the same technique cited by Hassan (1983) was used. The thermocouple emf was amplified x 100 before being fed to an oscilloscope and to an analogue to digital converter. The digital signals were fed to an ITT 2020 micro-computer which converted the signals to temperature. The sampling frequency was 2 HZ. The major problem of using fine wire thermocouples in coal flames was that the wires became coated with char particles. This coating was non-uniform with many voids. A greater radiation loss from the thermocouple resulted as a consequence of an increase in its size. An estimate of this loss is provided in section 4.3.1.

3.4.2. Gas-Concentration

Particle-laden gas samples were extracted from the furnace with the aid of a direct water-quench (shower) probe, see Fig. 3.6, which was a refined version of that used by Hassan (1983). The main advantages of the probe used were the improved cooling, the manufacturing technique and the materials used, enabling longer life of the probe. It was made of grade 316 stainless steel and the tip-end was machined from a block so that no welding was necessary in this critical vicintiy. The number of tubes that supplied cooling water was increased from 2 to 8. The assembled probe was filled with sand and bent in a specially made jig. This drastically reduced the number of welds (otherwise critical points of failure).

Water and char were separated from the gas sample with a disengager nearest to the probe, see Fig. 3.6. The moisture that was not trapped by the disengager was carried forward and condensed in the ice bath and then collected in the disengager located downstream. Gas samples were then passed through three dryers which contained calcium chloride for the removal of the remaining moisture before being supplied to the gas analyers via the suction pump.

Because the sampling system was under negative pressure, one of the major sources of operational difficulties was the leakage of air into the system. Test for any leakage was by operating the probe normally and introducing oxygen free nitrogen at atmospheric pressure to the probe tip and supplying the sampled gas to the oxygen analyser. Obviously if the system was free of any leakages, a zero oxygen concentration would be measured. The source of leakage was identified by introducing a high CO_2 content gas on the outside of the suspected areas whilst sampling air and observing the CO_2 concentration

measured by the analyser.

The other main difficulty was that the probe became blocked from time to time, especially when sampling very close to the burner and near the furnace axis. The probe had to be removed from the furnace for the blockage to be mechanically cleared. Although a high-pressure nitrogen purge was also sometimes employed to unblock the probe, it destroyed the seals at tube-joints and therefore this method was not frequently used.

The infrared CO_2 (ADC model 483) and CO (ADC model 336) and paramegnetic O_2 (Servomex model 540A) analysers were the same as those previously used by Hassan (1983). In addition a gas chromatograph with a Poropak-N column and a katharometer detector was used to measure unburnt hydrocarbons and also as a check on the species concentrations measured by the preceding dedicated instruments. The column and the detector and the system operating temperature were chosen so that the analysing time at a location did not largely exceed the sampling time.

3.4.3. NO_x Emission

A simple water-cooled sampling probe was designed, Seitz (1986), Fig. 3.7. The main feature being that only the first 70mm length from the probe tip was cooled. This allowed the gas sample to be quenched to 150°C so that the NO was not reduced to N_2 by char and CO. The temperature of the probe near the tip was measured so that the quenching rate of the gas samples could be controlled. The sample line up to the cyclone separator was wrapped with a heating tape, type GW 160W, Hot Foils Ltd. The assembly of the cyclone separator which was filled with glass beads, was immersed an in ice bath so as

to separate moisture from the gas sample. The glass beads improved the efficiency of the moisture collection by providing larger surface area for the moisture to condense and also provided more uniform temperature in the cyclone. The finer particles which carried over were trapped by a micro-(2μm)-filter. A Thermo-Electron chemiluminescent analyser model 12A was used to measure NO_x.

The sampling system performed well. The main operational problems were probe blockages and leakage of air into the system. The blockage was cleared mechanically and any leakages were detected by means similar to that described in section 3.4.2.

3.5. The Fuels Tested

The procedures described in British Standards, BS 1016 (1977) were used to determine the ultimate (elemental) and proximate analyses. The particle size distribution was determined by an air-jet sieve, Model 200 LS, Alpine Process Tech Ltd., and by the Malvern 2200 size analyser (Malvern Instruments, Malvern, England). For particles under 25μm only the later technique could be used. A detailed account of the coal characterisation tests is given by Ismail (1986). The results are provided in Tables 3.1 and 3.2.

Petrographic analyses provided by the suppliers of some of the fuel samples are given in Table 3.3. A summary of the value of such analyses is given in Appendix 3.A. Fuller details may be obtained in Stach (1982) and Neavel (1981).

3.6. Experimental Procedures

3.6.1. Furnace Operation

The igniter, see section 3.2.3, was switched on and then natural gas was supplied to the burner. The furnace was preheated by firing natural gas until steady refractory wall temperatures were observed. The natural gas supply to the furnace was then reduced and coal plus natural gas were fired simultaneously. Once a stable, anchored coal flame was established the natural gas supply and the igniter were turned off. The furnace was air-tight and its pressure was maintained at a slightly negative value (-5mm H_2O) to avoid any dust escaping the furnace when ports were opened to receive probes. The furnace was run on coal until equilibrum conditions were achieved.

The above processes lasted approximately three hours after which experimental measurements were commenced. The primary and secondary air exit temperatures were maintained at 353K and 600K respectively during all the experiments.

Operational difficulties were due mainly to slagging on the refractory walls and on the quarl. Because of the serious consequences (see section 4.3.3) due to slag build up especially in or near the quarl region, frequent cleaning from this critical region was required.

3.6.2. Inflame Combustion Measurements

The amplified (x100) output from the thermocouple was logged into an oscilloscope and to an anlogue to digital converter. Any electrical noise or an open circuit was indicated on the oscillograph. The digital signals were fed to an ITT 2020 micro-computer which determined the mean and the standard deviation of temperature. The

micro-computer also enabled the probe to be automatically traversed. The life of a thermocouple was usually sufficient for a complete radial profile at one axial location to be obtained. It was not desirable to reuse the thermocouple because of the char coating on it. Measurement time of 2 minutes per station was found to be sufficient to represent the mean temperature.

The gas analysers and the chromotograph were calibrated prior to any measurements. Gas concentrations near the furnace exit were always measured before sampling in the upstream region. The percentage of excess air allowing for unburnt carbon was compared to that at input. Any disparity between the two if any were due to leakage of air into the furnace or incorrect air or fuel flow rates. The faults were rectified before any further experiments were conducted. Gas sampling was then performed at the required axial location. The suction rate was adjusted such that the static pressure at the probe tip was nearly atmospheric.A typical flow rate of quench water was 0.35 l/min and that of cooling water 4 l/min. The transit time of the sampled gas between the probe and the first disengagor was five seconds. The analysers response time to achieve 90% of the gas concentration of the probe tip was 40 seconds. Analogue outputs from pre-calibrated CO_2, CO and O_2 analysers were connected to a chart-recorder and also to a micro-computer which logged in the data and controlled the probe radial position. A typical duration of ten minutes was necessary per sampling point.

3.6.3. Flame Stability

For a given ratio of the primary stream (coal plus air) to secondary air axial momenta ratio, R_m, the secondary air swirl number, S_s was reduced, while maintaining the overall input stoichiometry and preheat temperatures constant, until flame lifted off from the quarl. Lift-off was observed visually and also detected by the "Digiscan" flame monitor. The flame detector of this system was mounted so that its field of view covered the quarl region. The 48PT2 flame scanner which is connected to the D41 interlock system was mounted in the horizontal plane so that its axis was 200mm from the throat of the quarl. This avoided the inconvenience of automatic furnace shut-downs when a flame was lifted.

3.6.4. NO_x and O_2 Emission Measurements

The NO_x analyser was calibrated with three gas mixtures containing different amounts of NO:300,600 and 900 ppm NO in N_2. The calibration gas accuracy was $\pm$ 2% and that of the analyser was better than $\pm$ 3%. The flue gas sample was also analysed for oxygen (Servomex, model OA150). Analogue outputs from the two instruments were linked to a chart recorder. Also integrated values over one minute per sample were recorded manually.

Table 3.1

Analyses of Test Coals

	UK Grimethorpe (1)	UK Grimethorpe (2)	South African (A)	South African (B)	UK Gedling Normally Ground	UK Gedling Microfine	Low-Volatile Char BLVG
	Weight % as received						
Proximate Analysis							
Moisture	3.2	6.6	3.0	6.7	6.3	2.4	9.4
Volatile Matter	30.8	31.7	25.3	19.3	35.8	34.4	2.8
Fixed Carbon*	58.2	53.0	58.8	32.0	53.7	51.8	67.1
Ash	7.8	8.7	12.9	42.0	4.2	11.4	20.7
Ultimate Analysis							
Carbon	73.00	69.76	70.50	40.88	72.60	69.93	71.78
Hyrdogen	4.96	4.85	3.97	2.56	5.05	4.91	0.83
Nitrogen	1.76	1.55	1.63	1.04	1.29	1.43	0.39
Sulphur	1.14	1.38	0.41	0.40	1.55	1.24	1.30
Oxygen*	11.34	13.76	10.59	13.12	15.31	11.09	5.30
Gross Calorific Value + (MJ/kg)	29.26	28.21	27.83	15.12	29.29	28.70	25.80
Stoichiometry kg air/kg coal	9.66	9.16	9.03	5.03	9.49	9.30	8.36

* - by difference
+ - calorific value obtained from the expression of Jain and Sundararajan (1981).

Table 3.2

Particle Size Distribution of Test Fuels

Nominal Particle Size μm	UK Grimethorpe (1) Coal	UK Grimethorpe (2) Coal	South African (A) Coal	South African (B) Coal	UK Gedling Normally Ground	UK Gedling Microfine Coal	Low-Volatile Char BLVG
	CUMULATIVE WEIGHT % UNDERSIZE						
710	100	100	100	100	100	100	99
425	100	100	100	100	100	100	94
200	97	100	98	98	100	100	82
100	90	100	85	88	89	100	70
75	85	99	78	81	80	97	56
50	75	95	64	71	68	88	40
40	68	89	56	64	60	80	29
25	45	60	40	50	40	68	8
15	28	37	26	29	23	48	5
10	17	21	15	16	15	33	3
7	9	11	8	8	10	20	2
5	3	5	4	4	6	10	1
3	-	0.5	0.5	0.5	0.5	0.5	-
Weight Mean Size (μm)	42	20	50	43	45	11	73

Table 3.3

Petrographic Analyses of Test Coals

Maceral Analysis (mineral matter, coal shale free basis)	UK Grimethorpe Coal	South African (A) Coal	UK Gedling Coal
% Volume Vitrinite	78	21	72
Exinite	3	7	8
Inertinite	19	72	20
Mean Maximum Reflectance % (Total No. of points - 100)	1.04	0.65	0.64

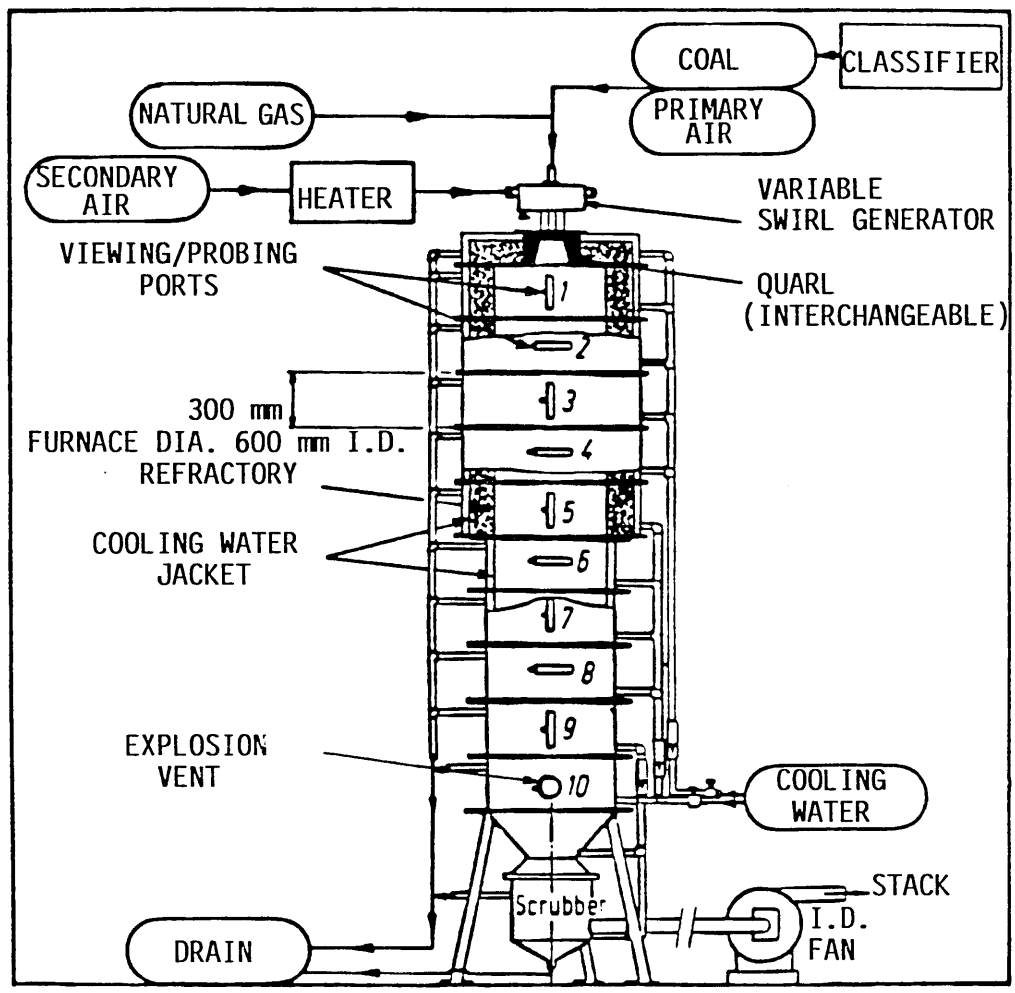


Fig. 3.1 Schematic of furnace.

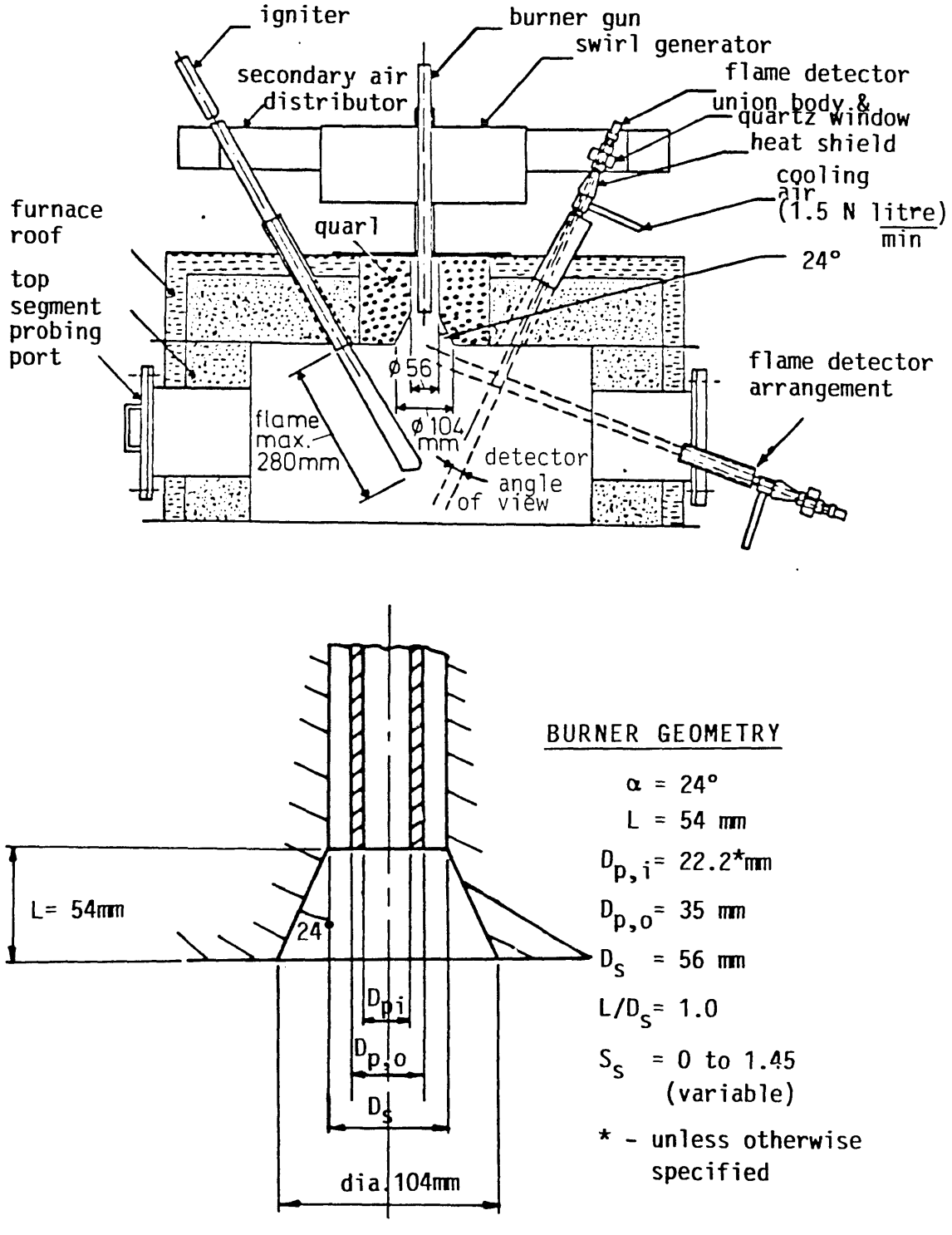


Fig. 3.2 Details of furnace roof and burner.

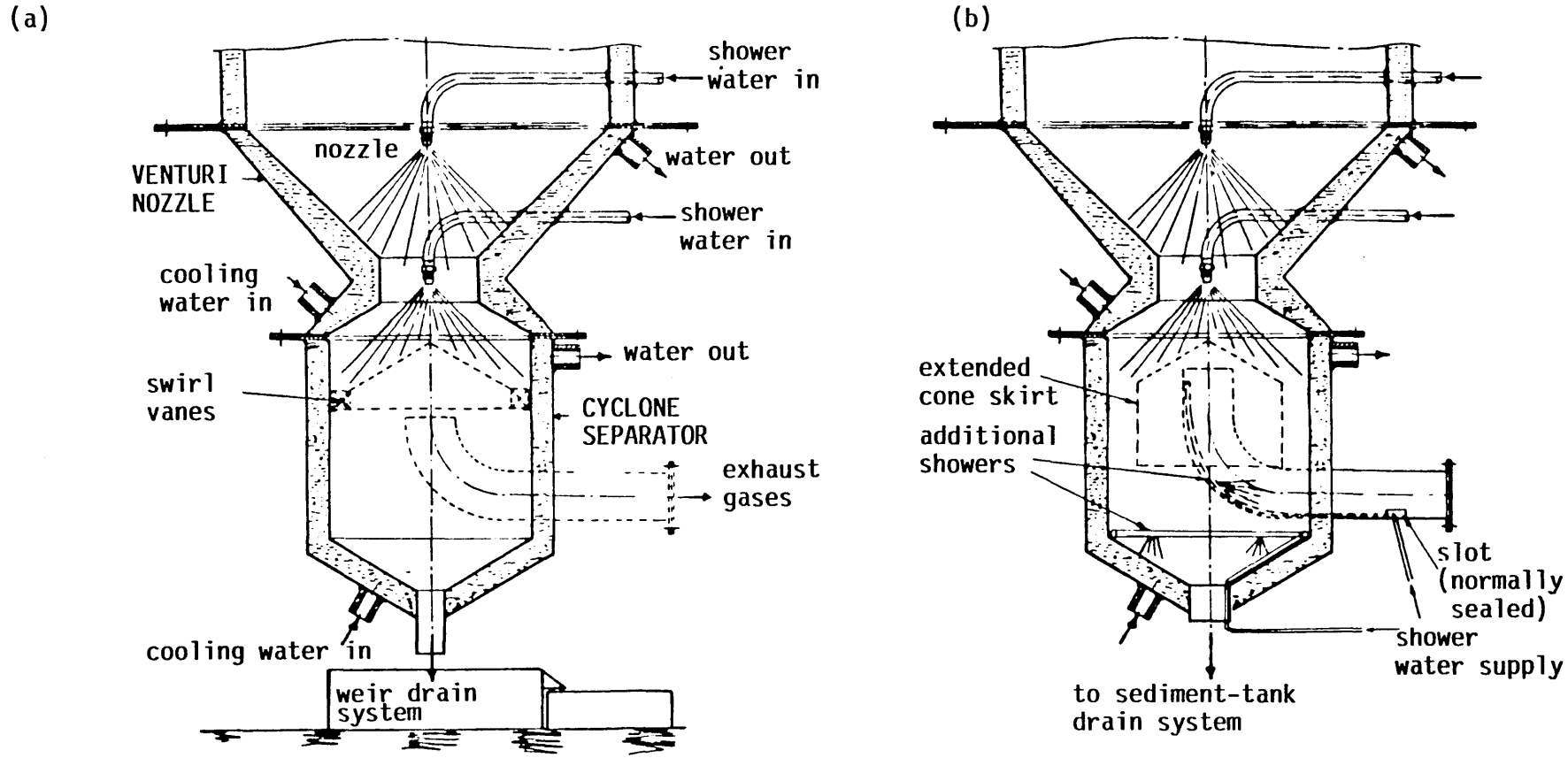


Fig. 3.3 Details of Scrubber.

(a) original version

(b) modified version

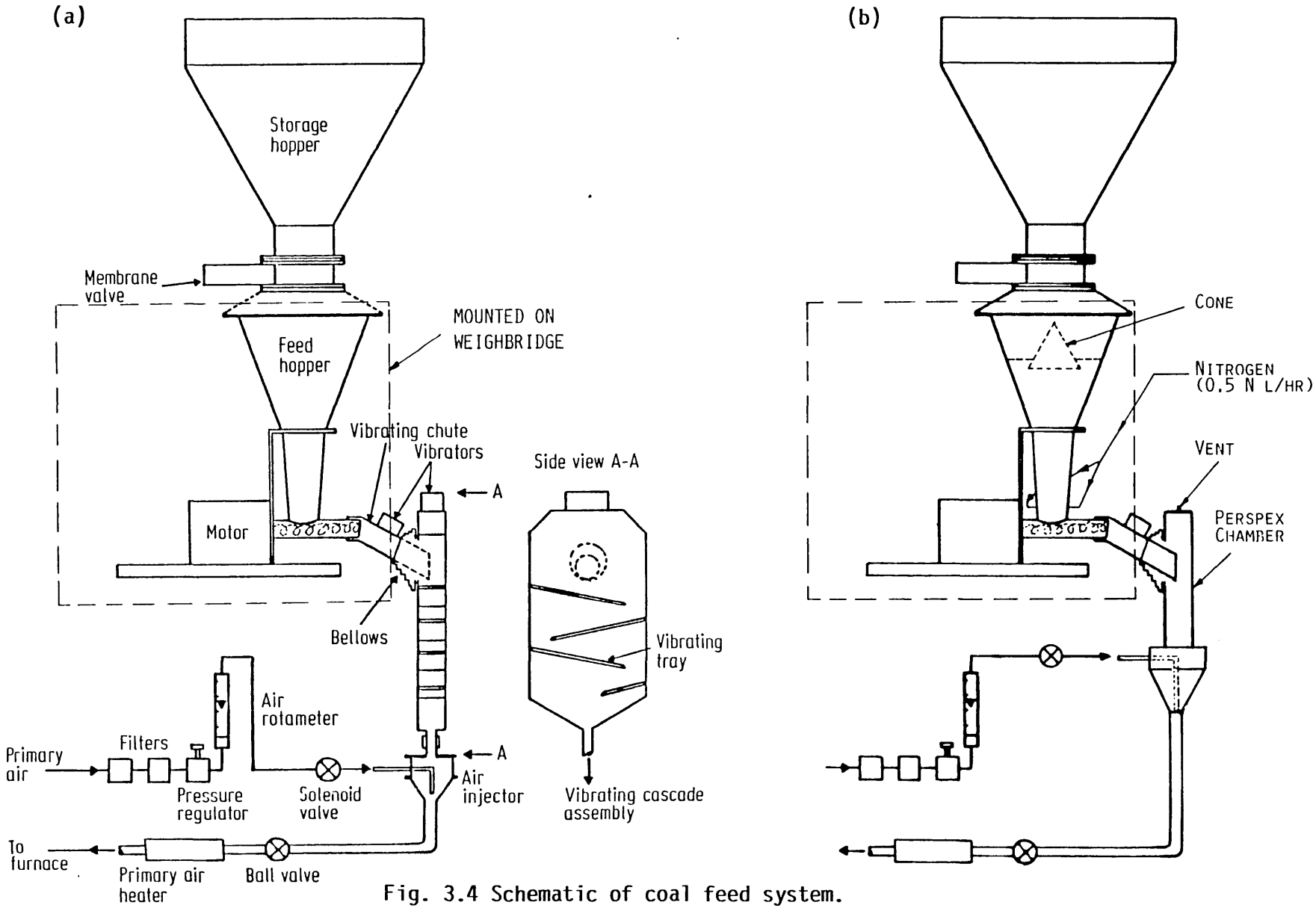


Fig. 3.4 Schematic of coal feed system.
(a) original version
(b) modified version

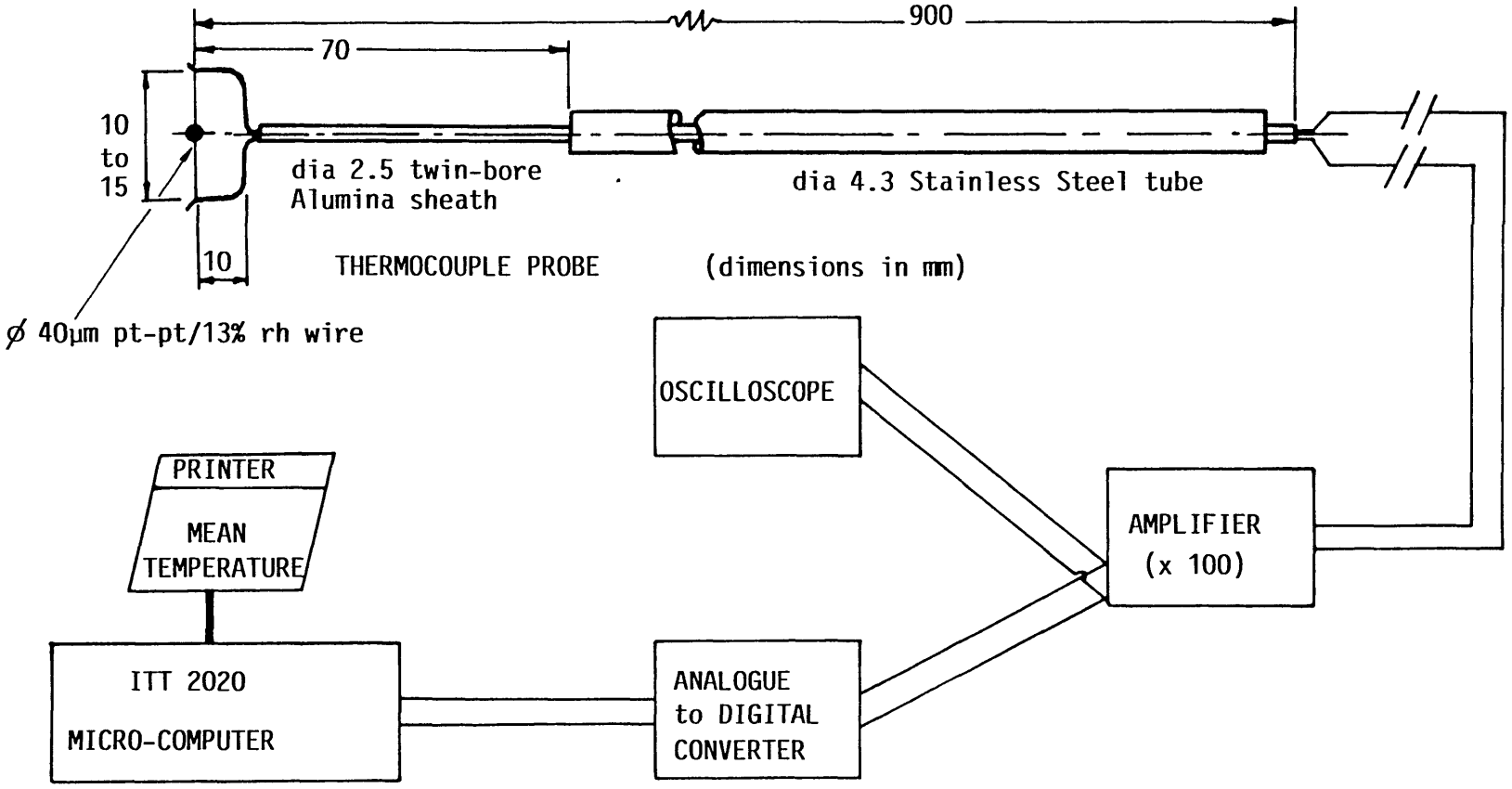


Fig. 3.5 Schematic of temperature measurement system.

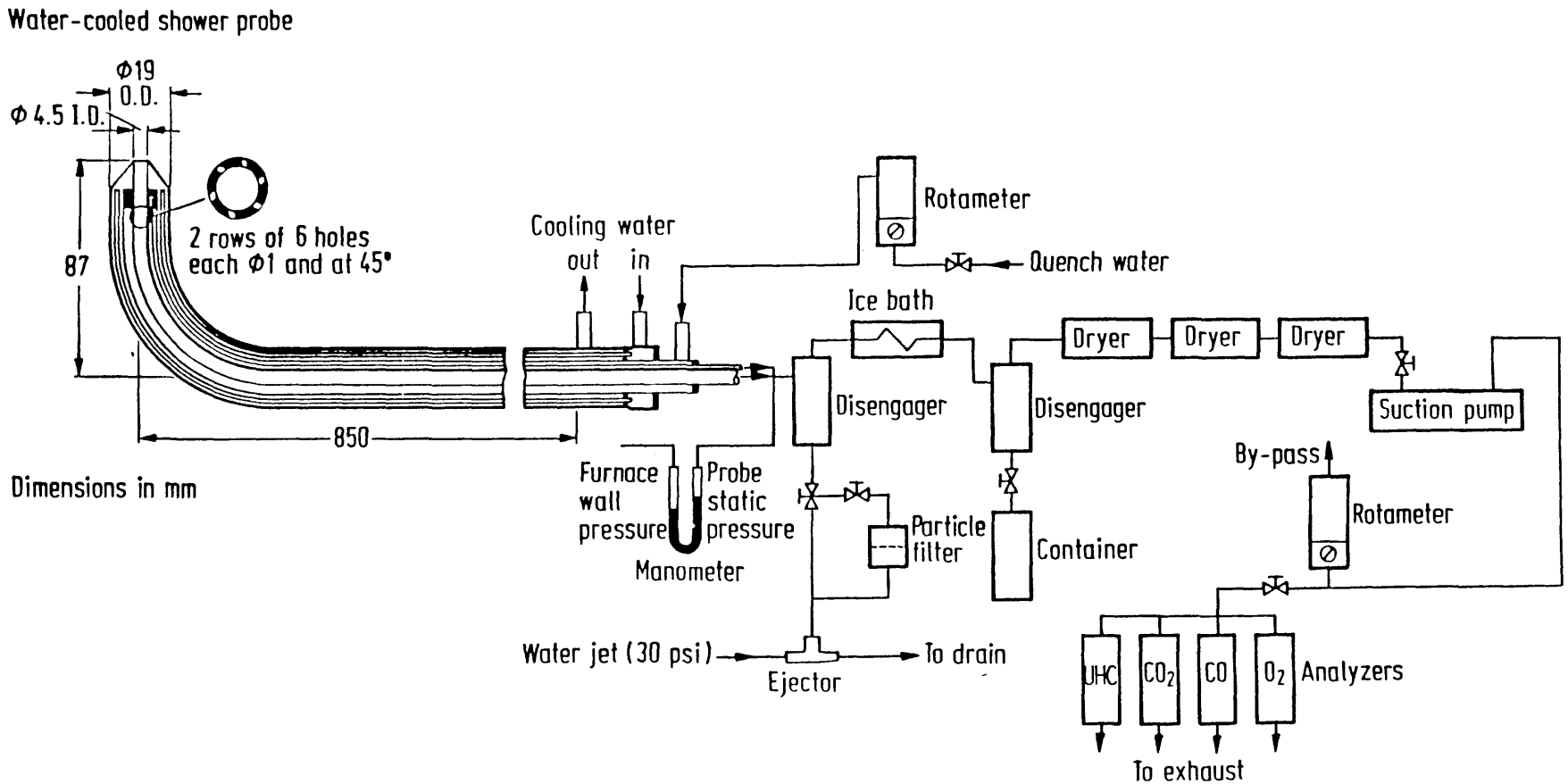


Fig. 3.6 Schematic of gas sampling system.

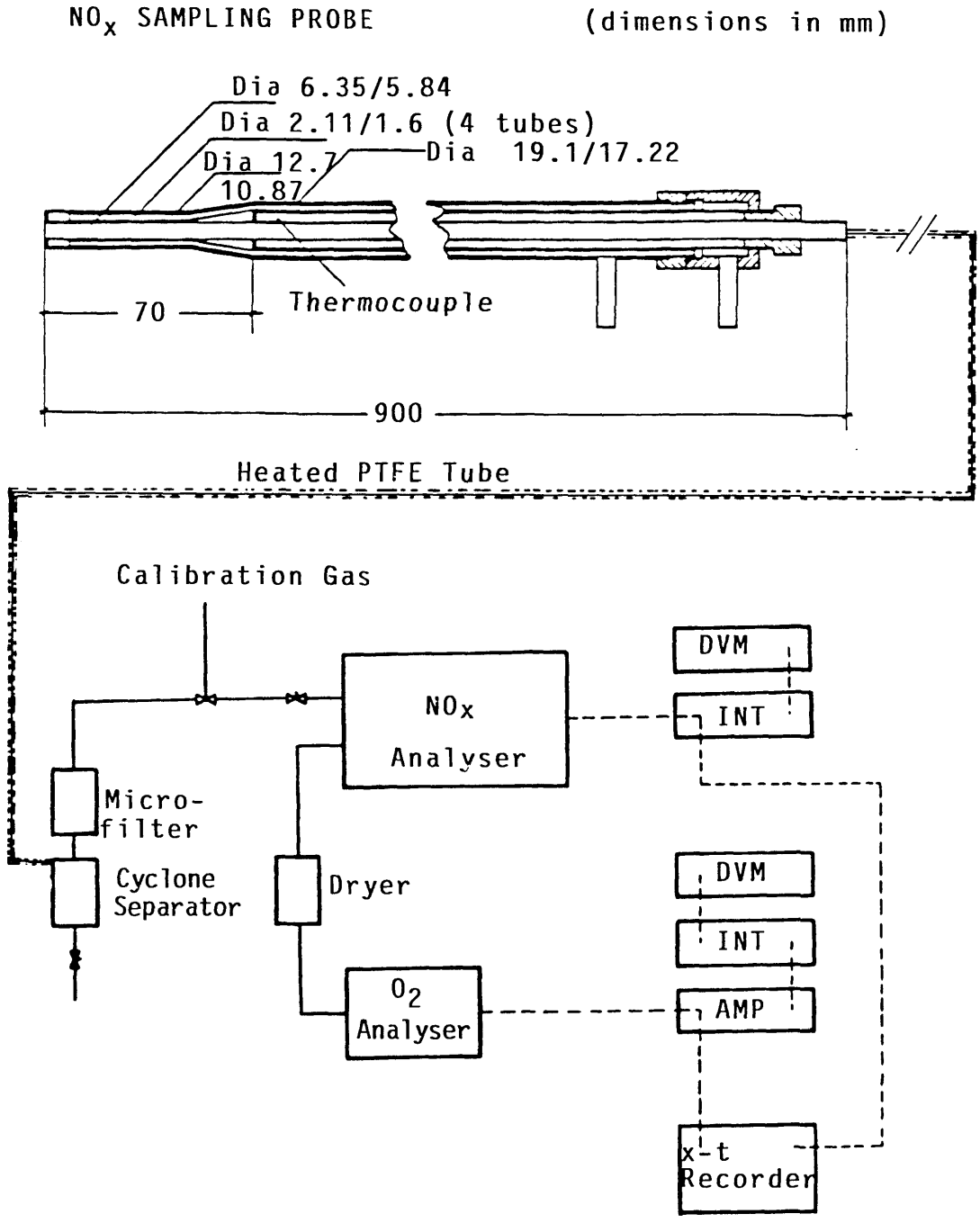


Fig. 3.7 Schematic of NO_x emission sampling system.

APPENDIX 3A

Petrographic Analyses of Coal

Coal is a sedimentary rock accumulated as peat and composed principally of macerals, subordinately of minerals, and containing water and gases in submicroscopic pores. Macerals are coalified plant remains whose form and/or structure is still preserved in the bituminous-coal stage. The discipline werein coal is studied as a rock constituted principally of macerals is called coal petrology.

Macerals are classified in three main groups: Vitrinite, Exinite (or Liptinite) and Inertinite. The progenitors of each of these constituents occurred in the orginating peat. If a hypothetical peat was metamorphosed to a higher rank coal, the relative maceral constituents would not be changed except for some differential loss of volatile products. However, the extent of the metamorphic alteration would affect the elemental composition and molecular structure of the various organic constituents. Coal may therefore be classified according to petrographic composition (type) and the extent of metamorphic alteration (rank). This means that two or more types of coal with different proportions of maceral constituents are found in the same coal rank and vice versa.

The macerals can be identified by observing a polished coal sample under a microscope. The reflectance of the incident light to the sample is measured with a phototube. Inertinite macerals exhibit bright areas, the vitrinite macerals, the intermediate gray and the liptinite or exinite macerals the dark areas in the photomicrograph of a polished sample.

In the context of relative reactivity, vitrinite and liptinite are

referred to as "reactives" and inertinite macerals are referred to as "Inerts". The reactive macerals are those that decompose when heated to about 400°C in an oxygen-free atmosphere. The inert macerals do not become plastic and evolve less volatile matter than do associated reactive macerals. The vitrinite macerals of a coal contains relatively more oxygen, exinite more hydrogen and the inertinite more carbon. In the higher rank coals, the properties of the macerals differ little and the organic petrography is of less significance.

The reflectants of vitrinite may be correlated with the volatile matter and carbon content of coal. Therefore quantitative determination of the rank of coal by making reflectance measurements on vitrinite is possible.

CHAPTER 4

INFLAME COMBUSTION MEASUREMENTS

4.1. Introduction

The performance of inflame measurements of large pulverised coal flames is a very difficult and a time consuming task. Experimentors have usually resorted to measuring just the exit conditions of large boilers. Others have conducted measurements in small scale furnaces to study the combustion behaviour of a single or a few particles or dilute particle suspensions, for example Howard and Essenhigh (1966 (a),(b)), Essenhigh (1976), Milne and Beachey (1977), Solomon and Colket (1978), Suuberg et al (1978), Mitchell and McLean (1982), Smith (1982), Solomon et al (1982), Timothy et al (1982), Bradley et al (1984), Jost et al (1984), to mention just a few. Data from large scale furnaces which utilise a burner configuration similar to that of the present study have emerged in the main from IFRF and from Smoot's group at Brigham Young University, Utah, USA.

Some of the recent IFRF works include those of Michel and Payne (1980) and Phelan and Bortz (1984) and those of the Smoot's group include that of Asay et al (1983). Of these, Michel and Payne (1980) present comprehensive sets of data for cement-kiln type long flames of zero swirl. Gas-species data in coal flame are provided by Phelan and Bortz (1984) at only a few cross-sections. Large asymmetries in their concentration data is noticeable. Asay et al (1983) provide the data for an unspecified swirl number and the near field data is not reported. These data throw light upon the process of NO_x formation in pulverised coal flames.

Several sets of inflame combustion data are presented in this chapter. The data will enhance further the physical understanding of the process of combustion of pulverised coal and are invaluable for the validation of computer prediction codes. The flow and experimental conditions are outlined in section 4.2, whilst the experimental method and accuracy is described in section 4.3 together with the various practical difficulties encountered which make coal combustion experiments so difficult. In section 4.4 axial gas species concentration and temperature data are presented and discussed for two swirl numbers and two levels of excess air as well as the radial data for the two swirl numbers. An attempt has been made to summarise in section 4.5 the findings of this chapter.

4.2.Experimental Conditions

It is necessary here to describe both the geometrical condition of the furnace and the input flow condition. The geometry of the furnace and the burner as well as the procedures for the calibration of air and coal flow rates have been described in chapter 3. It is worthwhile though to recollect on the choice of the furnace geometry. It is cylindrical, vertically orientated and down-fired so that the 3-D natural convention is minimised to render the flow axisymmetrical 2-D. The mode of firing also facilitates ash-collection. However, some ash is deposited on the furnace walls. The deposition is of two types:- fused-slag deposits and low temperature deposits. The bonding of the fused-slag deposits with the furnace walls is so strong that the deposits may be only removed by chiselling it out or by melting it with a high temperature torch. The coating of slag on the furnace walls which was very uneven, reached an equilibrum thickness of about

12mm. The effect of these deposits on the measurements is discussed in section 4.3.3. Low temperature deposits are weakly bonded to the furnace walls and can be easily removed mechanically. This was the form of the deposits near the relatively cool quarl exit, commonly known as the "eye-brow". During the experiments the quarl exit was kept free of such deposits.

For the purpose of validating mathematical models, knowledge of the inlet flow velocity profiles is ideally required. Because the burner is not easily accessible for probing, the velocity profile at the burner exit was not measured. However, the symmetry of the coal laden primary stream was checked by visually observing its outflow in a perspex enclosure. The outflow of the primary stream was symmetrical as expected because the nearest pipe bend to the burner exit was over 50 pipe diameters upstream. An IFRF variable swirl generator provided the secondary air swirl. The secondary air inlet to the swirler was distributed uniformly by a manifold. The preheat temperatures were measured in close proximity to the burner exit. The primary stream was maintained at 353K and the secondary air stream at 600K.

A United Kingdom Nottinghamshire Gedling coal, rank 802, was used for all the inflame and NO_x emission measurements. Much effort was devoted to obtaining the coal from a seam which was consistent so that future work could be continued with the coal of the same specification. Also the grinding of the coal was carefully supervised so that the coal sample was not contaminated with other coals. The ultimate and proximate analyses of the coal as well as the particle size distribution are provided in Tables 3.1 and 3.2 respectively.

The influence of excess air was studied by firing at 15% and 25% excess air levels, flames S7L and S7H respectively. Two levels of

swirl, S_s = 0.78 and S_s = 1.03 were used to evaluate the influence of swirl.

Table 4.1 provides the input flow conditions. The coal mass loading, $m_{c,p}$, is defined as the ratio of the coal mass flow rate to that of the primary air plus coal mass flow rates,

$$m_{c,p} = m_c/(m_c + m_p) \quad (4.1)$$

R_m is the ratio of the primary stream to secondary air axial momenta,

$$R_m = (m_c + m_p)V_p/(m_s V_s) \quad (4.2)$$

The Reynolds numbers are defined (air only basis) as:

$$Re_p = V_p D_{p,i}/\nu_p \quad (4.3)$$

for the primary air, and

$$Re_s = V_s (D_s - D_{p,o})/\nu_s \quad (4.4)$$

for the secondary air.

4.3 Experimental Methods and Accuracy

The experimental procedures have been described in section 3.6. It remains here to mention the difficulties encountered and to comment on the accuracy and the consistency of the data

4.3.1. Mean Temperature

Thermocouples of 40μm diameter were used for the measurement of mean temperature. The chosen size was due to its adequate mechanical strength to survive the impaction of particles upon it. Positioning of the thermocouples was accurate to within $\pm$ 2mm. Since only the mean temperature was measured, apart from an instrumental error of less than $\pm$ 1% in measuring the emf, the errors originated mainly from the radiation losses and to a lesser extent from the conduction

of heat to the supports of the thermocouple wires. Assuming that: the surrounding furnace walls and the thermocouple bead are grey surfaces; the area of the wall is much larger than that of the thermocouple bead; and that the radiation exchange between the wires and the gases is negligible, the steady state energy equation, Bradley and Mathews (1968) can be written as follows:

$$(2h/r)(T_g - T_t) = (2\epsilon_t\sigma/r)(T_t^4 - T_{wall}^4) - \delta/\delta x\ (k\ \delta T/\delta x) \qquad (4.5)$$

where h is the local heat transfer coefficient, r is the bead radius, T_g is the mean gas temperature, T_t the mean thermocouple bead temperature, ϵ_t the bead emissivity, σ the Stefan-Boltzmann constant, T_{wall}, the mean wall temperature, k the thermal conductivity of the wire, T the wire temperature and x the distance away from the thermocouple junction.

In the absence of the radiation exchange, the error in temperature due to conduction may be deduced from equation (4.5) as

$$\delta/\delta x\ (k\ \delta T/\delta x) - 2h/r\ (T - T_g) = 0 \qquad (4.6)$$

which gives, Eckert and Drake (1959)

$$((Tg - T_t)/T_g) = ((T_g - T_s)/T_g)\ \text{sech}\ (L\sqrt{(2h/rk)}) \qquad (4.7)$$

where T_s is the temperature of the supports and L is the half span of the wire. For the present case, $L = 5 \times 10^{-3}$ m, $r = 40 \times 10^{-6}$m ($\equiv$ 2xwire radius, a conservative value) and using the correlation quoted by Bradley and Mathews (1968) for an assumed minimal local velocity

of 1m/s, h = 1450 W/m^2K. From the correlation of Sato et al (1975), at 1200°C, k_{pt} = 80 W/mK and k_{pt-rh} = 32 W/mK. For a conservative estimate, using the higher thermal conductivity and T_s/T_g = 0.8, the conduction error amounts to 0.3% of the gas temperature. The error in measured temperature due to conduction may therefore be neglected, reducing equation (4.5) to

$$(T_g - T_t) = (\sigma\epsilon_t/h)(T_t^4 - T_{wall}^4) \qquad (4.8)$$

Difficulties in the estimation of the radiation error arise due to the lack of information on the local heat transfer coefficient, complicated also by the time dependency of the thermocouple bead size due to particle deposition, and the effective bead emissivity. Estimates of the radiation error are however presented in Fig.4.1 for the following conditions:

volumetric gas mixture : 15% CO_2, 3.5% O_2 and 81.5% N_2,

mixture properties : evaluated from Brokaw (1961) and Svehla et al (1962),

h: evaluated from $Nu = 0.42\ Pr^{0.2} + 0.57Pr^{0.33}\ Re^{0.5}$ ($0.01 < Re < 10000$, quoted by Bradley and Mathews (1968)).

ϵ_t : 0.3 (larger than that for the wires, Bradley and Entwistle (1961) but less than that for ash, Rizvi (1985)).

The major influence of the size of the thermocouple bead on the radiation error is clear from Fig 4.1. For example by increasing the diameter from 100μm to 200μm, the error increases by a factor of 1.7 when T_t = 1500K and T_{wall} = 1200K.

Bare wire thermocouples also suffer from catalytic activity on their

surfaces. The consequent errors cannot be easily quantified. Since high temperature excursions were not evident in the measurements, the catalytic effects are not dominant in this case. The catalytic effects were observed by Heitor (1985) to be negligible compared to the increase in the radiation loss as a consequence of an increase in the size of the thermocouple.

Suction pyrometers are commonly used for measurements in large scale furnaces but they are not free from any of the above errors. Indeed their performance is somewhat inferior, Attya and Whitelaw (1981)and they tend to block very frequently. More precise and time resolved temperature measurements may be possible by using optical methods; for example the two colour pyrometry, Mitchell and McLean (1982), Tichenor et al (1984) or Raman Spectroscopy, but the instrumentation is expensive and so far it has not been used in large scale furnaces.

4.3.2. Mean Gas-Species Concentration

The ideal sampling technique should isolate a gas volume from the immediate vicinity of the sampling point and prevent any further chemical reaction in the constituents, Tine (1961). The use of solid probes in a fluid stream and the disturbance caused by the suction of a fluid sample in the probe distort the flow pattern of the stream. In this study, the fluid stream is heterogeneous and therefore the requirement of isokinetic sampling is more important. However since the flow is swirling, recirculating and highly turbulent, the concept of isokinetic sampling has little meaning, Bilger (1977). An attempt was nevertheless made to balance the static pressure near the probe tip with that of the furnace.

Quenching of the gas (and particle) samples was by means of dilution

with water. Due to the highly turbulent spray of water in the probe, a fast quenching rate was possible. Furthermore, the large heat capacity of water means only a small temperature rise of the fluid as the hot samples pass through the probe. This method of sampling has been compared with that by means of a water-cooled probe by Hassan et al (1983) and by Lewis and Smoot (1981). The results of both indicate that the gas samples were inadequately quenched in a water-cooled probe compared with those obtained from a water quench probe.

The main disadvantage of using a direct water quench probe is that some gaseous species, for example CO_2 and UHC dissolve in water. The extent of CO_2 dissolved in water was measured by operating the sampling system for a typical condition, see section 3.6.3, and supplying to the probe tip two samples of calibrated gases containing 12% CO_2, and 18% CO_2 in nitrogen. The error in the CO_2 measured was about -3% of the calibration gas. The estimation of the amount of CO_2 dissolved in water is in close agreement with the 4% measured by Lewis and Smoot (1981). The dissolution of a gas in a fluid follows Henry's Law which states that the amount of gas dissolving in a fluid is directly proportional to its partial pressure. The constant of proportionality for CH_4 is two orders of magnitude smaller than that for CO_2. The amount of UHC which dissolved in water is therefore estimated to be negligible. The reduction of the sample volume due to the dissolution of these species resulted in an error of about +1% in the volumutic measurement of all the gas species. Despite these errors, the water-quench probe sampling method was preferred to the water-cooled one because of its self washing nature so that blockages were minimised and because of the rapid quenching of the sampled gas.

Other probe designs for example that of Vranos and Knight (1984) utilises near the probe tip the cyclone principle to separate the particles from the gas to alleviate blockages. However the indirect freezing of the sample by water cooling is likely, as discussed above, to result in inadequate quenching rate. Optical techniques such as Raman Spectroscopy may permit the measurement of time resolved information but this technique is expensive in terms of equipment and man hours of experience, Jones and Whitelaw (1984).
The sampling probe could be located to within ±1mm of the desired position. The instrumental error amounted to less than ±1% of the measured concentration values.The repeatability of the data, refer to section 4.3.3, gives an estimation of the accuracy of the data. Quantitative error analysis is not presently possible because of the lack of the velocity data.

4.3.3. Consistency of Data

The measurements conducted required periods of long durations of furnace firing, typically eight hours a day over a number of weeks. It follows that much care had to be taken as to the material uniformity of the fuel, the consistency of fuel and air flow rates, the preheat temperatures and the geometry and condition of the burner and the furnace. In order to verify the consistency of the measured data from one day to another, the gas-species concentration near the furnace exit was always measured prior to the inflame measurements. A-priory measurement of particle burnout at the furnace exit, typically 98%, permitted the calculation of the theoretical gas species concentration. The disparity between the two in the oxygen concentration was not permitted to exceed ± 10% of its theoretical

value.

The choice of measuring the gas species concentration near furnace exit rather than the measurement of temperature is due to the better sensitivity, especially of CO and O_2 concentrations to the operating conditions. For example, the symptoms of poor combustion and in-leakage of air near the furnace exit would both result in lower temperature. However, the concentration of CO would remain unchanged but that of O_2 would increase from that of the normal operation as a consequence of an in-leakage, and the CO concentration would increase as a result of poor combustion.

The self consistency of the data whereby CO_2 increased when O_2 decreased and vice versa was also checked from their measurements near the furnace exit. Any malfunctioning of the instrumentation could be identified from this test.

Following the above checks, an account of the material balance ($m_{in} = m_{out}$) was made using ash as a tracer. Typically the outflow was deficient by less than 5% of the inflow. However, its calculation involves a number of assumptions and includes experimental errors from the measurements of all the involved quantities. As long as the oxygen concentration at furnace exit was within $\pm$ 10% of its theoretical value, a material balance was not necessary. A heat balance was calculated from the measurement of the cooling water flow rates and the temperature rise as well as the exhaust gas flow rate and temperature. Typically 5% of the heat input was not accounted for.

Any inconsistencies in the gas species concentrations near the furnace exit were most frequently due to inaccurate coal feed rate or the ingress of air. The latter was minimised by maintaining the

furnace pressure at -5mm H_2O. The coal feed rate had to be calibrated from time to time to allow for the changes in its flow properties, see section 3.3. However, on a few occasions, even when the gas species concentration near the furnace exit was consistent, the inflame measurements were not. An example of such an inconsistency is illustrated in Figs. 4.2 (a) and (b). The gas concentration profiles are vastly different from each other. Because the concentration profile, Fig. 4.2.(b), was altered both near the central flame region as well as in the outer region, it was thought to be due to a change in the near-field flow pattern. An inconsistent level of the NO_x emission also reflected the changes in the near-field flow pattern. Furthermore, for the worst inconsistencies, the flame stability performance near the limits were altered as well. The causes of such changes in the flow profile were thought to be due to:

(a) instrumental errors : leakages in the sampling system,

(b) input flow conditions: calibrations, coal type, preheat temperatures, and inlet flow profiles,

(c) the burner geometry : misalignments, position of the primary tube, asymmetrical surfaces or slagged quarl,

(d) the swirler condition : damage, and

(e) furnace geometry : ash-fouled walls or exit geometry.

The instruments were re-checked against the gas chromatograph and the air flow rates were re-calibrated. The coal analyses and the size distribution were re-examined. The swirler was visually checked for any damage or blockage. The burner alignment was visually observed from the furnace exit.

In order to visualise the flow patterns, a small acetylene flame was traversed radially and axially inside the furnace using a water-

cooled probe. This test was conducted for both isothermal conditions and when coal firing. It was observed that the flow was grossly asymmetrical, and three dimensional. For example, forward axial flow was observed near one side of the wall whereas reverse axial flow near the opposite wall. Measurement of velocity under isothermal conditions using hot-wire anemometry revealed that the flow was steady. However, when coal firing, the flow was time-dependent. The periodicity of the flow pattern changes was a variable, sometimes ten minutes, one hour or even a day! Time-dependent rotating symmetrical flows are associated with "vortex breakdown", Harvey (1962), Sarpkaya (1971 (a) and (b)), Faler and Leibovich (1977), Leibovich (1978). Vortex breakdown represents a transition between the rotating flows which do (subcritical) and those that do not (supercritical) exhibit axial velocity reversal.

Time-dependent flow may also be encountered due to the presence of the precessing vortex core (PVC), Syred and Beer (1974). The frequency of the instabilities due to the PVC's for the present combustion situation would be between 10 to 70 Hz, Syred (1985). Therefore flow changes with the long-time periodicity cannot be accounted for by the PVCs. Because steady (with reverse flows) stable running of the furnace was normally possible, the instability was thought to be due to a geometrical change of the burner or the furnace, or due to large in-leakages of air into the furnace. The ingress of air into the furnace was ruled out because of the near atmospheric value of the furnace operating pressure. The walls were deslagged. This did not improve the flow symmetry. Therefore the flow asymmetries were suspected to be due to a change in the burner geometry.

After several experiments, using the acetylene flame flow visualisation technique and systematically varying the important parameters, it was observed that the flow was very sensitive to the alignment of the primary air tube. The overall flow pattern was dominated by the swirling secondary air flow; the flow was also strongly influenced by the non-uniformly deposited slag at the quarl exit (eye brow); and that rough and non-uniform geometrical profile of the divergent section of the quarl resulted in flow asymmetries.

An important observation was made as a corollary of the above experiments. A significant change in the flow characteristics occur due to combustion, Escudier and Keller (1985), Syred et al (1974). When the flow was symmetrical under cold flow conditions, it did not necessarily imply flow symmetry under a combustion situation. The asymmetrical patterns were dependent on the swirl number, the Reynolds number, the primary to secondary air axial momenta ratio, the burner geometry, and the ratio of the mass flow rates of the primary to secondary air.

Flow asymmetry and consequently the lack of repeatability of inflame measurements, may also be detected from inconsistent NO_x emissions. When the concentration profiles were symmetrical about its axis to within $\pm$5% CO_2, $\pm$ 10% O_2 and $\pm$ 20% CO of the ensemble mean values, the repeatability was good (better than $\pm$ 10% of the mean O_2). The larger error band of CO is a result of its lower concentrations.

It is obvious from the above accounts that precise, repeatable experiments in large-scale coal fired furnaces are time consuming and tedious. For example, monitoring of the time-dependent slagging near the quarl exit during coal firing and the subsequent deslagging processes are not without practical difficulties and it may be added

not easy to predict either, by mathematical modelling.

It must be mentioned that due to the inhomogeneous nature of coal, its structure and constituents can differ from one particle to another, Neavel (1981). Furthermore, the grinding process may lead to the segregation of coal constituents with the particle size, Milne and Beachey (1977), Left (1983), Hirji et al (1986). Hence the variation of coal combustion measurements are inevitable and the measurement accuracies that can be achieved for example when gas firing may not be reached.

4.4. Discussion of Results

4.4.1. The Axial Data

Volumetric concentration on dry-analysis basis of CO_2, O_2 and CO for 15% excess air and swirl numbers S_s = 0.78 and S_s = 1.03 are illustrated in Fig. 4.3. The concentration trends for both of these swirl conditions can be summarised as an initial region, X/D_s = 0 to 10, of intense pyrolysis and combustion indicated by steep O_2, CO_2 and CO gradients followed by slower conversion of CO to CO_2 between X/D_s = 10 and 30. The central zone near the furnace axis where the combustion takes place is diluted with the excess oxygen from the outer region of the flame, resulting in a flatter profile as the flow approaches the exit of the combustion chamber. The main differences between the two sets of concentration profiles are that for S_s = 1.03 a more compact reaction zone (characterised by X/D_s where O_2 is a minima) is evident and a larger extent and rate of pyrolysis indicated by steeper and larger concentration of CO.

The effect of excess air on the combustion is highlighted in Fig. 4.4 (a) and (b) for the swirl number S_s = 1.03, and excess air levels of

15% and 25%. A noteable change on increasing the excess air is in the profile of CO. A faster rate of production and decay of CO is evident. The position of minimum O_2 concentration is unchanged from that for λ = 1.15. The change in this CO profile is therefore most probably due to the pyrolysis of coal.

The axial temperature profiles pertaining to the two levels of swirl numbers and the two excess air levels are presented in Fig. 4.5. The obvious effect of the increased excess air resulting in lower temperatures may be clearly observed. Near the burner, steeper temperature rise and higher temperature is reached when S_g = 0.78 compared with that for S_g = 1.03. With the higher level of swirl, the region of more intense mixing and combustion may be occurring away from the axis. At X/D_g > 20 higher temperature is afforded with S_g = 1.03 compared to that for S_g = 0.78 due to the dilution with the hotter products from the regions away from the furnace axis.

4.4.2. The Radial Data, λ = 1.15, S_g = 0.78

Fig 4.6 (a) illustrates the radial concentration profiles for X/D_g = 2.09. These profiles can be conveniently divided into two zones: the inner zone 0 < r < 100mm and the outer zone 100 < r < 300mm. Most of the chemical reactions take place in the inner zone resulting in steep gradient of CO_2 and O_2. The production of CO is either by the pyrolysis of coal, Howard (1981) or by the incomplete mixing-limited combustion of carbon. High and uniform CO_2 concentration in the outer zone is the result of back mixing due to an external recirculating bubble. At X/D_g = 7.45, see Fig. 4.6 (b), the gradients of CO_2 and O_2 span the whole cross-section. The reaction zone is wider due to the expansion of the central jet flow. The CO gradient however is very

steep near the axis and it decays rapidly up to r = 75mm. In this central region of low oxygen concentration, the presence of CO is probably due to the fast reaction C + 1/2 O_2 ⟶ CO and due to incomplete combustion of the released hydrocarbons, although some of it emanates from the pyrolysis of coal. The latter fact is confirmed by the O_2 profile which is not as steep as that of CO in this central region.

The profiles at X/D_s = 12.80 are presented in Fig. 4.6 (c). The trends are similar to those for X/D_s = 7.45. However, the CO concentration at the axis is lower and CO diffuses further outwards from the axis. By X/D_s = 18.16, Fig 4.6 (d), the maximum CO level has dropped to 0.2%. The gradients of CO_2 and O_2 are evident at r < 260mm but flatter profiles of these appear at 260 < r < 300mm. This outer region containing flat CO_2 and O_2 profiles increase in their annular width as X increases. At X/D_s = 23.52, Fig. 4.6 (e), this width is 200 < r < 300mm. The CO level is very low (0.03%), indicating the position of the flame tip. Further downstream, see Fig. 4.6 (f), the profiles of CO_2, O_2 and CO are flatter, approaching plug-flow profiles as the flow nears the furnace exit.

The unburnt hydrocarbons (UHC) profiles are illustrated in Fig. 4.7. The major UHC species in descending order are CH_4,C_2H_4 and C_2H_2. The results are in agreement with the findings of various researchers on the compositions of gaseous products of coal pyrolysis, summarised by Howard (1981), which indicate that methane is a major constituent whilst carbon oxides, hydrogen and light hydrocarbons account for the rest.

The UHC profiles follow the trend of the CO profiles. Maximum levels of UHC, like CO maximum were measured at X/D_s = 7.45. These

observations are compatible with the earlier comment on the existence of CO due to the pyrolysis of coal.

The temperature profiles for various X/D_s are presented in Fig. 4.8. At X/D_s = 2.21 the temperature profile portrays a double-minima trend. The region bounded between 0 < r < 25mm exhibits an increase in temperature associated in the usual combustion terms as preheat and reaction zones. This radial width corresponds to a width of a jet expanding at 10° included angle. The adjacent width from r = 25mm to r = 110mm includes at r = 60mm a second temperature minima. This complicated profile may be explicable by the existence of an annular inner recirculation zone within this radial width. Colder incoming air plus fuel pass through 25 < r < 60mm. At 60 < r < 110mm, the combustion hot products are brought back from downstream. The flat profile at 110 < r < 300mm is a consequence of an external recirculating bubble. At X/D_s = 3.64, Fig 4.8 (b), the temperature profile exhibits one peak only, a typical characteristic of a diffusion flame. A mild temperature gradient exists up to r = 50mm. A steeper gradient is not evident because of the strong radiation exchange between the char particles and the refractory walls which tend to diffuse the temperature gradients.

By X/D_s = 5.07, mixing between the fuel and oxygen at the axis is sufficient to permit their combustion, leading to a steep temperature increase between 0 < r < 50mm. This region is followed by a flat profile up to r = 260mm. There then follows a decrease in temperature up to the wall because of the arrival of the relatively cold secondary air which was deflected outwards due to the swirl.

At X/D_s = 9.00, the central region consists of only a mild temperature gradient; the outer region follows the temperature trend

of the previous profile at X/D_S = 5.07. By X/D_S = 14.36, the temperature profile is flat between 0 < r < 270mm despite the gradients in the gas species concentrations. This further demonstrates the effect of the refractory walls in diffusing the temperature gradients.

4.4.3. The Radial Data, λ = 1.15, S_S = 1.03

The data illustrated in Fig. 4.9 show the trends generally similar to those for S_S = 0.78. Only the main differences between the two are highlighted here. The central reaction zone width at X/D_S = 2.09 is slightly more compact than that for S_S = 0.78. Higher CO_2 concentration is also observed in the outer regions indicating a larger extent of burnout of coal. The CO profile exhibits a maximum at r = 30mm, whereas that for the S_S = 0.78 was at the axis. This is probably due to the stronger swirl used which causes the particles to be flung outward towards the wall.

At X/D_S = 7.45, Fig 4.9 (b) higher level of CO may be observed together with higher and flatter concentration of CO_2 in the outer region compared with the equivalent for S_S = 0.78. This demonstrates the faster production of CO, hence faster pyrolysis (see also Fig. 4.10) and the faster combustion due to better mixing of the fuel and air. At X/D_S = 12.80, Fig. 4.9 (c) much lower (0.45%) CO was measured at the axis compared to 1.15% CO observed for S_S = 0.78. The CO_2 and O_2 profiles are generally flatter and exhibit the effect of higher swirl in the more rapid decay of the species concentration field.

Figure 4.10 exhibits the UHC profiles. As before, the trends follow those of the CO. Maximum concentrations of UHC were measured at X/D_S = 7.45. Compared to the profiles for S_S = 0.78, higher concentrations

of UHC were measured at X/D_s = 2.09 and 7.45 but much lower UHC concentrations were observed at X/D_s = 12.80. This is indicative of faster pyrolysis and also faster decay of gaseous volatile products. Note also that at X/D_s = 2.09 small concentrations ($\simeq$ 30ppm) of C_2H_6 were measured.

4.5. Summary

It is commonly known that combustion measurements of pulverised coal flames are difficult. A few of these difficulties have been highlighted in section 4.3. Horn et al (1966) commented that repeatability tests were not conducted for their measurements. Some authors have mentioned flow asymmetry difficulties associated with a certain burner geometry, for example, Leuckel and Fricker (1976). Others prefer not even to mention such fundamental details about the flow and the repeatability. It is possible that the checks made for the present experiments were not conducted by others or that their flow conditions were perfectly symmetrical. The present data are accurate to within $\pm$ 10% O_2 which is believed the best that can be currently achieved.

The on-axis data have illustrated that increasing swirl results in more rapid evolution of the volatiles and more rapid combustion. Increasing the excess air results in the faster production and decay of CO.

The radial data for S_s = 0.78 and S_s = 1.03 both indicate the penetration of the central primary jet at least up to X/D_s = 2.09. This central flow was probably surrounded by an annular inner recirculation zone. The unburnt hydrocarbons persisted up to X/D_s = 13, the major species being CH_4. An increase of the swirl resulted in

the particles being flung further away from the axis. As expected, a more rapid decay of the species concentration results due to the increase in swirl. The temperature data are informative only very close to the burner. Further downstream the temperature profiles were flat due to strong radiation exchange, although strong gradients of the gas species concentrations were still evident at these locations. The combustion of pulverised coal is, apart from other factors, strongly flow dependent which in turn depends upon the geometries of the burner and the furnace. Also because any two types of coal are rarely identical, the data cannot be easily compared with others. There is a strong incentive therefore to mathematically model the combustion process. The computer prediction codes have to be validated with accurate and preferably 2-D data. For this reason it is expected the data presented here will prove invaluable.

Table 4.1: Run Conditions: Inflame Measurements

$\dot{m}_c$ = 12 kg/hr											
Flame	S_s	λ	R_m	$\dot{m}_{c,p}$	$\dot{m}_p$ kg/hr	$\dot{m}_s$ k_g/hr	V_p (m/s)	V_s (m/s)	V_p/V_s	Re_p	Re_s
S6L	0.78	1.15	0.231	0.303	27.47	103.39	19.7	32.5	0.60	21250	13330
S7L	1.03	1.15	0.231	0.303	27.47	103.39	19.7	32.5	0.60	21250	13330
S7H	1.03	1.25	0.186	0.303	27.47	114.96	19.7	36.2	0.54	21250	14820

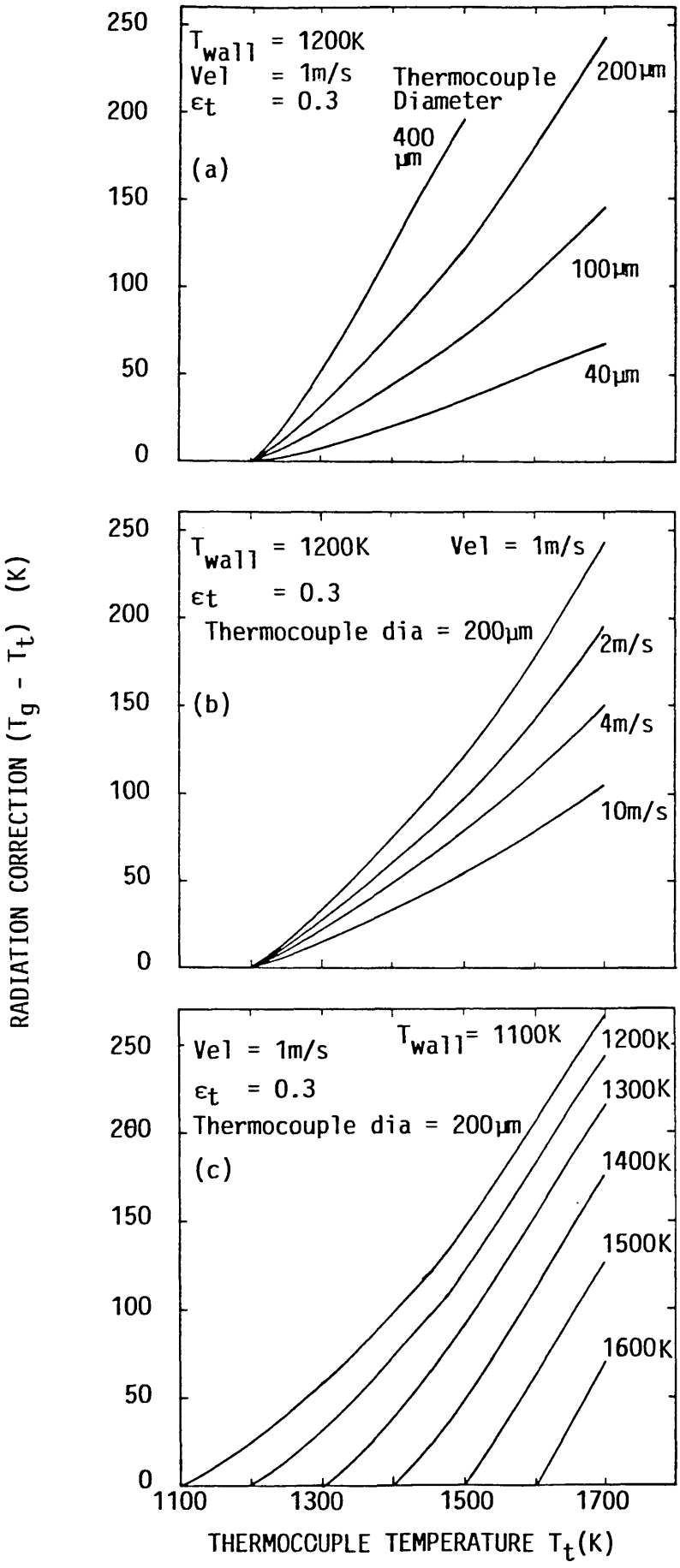


Fig. 4.1 (a) Influence of thermocouple diameter on radiation correction.
(b) Influence of velocity on radiation correction.
(c) Influence of wall temperature on radiation correction.

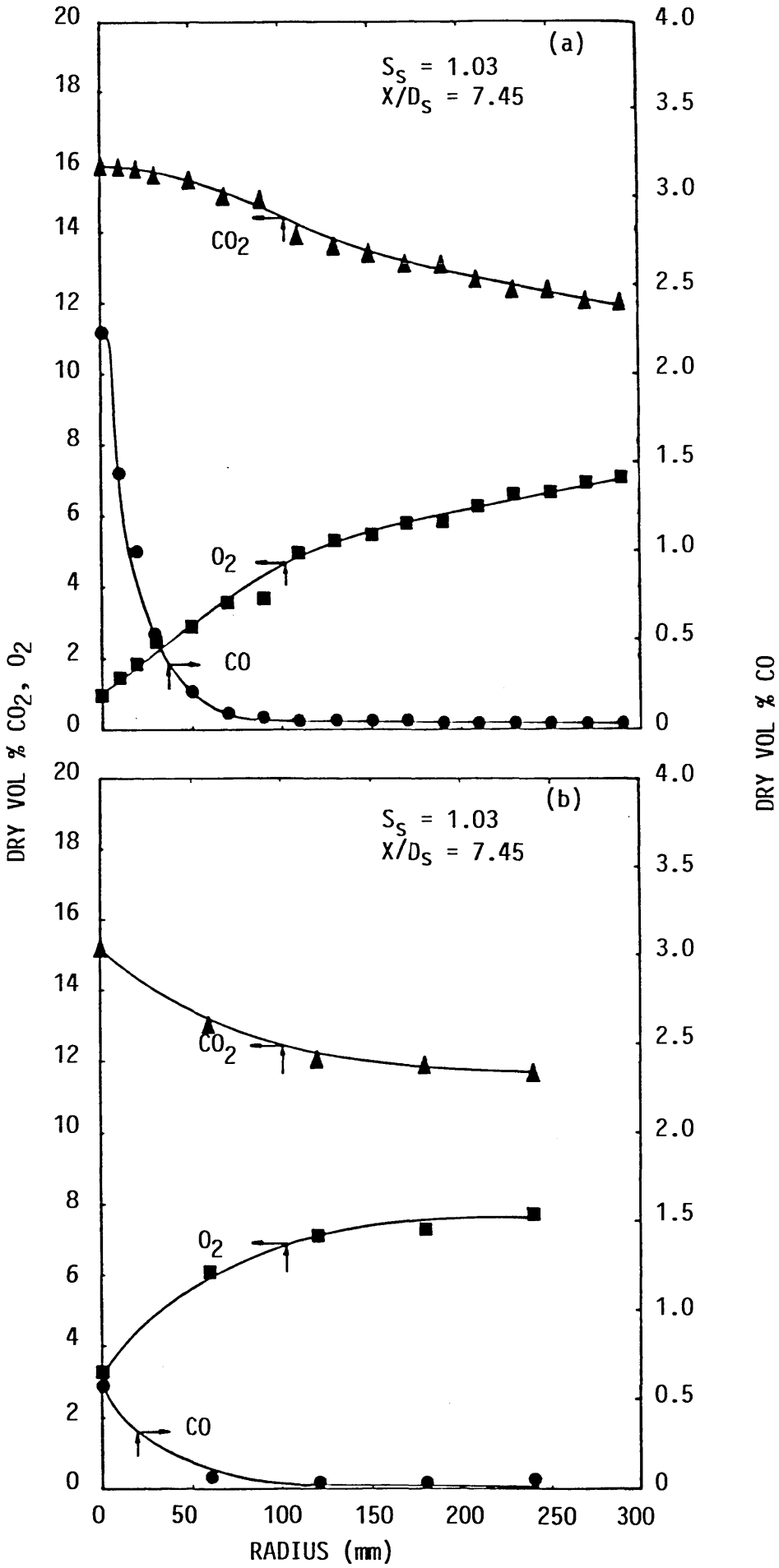


Fig.4.2 Consistency of gas-species concentration data. Radial profile, flame S7L, X/D_S = 7.45.
(a) Flow symmetrical
(b) Flow asymmetrical

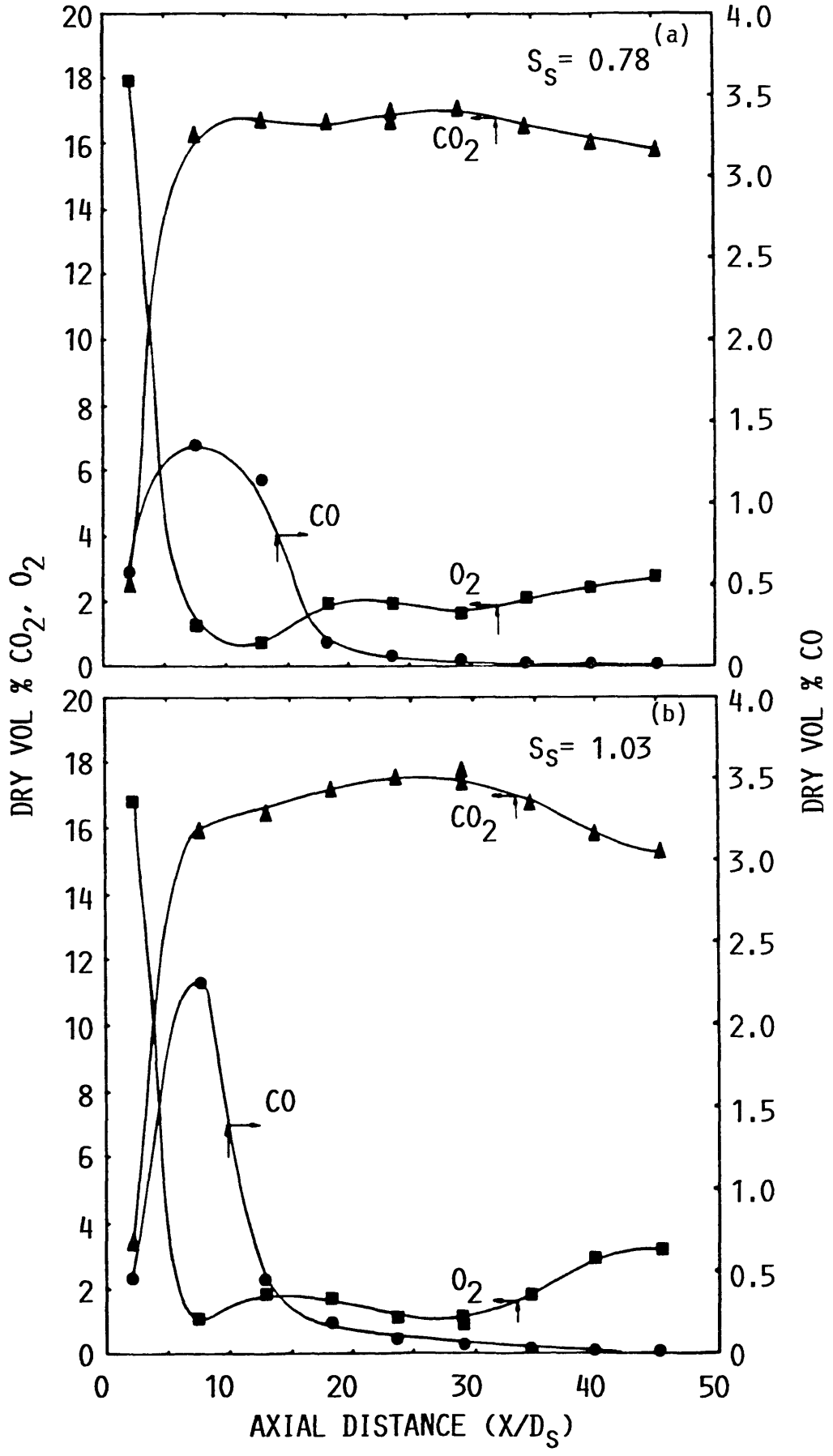


Fig. 4.3 On-axis gas-species concentration profiles. Effect of swirl (15% excess air).

(a) S_S = 0.78

(b) S_S = 1.03

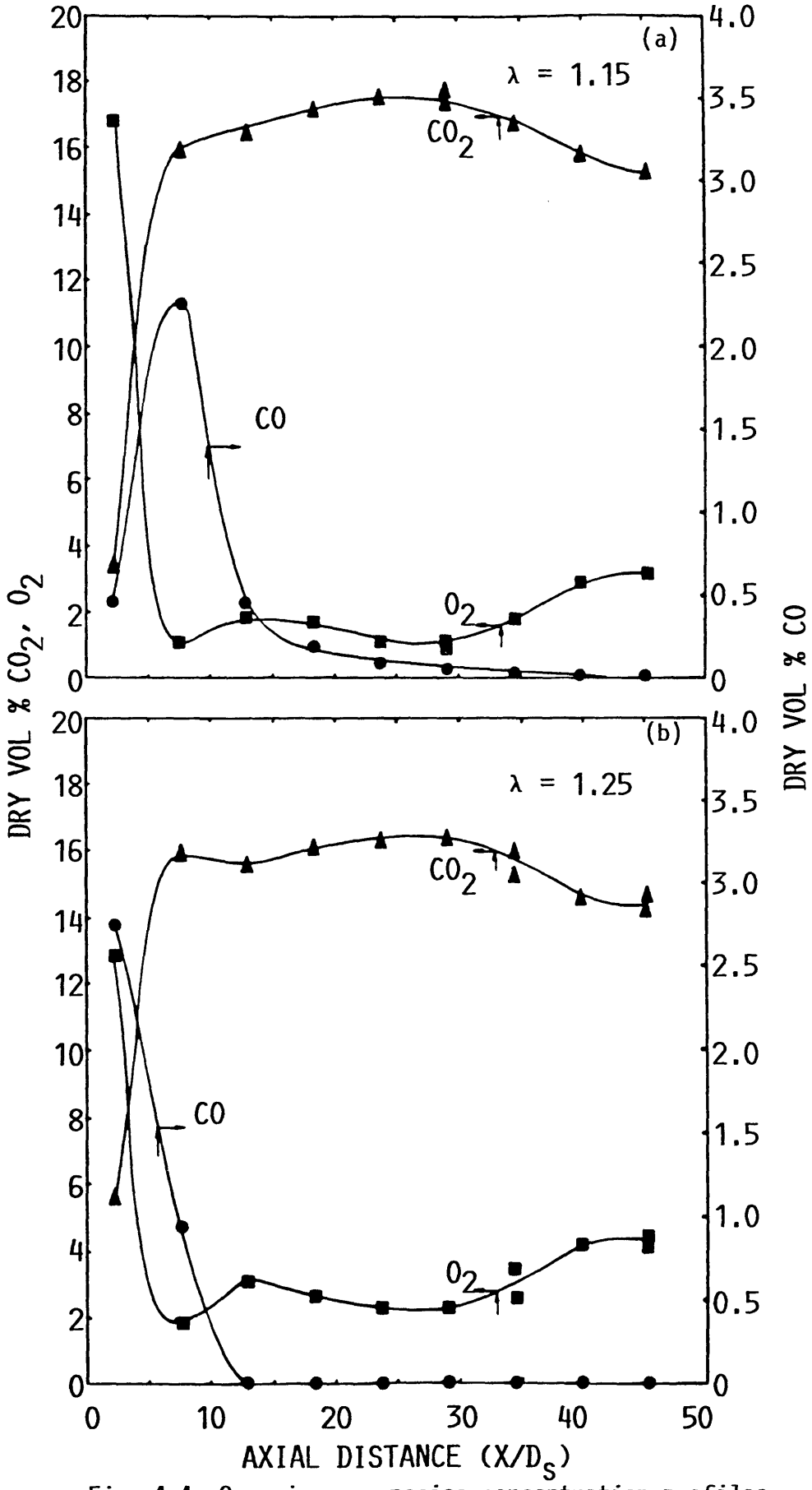


Fig. 4.4 On-axis gas-species concentration profiles. Effect of excess air (S_s = 1.03).

(a) 15% excess air

(b) 25% excess air

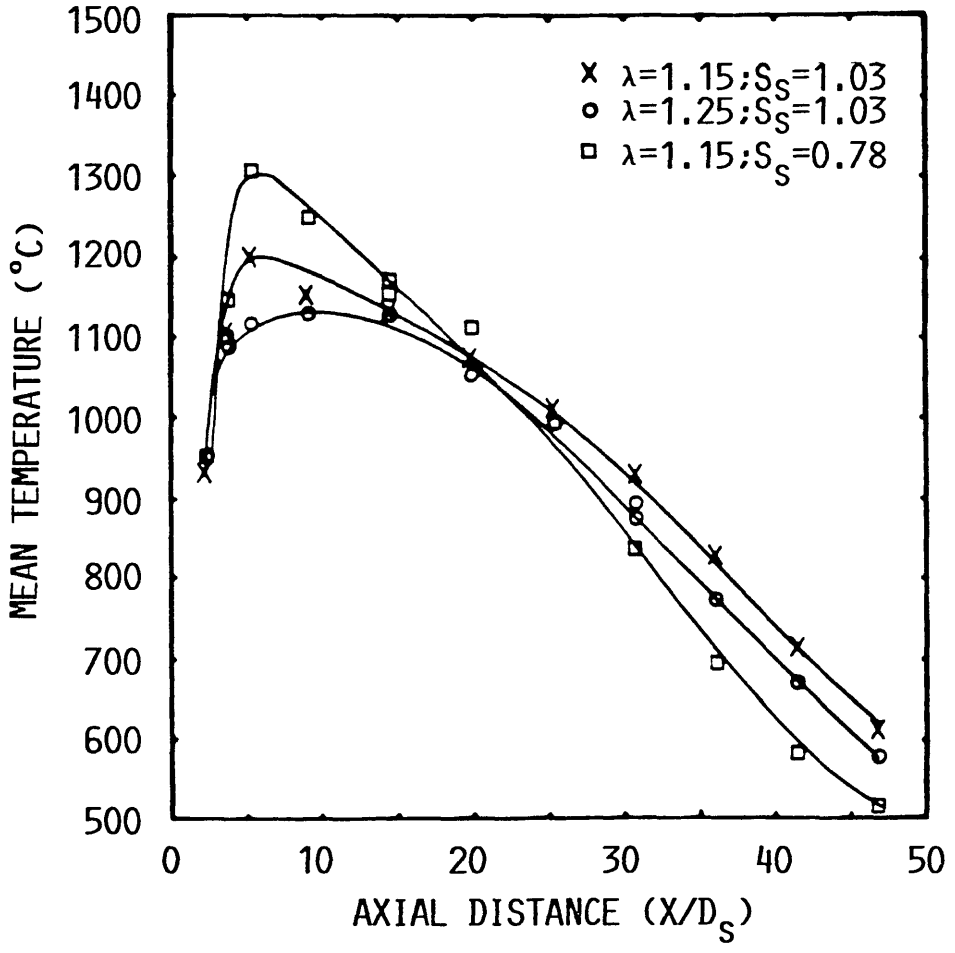


Fig. 4.5 On-axis temperature profiles.

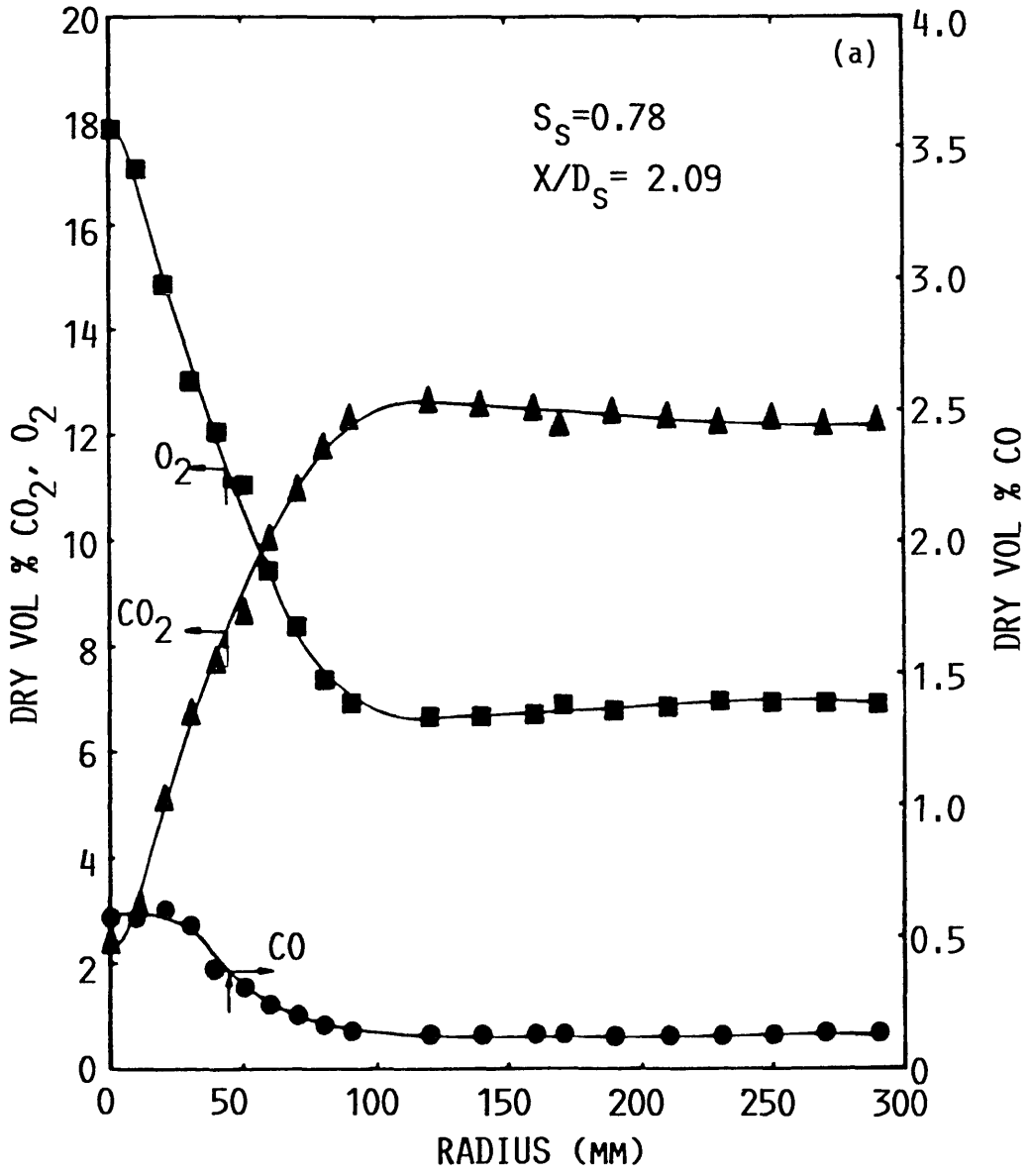


Fig. 4.6 Radial gas-species concentration profiles. Flame S6L, 15% excess air, S_s = 0.78.
(a) X/D_S = 2.09

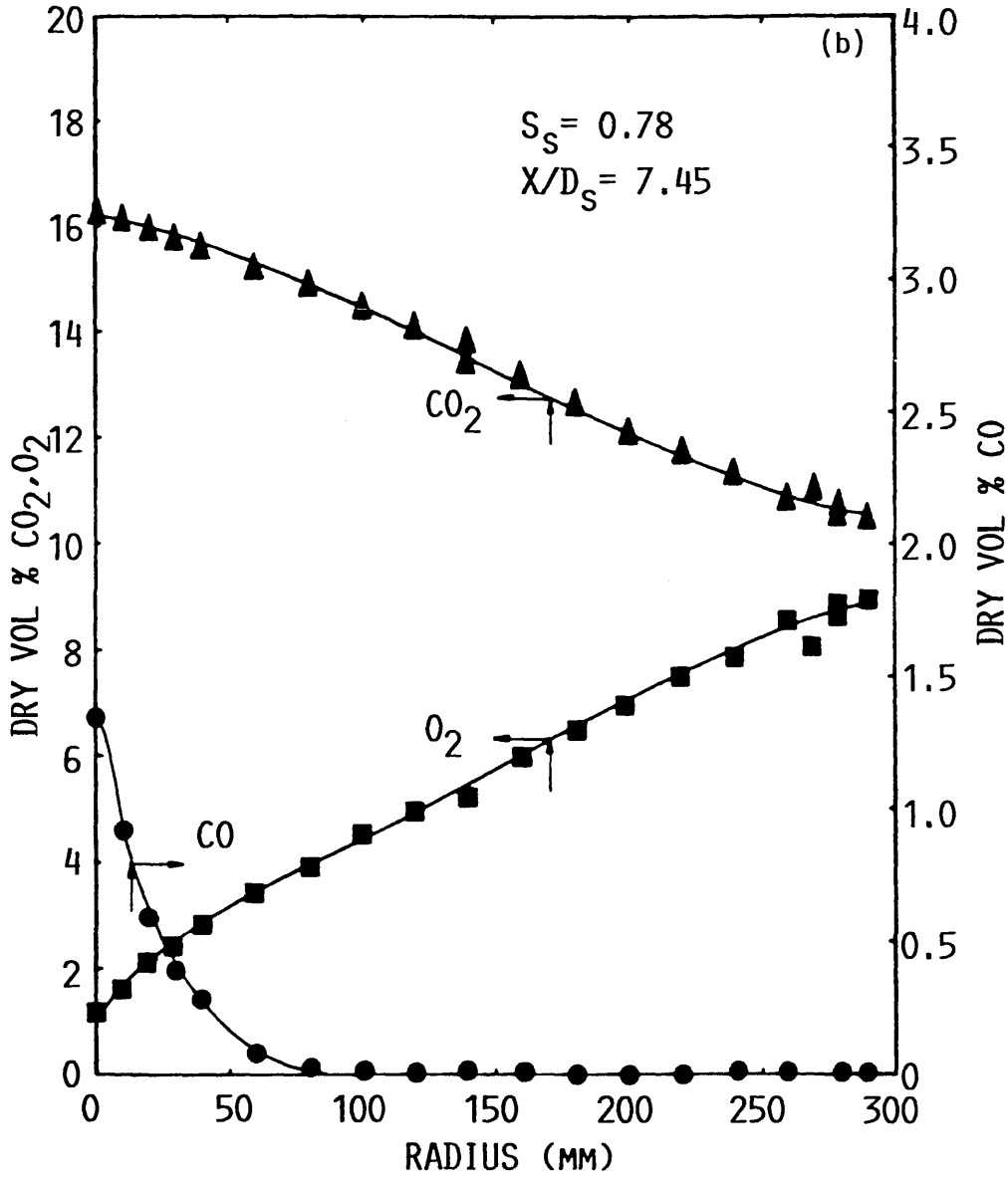


Fig. 4.6 Radial gas-species concentration profiles. Flame S6L, 15% excess air, S_S = 0.78.

(b) X/D_S = 7.45

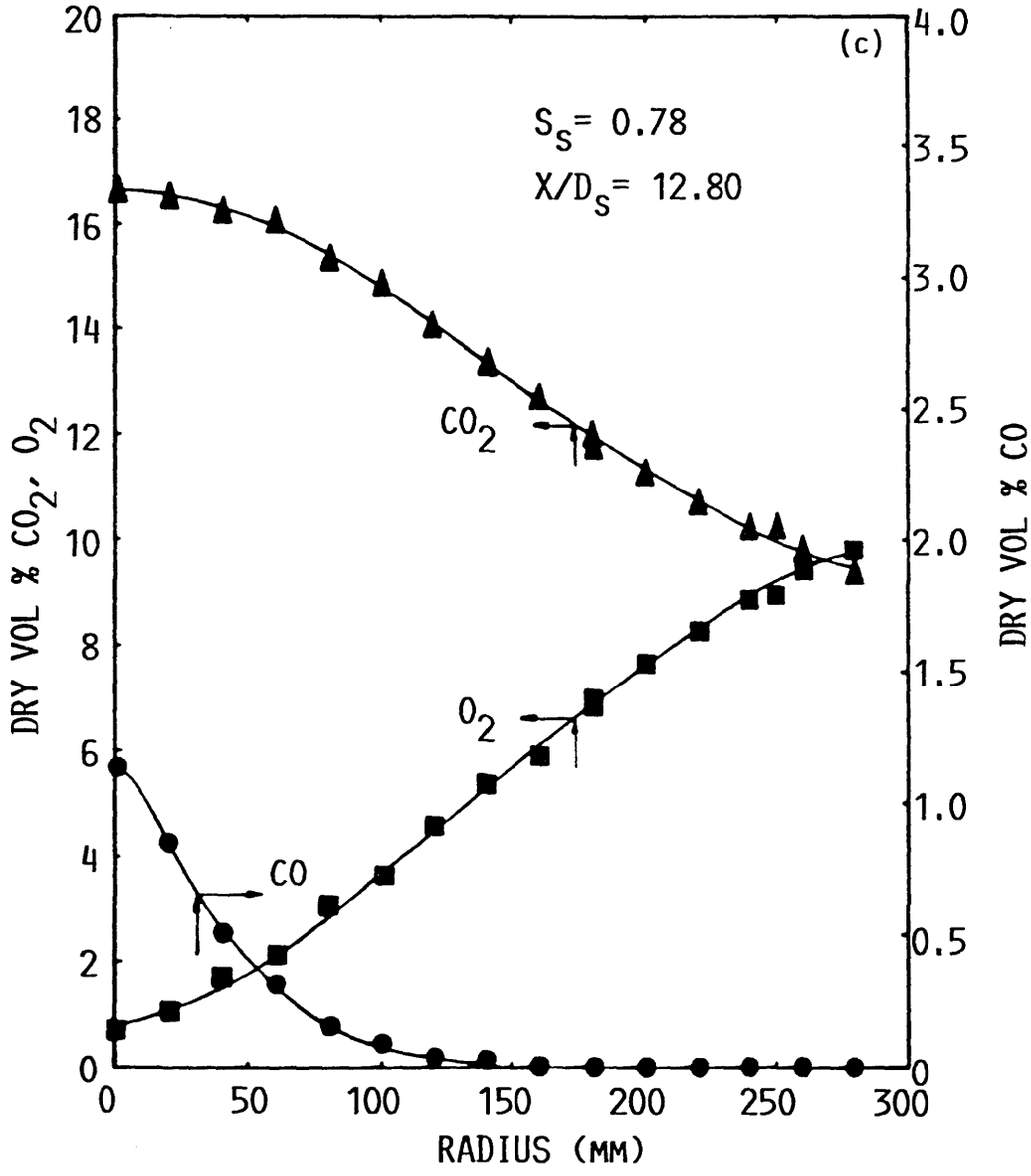


Fig. 4.6 Radial gas-species concentration profiles. Flame S6L, 15% excess air, S_S = 0.78.

(c) X/D_S = 12.80

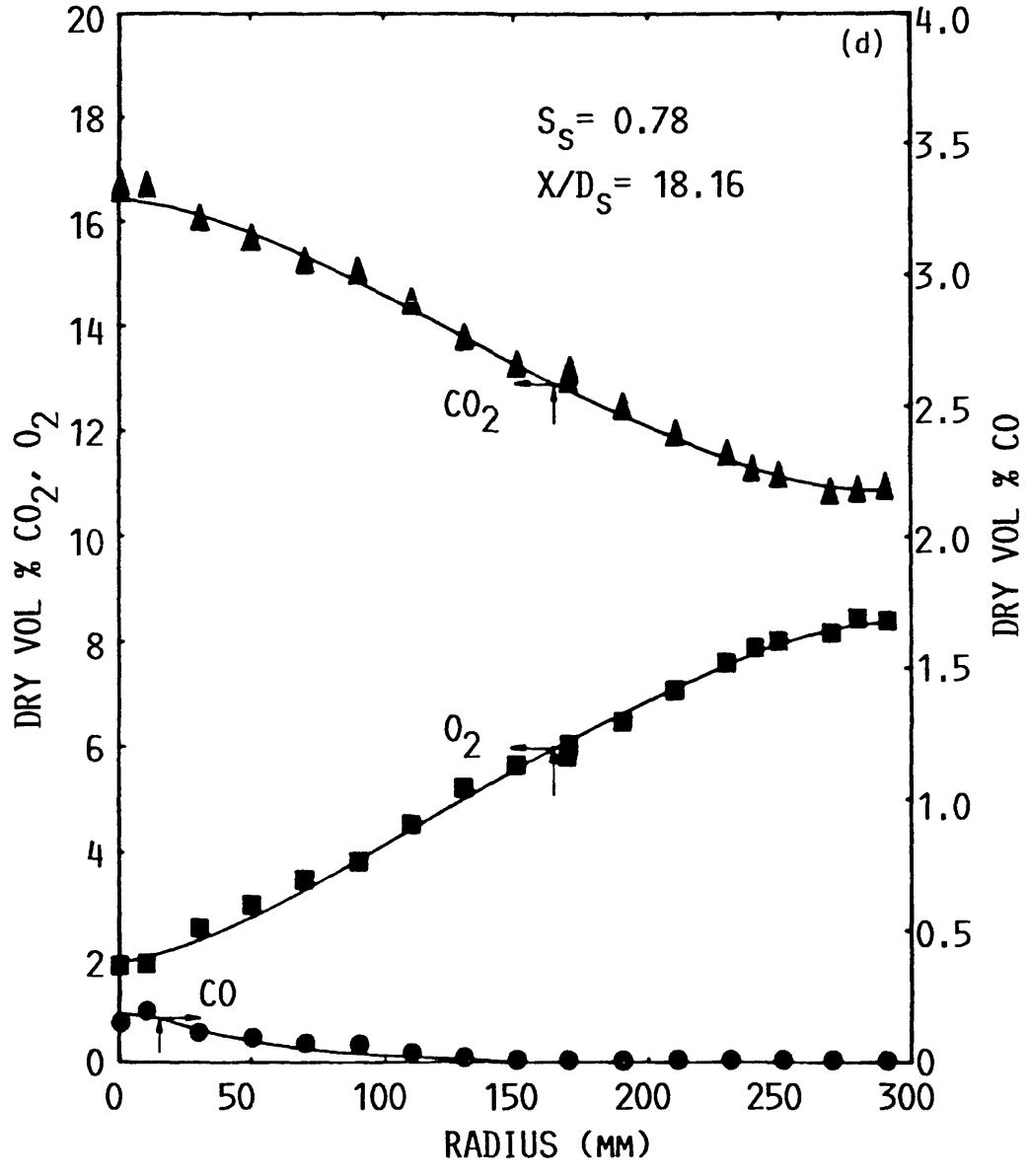


Fig. 4.6 Radial gas-species concentration profiles. Flame S6L 15% excess air, S_S = 0.78.
(d) X/D_S = 18.16

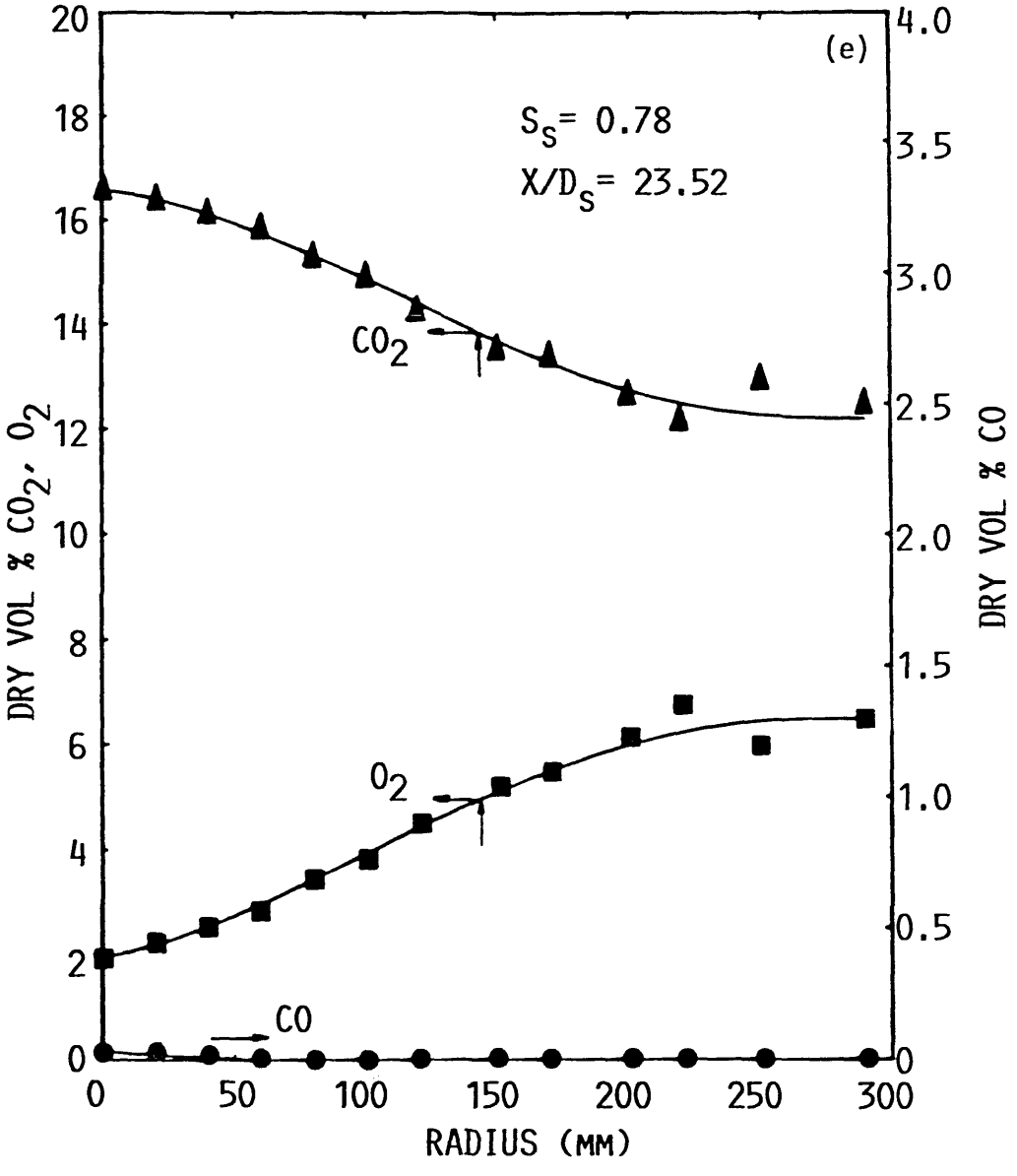


Fig. 4.6 Radial gas-species concentration profiles. Flame S6L, 15% excess air, S_S = 0.78.

(e) X/D_S = 23.52

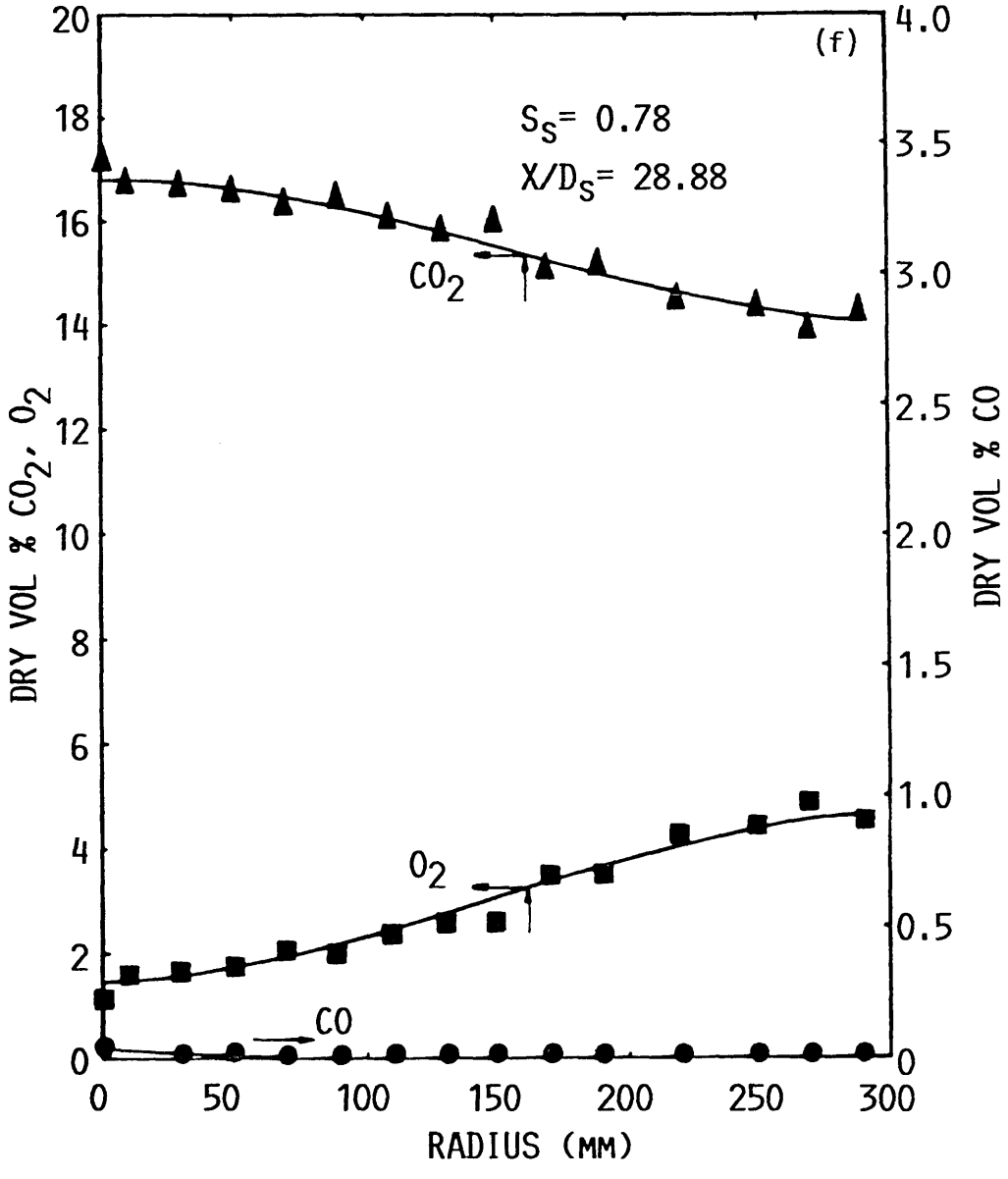


Fig. 4.6 Radial gas-species concentration profiles. Flame S6L, 15% excess air, S_S = 0.78.
(f) X/D_S = 28.88

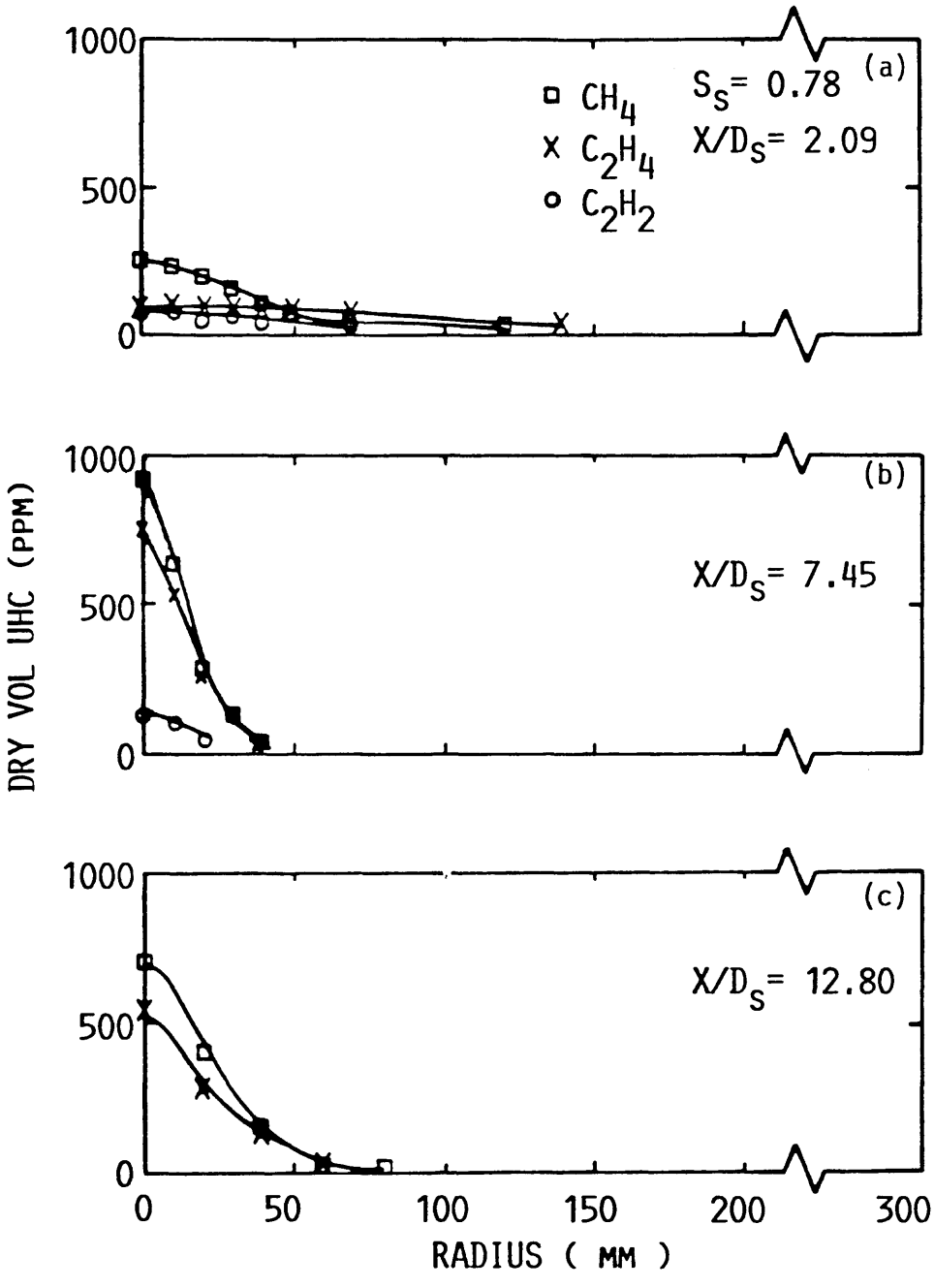


Fig. 4.7 Radial unburnt hydrocarbon profiles. Flame S6L, 15% excess air, S_S = 0.78.

(a) X/D_S = 2.09
(b) X/D_S = 7.45
(c) X/D_S = 12.80

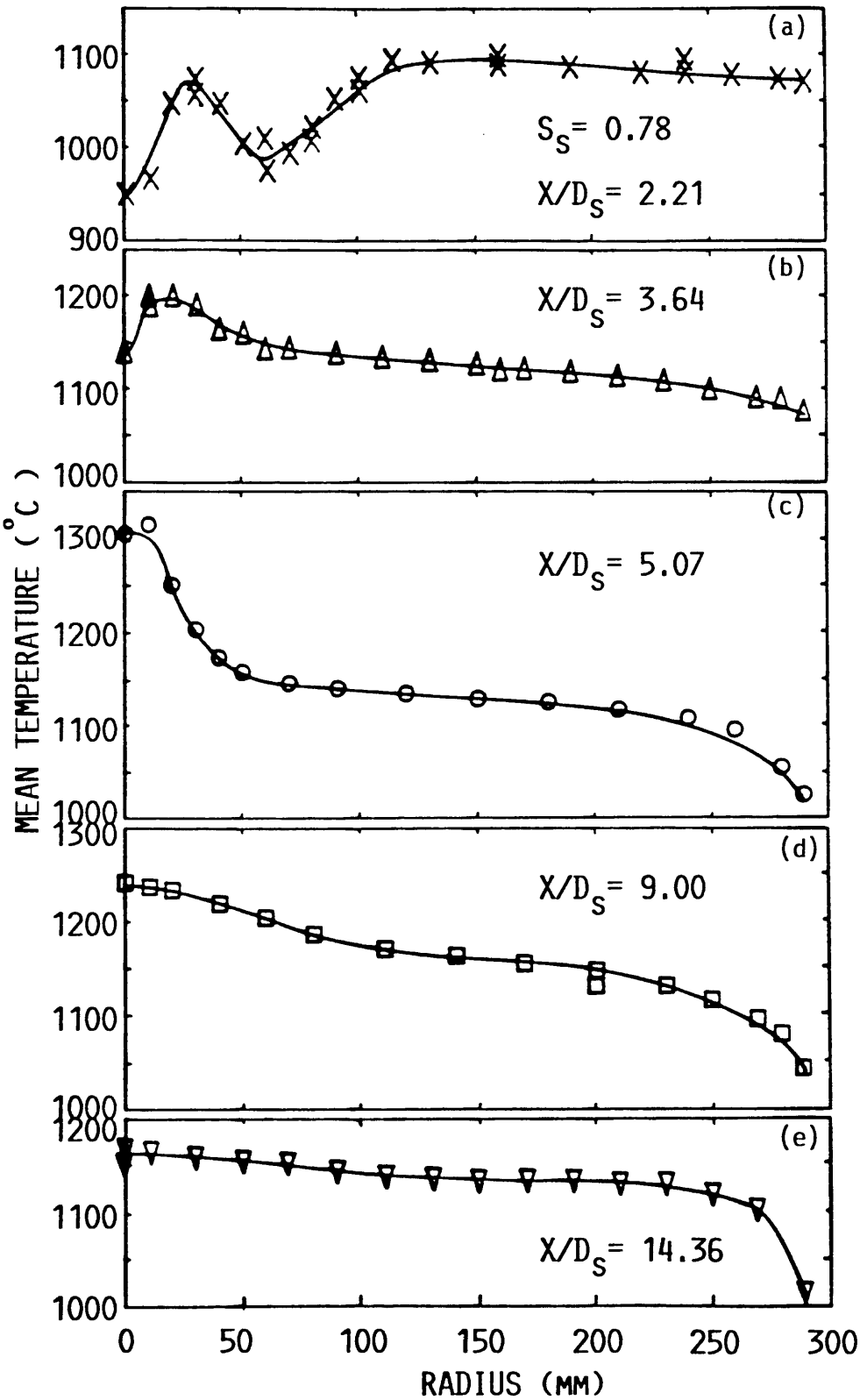


Fig. 4.8 Radial temperature profiles. Flame S6L, 15% excess air, S_S = 0.78.
(a) X/D_S = 2.21
(b) X/D_S = 3.64
(c) X/D_S = 5.07
(d) X/D_S = 9.00
(e) X/D_S = 14.36

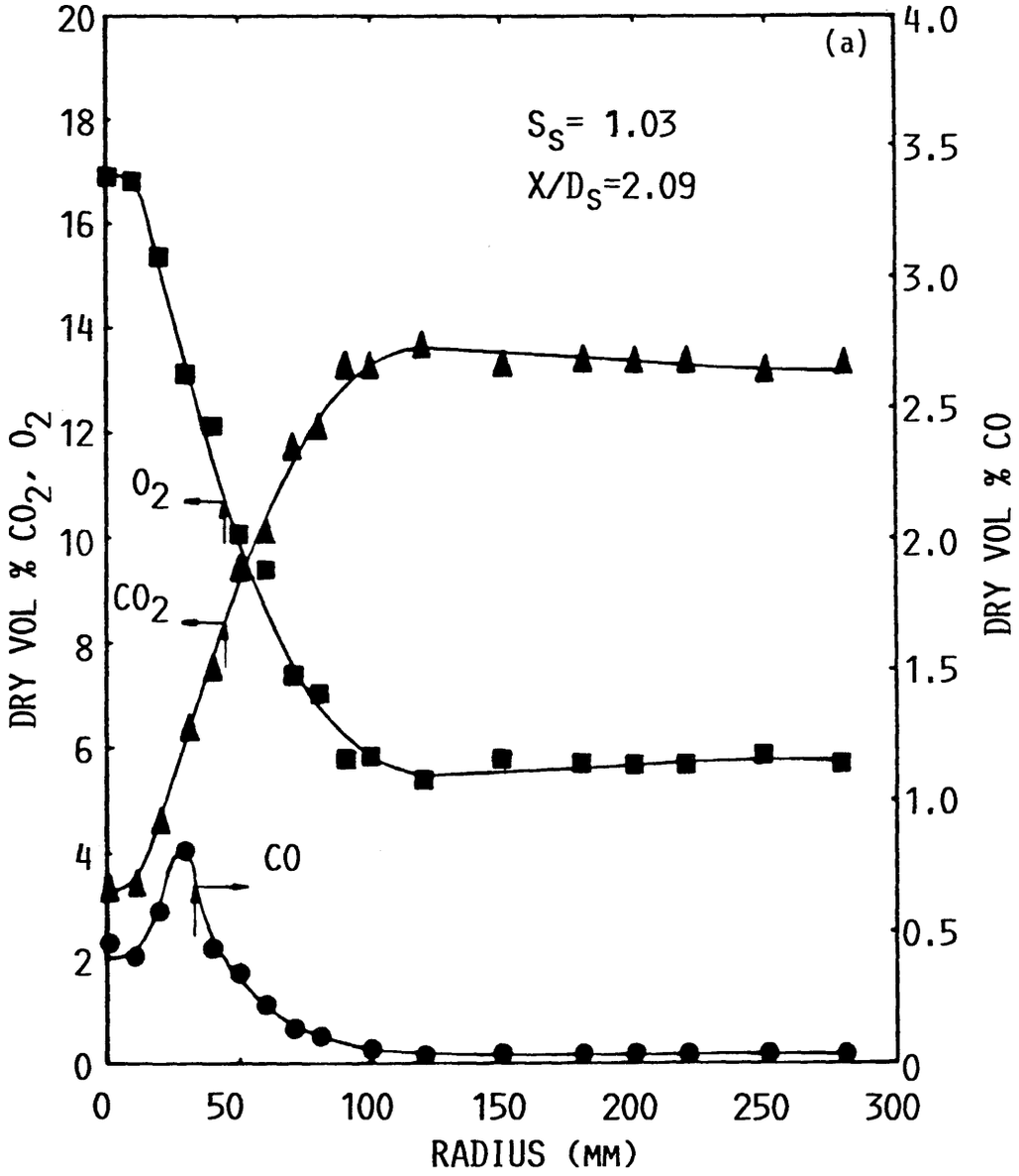


Fig. 4.9 Radial gas species concentration profiles. Flame S7L, 15% excess air, S_S = 1.03.

(a) X/D_S = 2.09

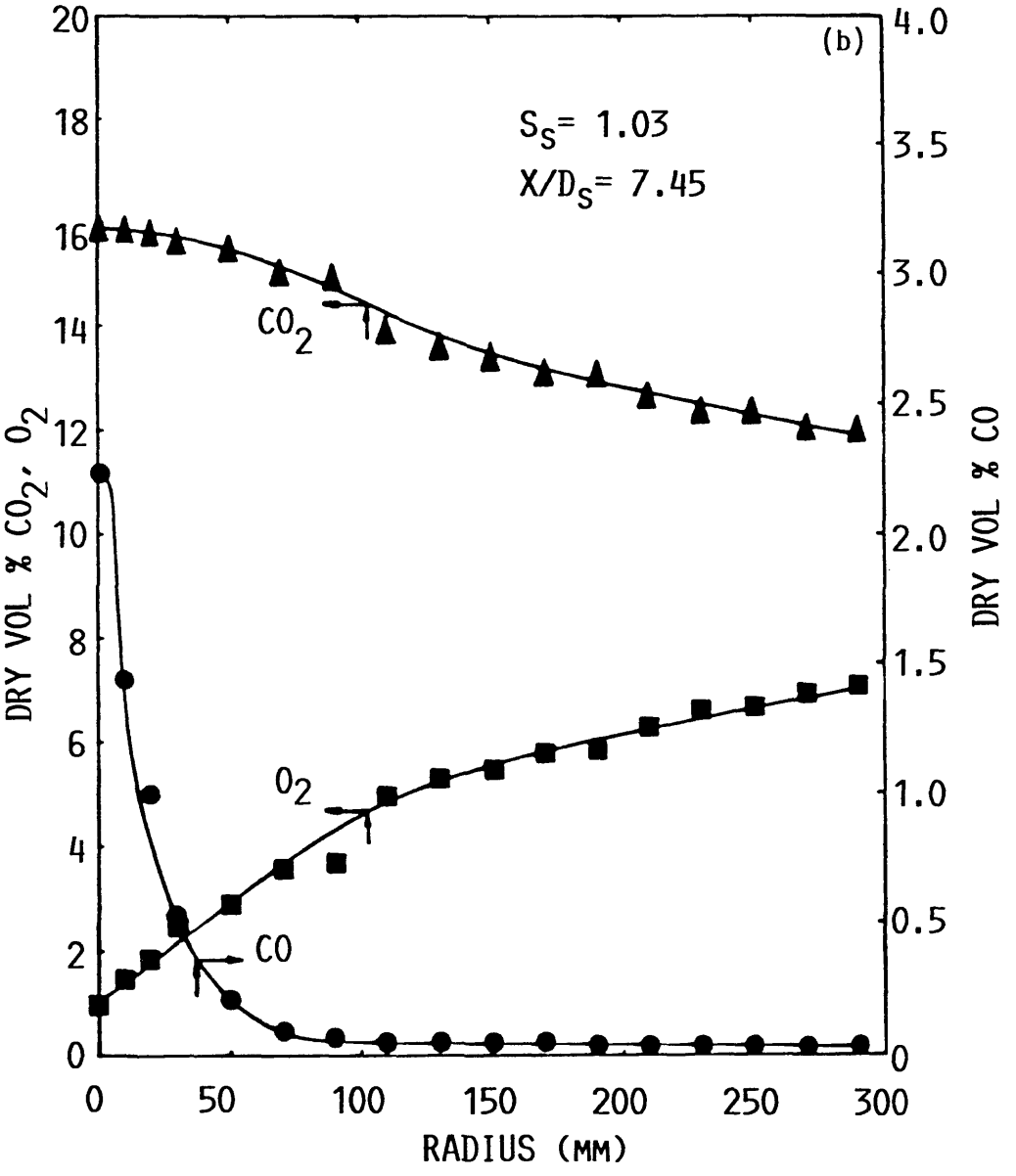


Fig. 4.9 Radial gas-species concentration profiles. Flame S7L, 15% excess air, S_S = 1.03.
(b) X/D_S = 7.45

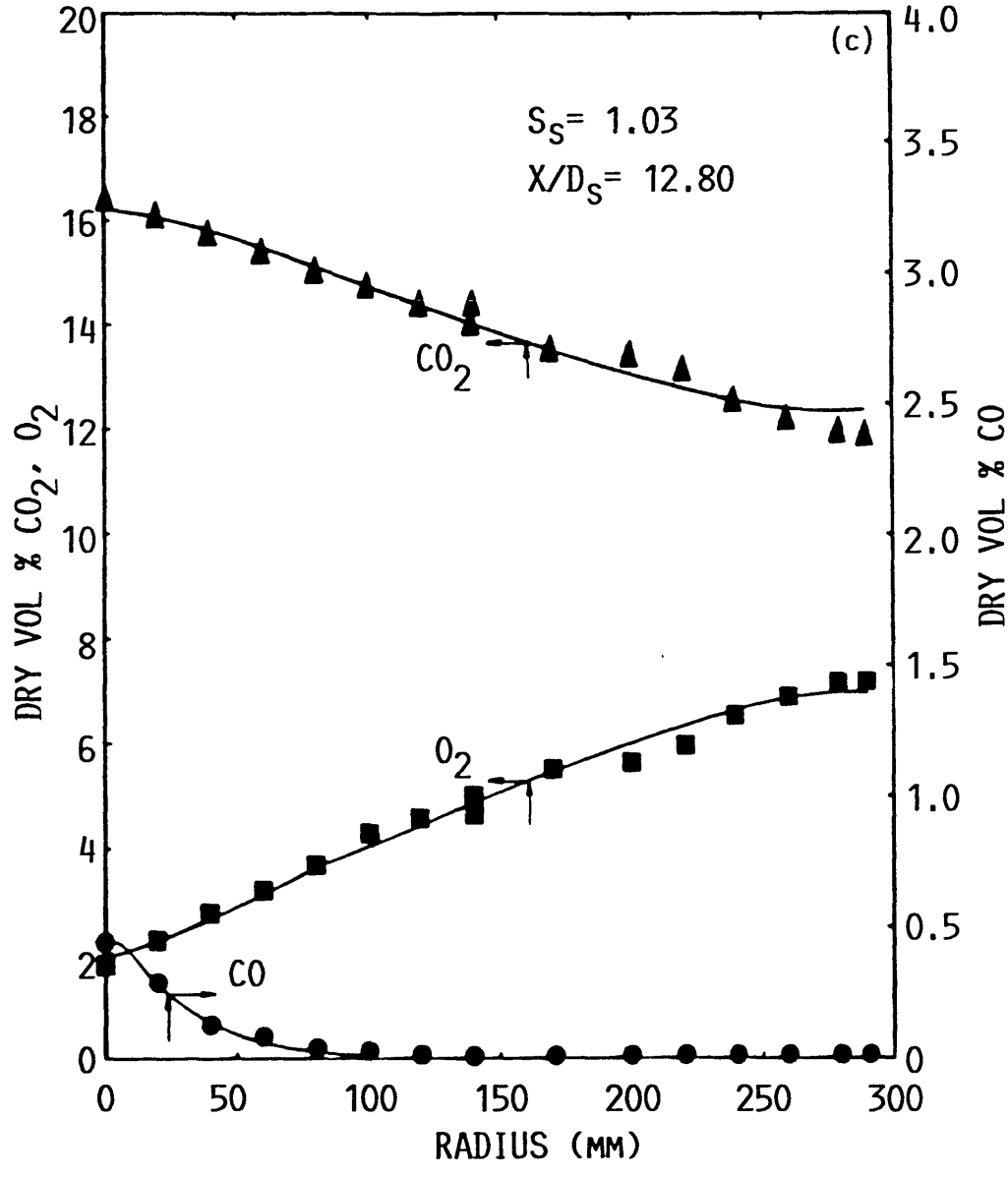


Fig. 4.9 Radial gas-species concentration profiles. Flame S7L 15% excess air, S_S = 1.03.

(c) X/D_S = 12.80

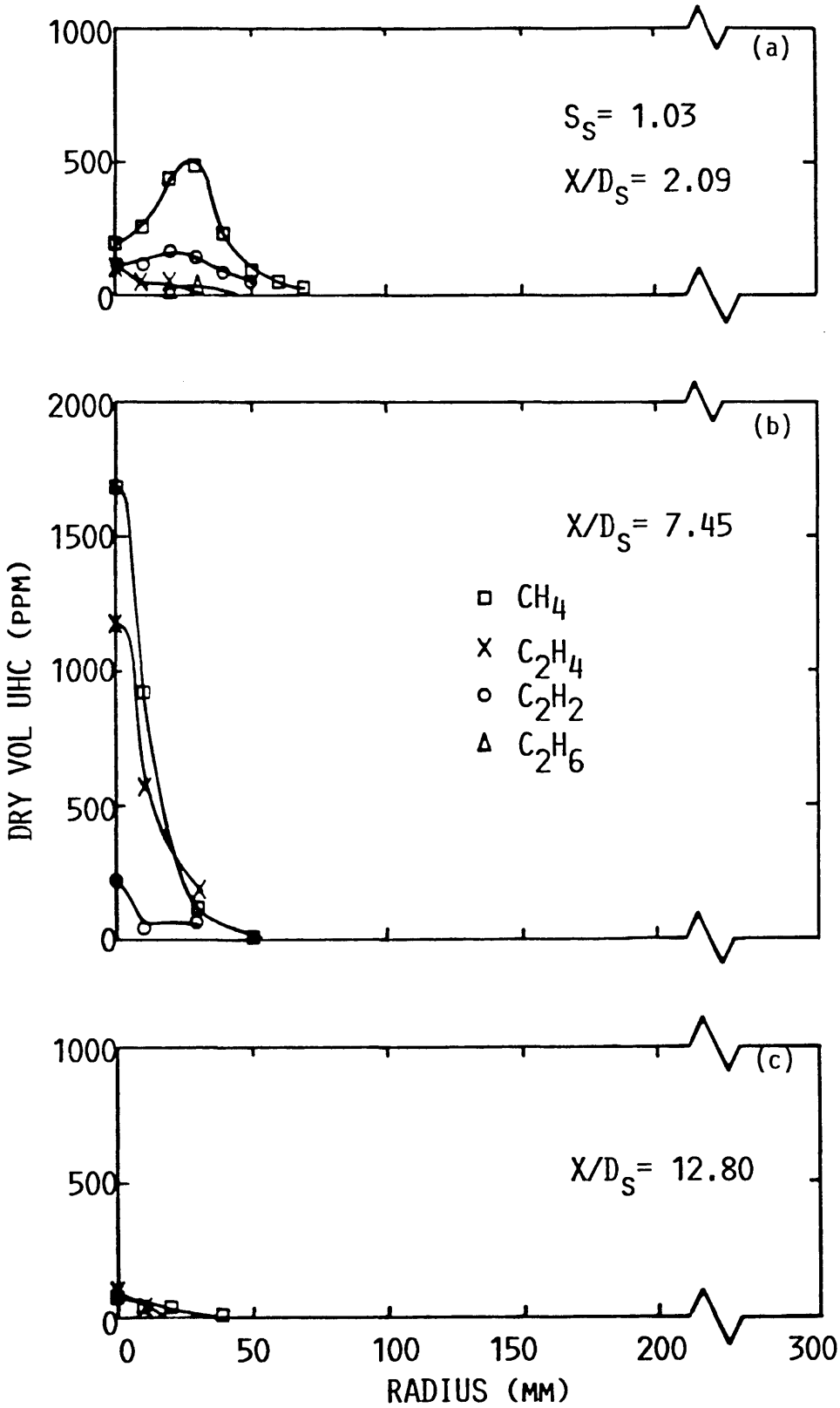


Fig. 4.10 Radial unburnt hydrocarbon profiles. Flame S7L, 15% excess air, S_S = 1.03.

(a) X/D_S = 2.09

(b) X/D_S = 7.45

(c) X/D_S = 12.80

CHAPTER 5

STABILITY LIMITS OF PULVERISED COAL FLAMES

5.1. Introduction

The availability and low cost of coal makes it an attractive energy source for large consumers such as the power generating industry. These users commonly burn coal in pulverised form (pf). One of the several disadvantages of coal fuel compared with the more convenient, but more expensive, oil or gas fuels is the restricted range of burner operating conditions for which stable flames are obtainable. The loss of the burner flames on turn down constitutes an unacceptable dust explosion risk. It is common practice in power stations to "support" pf flames during periods of low burner load by firing oil, or less frequently, gas. This is expensive, and therefore is motivation for new research on the stability of pulverised coal flames.

The literature on the subject is reviewed in chapters 1 and 2. The experimental conditions and procedures are presented in section 5.2. The criterion for flame stability is defined in section 5.3 and the data are presented in section 5.4. Preliminary results and the influence of coal type are discussed in section 5.5. Discussion of the effects of burner load and excess air are presented in section 5.6 and that pertaining to the effects of coal micro-fineness and volatiles content in section 5.7. A summary of findings is provided in section 5.8.

5.2. Experimental Conditions and Procedures

The furnace geometrical conditions and the input flow conditions have been described in section 4.2. The analyses of all the tested fuels

are listed in Tables 3.1. to 3.3. Three series of experiments have been conducted. Test series CT covered three bituminous coal types, each for two firing rates and two excess air levels. For one coal type (Grimethorpe), two finenesses of grind were considered; the coarser grind designated (1) and the finer one as (2). The standard 22.2mm internal diameter central burner pipe was utilised for all the tests. For the South African (B) coal a 31.0mm internal diameter burner pipe was used as well. The run conditions for these tests are listed in Table 5.1. The primary and secondary air exit velocities and the coal mass loading for all the experiments are given in the relevant flame stability graphs. The primary and secondary air temperatures were respectively maintained at 353K and 600K throughout the study.

Test series BL was performed on United Kingdom Gedling bituminous coal to evaluate the effects of burner load and excess air on the burner flame stability. The test conditions for series BL are given in Table 5.2. Test series MS was conducted to evaluate the flame stability performances of microfine Gedling coal and a low volatile char. Due to an instrumentation failure, the primary air was not preheated when firing the microfine coal. Previous sensitivity tests indicated that the lack of primary air preheat has insignificant effect on flame stability. For the char, a 31mm internal diameter central burner pipe was used. The run conditions for these tests are given in Table 5.3.

The experimental procedures have been described in section 3.6. Briefly, the trials were conducted by progressively reducing the secondary air swirl number, all other conditions being maintained constant, until flame lift off, detected both visually and by an

infrared monitor occurred. The flame lift off distance was approximately 100mm from the quarl exit. The repeatability of the experiments is indicated by the cross-hatching on the stability curves. The variance about the curve is due to the hysteresis character of the critical ignition and extinction condtions, Vulis (1961), which is influenced also by the fluctuations in the input flow conditions.

5.3. Criterion for Flame Stability

A stable flame is here defined as one that initiates at or within the burner quarl. It is distinguished from a lifted flame which may stabilize several burner diameters downstream provided that the criteria for ignition are met, otherwise blow-off results. Flame stability is synonimous to the phenomena of ignition and extinction of flames. These are affected in the main by the state of the reactants near the burner.

The ease and speed with which pulverised-coal may be ignited in a turbulent-diffusion flame depends on the 2-phase flow pattern, the extent and rate of mixing between the combustibles and their products, the particle heating rate and the attained particle temperature (therefore the residence time of particles near the burner region), the coal type and the condition of coal. These points have been reviewed in chapter 2. In the near burner region, whether the ignition is due to the gas-phase volatiles combustion or the heterogeneous reaction, for a given coal the speed of combustion is governed almost entirely by the speed of mixing of fuel and oxidant, Thring (1962), Michael and Payne (1980) and Truelove et al (1982).

5.4. Presentation of the Data

A similarity criterion for mixing in confined single non-swirling jets was first derived by Thring and Newby (1952). Beer et al (1963) modified the criterion for double-concentric jets. Steward and Tennankore (1976) used two similarity parameters, the Craya-curtet and the swirl number to represent single swirling jets. Gurac and Ilicali (1981) provide for non-swirling double-concentric burners a similarity criterion based on the Craya-Curtet number. Similarity parameters like those just referred to for particle laden double-concentric burners with swirl have not been reported.

Beer and Chigier (1972) have shown that the swirl number is the significant similarity criterion for swirling flows. Since two jets are utilised in double-concentric jets, the rate of shear at the boundary of the central jet determines the intensity of mixing between the two streams. The mixing will be a function of the velocity ratio of the two streams. Wroblewska et al (1976) successfully correlated for fixed burner geometries the mixing process with the swirl number and the momentum ratio. In order to derive a complete similarity parameter for the combustion of pulverised coal in a double-concentric swirl burner the loading and size distribution of the coal particles in the primary stream as well as the flow characteristic measures of the hot to cold thermal property ratios should also be considered.

For this study, flame stability data are presented, for a fixed burner geometry, constant stoichiometry and heat input, high Reynolds number ($>10^4$), and for specified coal type and conditions, in terms of the secondary air swirl number, S_g, and the ratio of the primary stream (coal plus primary air) axial momentum to that of the

secondary air stream, R_m. These parameters are defined as:

$$S_s = \frac{2G_\theta}{G_{ax}D_s} \tag{5.1}$$

where $$G_\theta = \int_{r=D_{p,o}/2}^{r=D_s/2} (Wr)\rho_s V_s 2\pi r dr \ , \tag{5.2}$$

$$G_{ax} = \int_{r=D_{p,o}/2}^{r=D_s/2} V_s \rho_s V_s 2\pi r dr \ , \text{ and} \tag{5.3}$$

$D_s/2$ = burner throat radius (28mm in this case); and

$$R_m = \frac{(m_c + m_p)V_p}{m_s V_s} \tag{5.4}$$

The inlet flow profiles were not measured so the definition of the swirl number does not include the pressure term, Beer and Chigier (1972). Also uniform axial primary and secondary air velocity profiles were assumed.

A typical flame stability curve, see Fig.5.1(a) is characterised by a minimum limiting swirl number, $S_{s,min}$, and a maximum momentum ratio, $R_{m,max}$, neither of which must be exceeded if a stable flame is to be maintained. For each value of R_m within the stability envelope there exists a critical swirl number, $S_{s,crit}$ below which an unstable flame was observed. Lower critical swirl numbers were generally possible for smaller magnitudes of the momentum ratio, R_m.

The flame root appearance for stable flames was always very luminous and its diameter for a constant R_m was larger at higher values of swirl numbers. As the momentum ratio was increased or the swirl decreased, the flame base was observed to "neck" or decrease in diameter until eventually the flame lifted off. Visible flame lengths

of between 1 to 1.5m were observed, the length increasing more or less linearly with an increase in the burner load. For the primary stream feed system there exists for a given coal loading a minimum primary air velocity below which the pulverised coal was not uniformly transported. This limit was placed for the lower value of R_m for a given coal throughput. The coal mass loading, $m_{c,p} = m_c/(m_c + m_p)$, as well as the primary and secondary air exit velocities for the experimental points have also been marked on the absissa.
Results of the preliminary experiments are presented in section 5.5. The analysis of the results led to further experiments, the results of which are given in section 5.6 and 5.7.

5.5. Preliminary Results and Influence of Coal Type

The results discussed here emerge from the series CT of the tests. The Grimethorpe (1) data are discussed first. Subsequently the results for the other types of coal are compared with the Grimethorpe (1) data.

5.5.1. Effect of Burner Load

The results for the Grimethorpe (1) coal for two firng rates, (heat input values of 98kW and 68kW, see Figs.5.1(a) and (b)) show that at the lower firing rate the $R_{m,max}$ limit is increased. Since increasing heat input in a furnace would result in a decrease in the relative fraction of heat absorbed by the furnace walls by radiation, Thring (1962), that is to have the opposite effect to that observed here, some other factor influences more significantly the flame stability for this case. This factor may be related to the ratio of the particle relaxation time, τ_p, to the fluid particle residence time

scale, τ_g. τ_g may be assumed to be inversely proportional to the primary air velocity. Since the same coal was used for both the tests, the particle relaxation time ($\tau_p = (d_p)^2\rho_p/18\mu_f$ for Stokes flow) remains constant whereas the fluid particle residence time ($\tau_g \propto 1/V_p$) decreases for the higher firing rate, τ_p/τ_g was not maintained constant for these two test cases. The decreasing fluid particle residence time (or increase in τ_p/τ_g), for the higher firing rate resulted in a greater proportion of the coal particles transgressing the near burner inner recirculation zone. In order to maintain the quantity τ_p/τ_g constant for both the cases, the fineness of grind would have to be reduced for the higher feed rate. This was not done here nor is this practical for industrial applications. The effect of burner load is studied in more detail in section 5.6.

5.5.2. Effect of Excess Air

Comparing Figs. 5.1(b) and (c) it is realised that flame stability is enhanced by increasing the excess from 23% to 30%. For enclosed diffusion flames the higher the amount of excess air, the shorter the time taken for fuel particles to find oxygen and hence the shorter the flame length. However, for a given swirl number and momentum ratio, there is a limiting excess air beyond which the fluid temperature drops due to the presence of the diluents,(nitrogen and excess oxygen in the air). It has been observed that for fixed burner and furnace geometries, there are optimum levels of swirl number, momentum ratio and excess air which provide a balance between the recirculating products (higher local temperature) and excess air (higher local oxygen concentration), Hedley and Jackson (1966) and Lenze (1982). For the present study only two levels of excess air

were used and the results show that for the whole range of experimental conditions the higher excess air enhanced flame stability. Further results on the effects of excess air on flame stability are provided in section 5.6.

5.5.3. Effect of Fineness of Grind

Examination of the results for the finer Grimethorpe coal (99 Wt% < 75μm), see Figs. 5.2(a) to (c) shows that the dependencies on firing rate and excess air are the same as those for the less finely ground coal (85 Wt% < 75μm), Figs. 5.1(a) to (c). Comparison of these figures show that increasing the fineness of grind considerably extends the limits of flame stability in terms of both $S_{s,min}$ and $R_{m,max}$. This trend was expected because finer coal particles are able to follow the gas flow more readily, they devolatilise more rapidly, and the diffusion of oxygen to their surfaces is faster. Enhanced flame stability for finer particles (though much coarser than that for present study) was observed also by Beer (1964) for anthracite coal and Chedaille and Hemsath (1965). It must be mentioned that the coal analyses of the finely and coarsely ground Grimethorpe coals, see Table 3.1, differ slightly. This is due to the variability of coal and the consequent difficulty of maintaining batch consistency. Additional results on the effects of fineness of grind are presented in section 5.7.

5.5.4. Effect of Coal Type

The dependencies for both the South Africa (A) and (B) coals, see Figs. 5.3 and 5.4 on firing rate and on excess air are generally the same as for the United Kingdom Grimethorpe (1) coal. The South

African (A) coal performs less well than the Grimethorpe (1) coal. In part this is because of the lower volatiles (30.1% cw 34.6% daf) and higher ash (12.9% cw 7.8%) content of the South African coal. And in part it is because of the coarser grind (78 Wt% < 75μm cw 85 Wt% < 75μm) of the South African (A) coal. In industrial grinding mills it is very difficult to control the fineness of grind for a limited quantity of a coal sample whereas the quantity of coal used for present experiments was too large to grind under laboratory conditions.

The South African (B) coal, in spite of its much higher ash content (42% cw 7.8%) performs very well compared with Grimethorpe (1) coal, see Figs. 5.4(a) and 5.4(c). Although the volatiles content of the South African (B) coal on as received basis is low (19.3%), on a dry-ash free (daf) basis it is higher than that for the Grimethorpe (1) coal (37.6% cw 34.6% daf), hence the improvement of flame stability performance. The enhanced stability Of the South African (B) coal may also be due to the larger amount of finer particles (50 Wt% < 25μm cw 45 Wt% < 25μm). It must be mentioned here that the flame root of this very high ash content coal was not as luminous in appearance as that of the other coals studied and the distinction between lifted and lit back flames was difficult to make. The luminosity in pulverised coal flames is due to the cracking of the devolatilised hydrocarbons. In this case therefore the rate of release of volatiles is probably inhibited by the high ash content in the coal.

5.5.5. Effect of Burner Geometry

The high ash content South African (B) coal burned with increased luminosity when the primary tube internal diameter was increased from 22.2mm to 31.0mm, presumably because of the longer near burner fluid particle residence times. Curiously the stability limits on $R_{m,max}$ are somewhat lower for 23 percent excess air, compare Figs. 5.4(c) and 5.5(b). This may merely be an indication that the choice of R_m as a characterising variable is less than ideal. More importantly it must be observed that stable flames are possible for lower swirl numbers for the larger primary tube, especially for the higher loading, compare Figs. 5.4(a) and 5.5(a).

5.6. Influence of Burner Load and Excess Air

The flame stability data for the test series BL are presented in Figs.5.6 and 5.7 for various coal feed rates and 15% to 25% excess air levels. The United Kingdom Gedling coal was used for all the experiments. This coal was chosen because of the consistency of its properties. The content of these figures is summarised in Fig. 5.8 and 5.9 which portray the dependencies of the limiting values of the minimum swirl number and the maximum momentum ratio on the coal feed rate and on the excess air. The results are discussed in the following two subsections.

5.6.1. Dependency of the Minimum Swirl Number

The limiting value of $S_{s,min}$ at low values of R_m may be linked with the magnitude of swirl required to produce an internal recirculation zone. The value of $S_{s,min}$, see Fig 5.8(a), for the studied range of coal feed rates is between 0.45 and 0.67. It is known that the inner

recirculation zone (IRZ) is established for swirl numbers of this magnitude, Beer and Chigier (1972). Because the flow field was not measured, the precise value of S_s for the formation of an IRZ is not known for the present geometrical configuration, and in any case the presence and characteristics of an IRZ will depend amongst other factors also on the magnitude of the momentum ratio, R_m. The effect of the axial momentum of the central primary jet on the swirling secondary air stream may be taken into account approximately by defining the total swirl number, S_t, as:

$$S_t = \frac{2G_\theta}{(G_{ax,s} + G_{ax,p})D_s} \tag{5.5}$$

which may be reduced to

$$S_t = \frac{S_s}{(1 + R_m)} \tag{5.6}$$

Furthermore, to evaluate the effect of the presence of coal on the flow, the momentum of coal may be deducted from the definition of R_m, and a modified total swirl number, S_t', may be defined as

$$S_t' = \frac{S_s}{1 + R_m(1 - m_{c,p})} \tag{5.7}$$

Plots of the minimum total swirl numbers, $S_{t,min}$ and $S_{t,min}'$ are illustrated in Figs. 5.8(b) and (c) respectively. The trends of $S_{s,min}$, $S_{t,min}$ and $S_{t,min}'$ versus the coal feed rate are similar. The results show the dominant influence of S_s on flame stability and indicate also that at the low magnitudes of R_m, the momentum of coal has a negligible effect on flame stability (hence the flow field). The figures show that increasing the excess air results in only a marginally better stability performance and that there is also a

small but definite improvement of flame stability with increasing the burner load. Stability deterioration at the lower feed rates is most probably due to the rising ratio of the rate of the radiation heat loss to the walls to the rate of the heat release.

This last argument has been roughly demonstrated by a simple model in which it is assumed that the flow in the flame zone well stirred. It is further assumed that, the rate of volatiles release is given by a single reaction model; the mixing and combustion of volatiles is instantaneous; the rate of particle burnout is governed by the combined chemical and physical rates; and since the particle concentration is independent of the firing rate, that the flame emissivity is also constant. Using this model, which is presented in more detail in Appendix 5.A, the ratio R_H of heat radiation to the wall to burner zone heat release was evaluated as a function of the coal feed rate. The result is illustrated in Fig. 5.10. The similarity between the shape of this curve and those of Fig. 5.8 should be noted.

5.6.2. Dependency of the Maximum Momentum Ratio

Maximum possible momentum ratios, see Fig. 5.9, at low coal loads (m_c < 16kg/hr) are small, again presumably due to the relatively high heat losses. However, the initial trend is such that as the coal feed rate is increased from 8 to 16kg/hr, $R_{m,max}$ decreases. A similar trend was also observed in the previous experiments, see Figs. 5.1. Better stability at lower loads is probably due to longer fluid particle residence time in the near burner region due to the smaller inlet velocities. The reader is referred to section 5.5.1 for a more complete discussion. It should also be noted that for these low loads

increasing the excess air adversely affects stability. Since higher magnitudes of velocity were utilised than the case of 15% excess air, shorter fluid particle residence times are to be expected, hence the observed trend.

For the higher loads (m_c > 16kg/hr) these trends are reversed. Stable flames are possible for much higher values of $R_{m,max}$ and $R_{m,max}$ increases very rapidly with increasing burner load. Also, increasing the excess air from 15% to 25% enhances flame stability. The improvement in $R_{m,max}$ may be partially due to the lesser relative amount of heat lost to the walls so that higher temperature of both the fluid and the particles results. Because the chemical reactions are generally described by an Arrhenious type expression (exponential dependency on T), Glassman (1977), then their rates will be enhanced substantially. However, the marked rapid improvement in the $R_{m,max}$ stability limit with increasing load (m_c > 16kg/hr) is more likely to be due to a change in the flow and mixing patterns of the fluid and solid particles flow because the combustion of gaseous volatiles will be limited in the main by the mixing process. Since the flow patterns were not measured, the comments made here can not at present be substantiated.

5.7. Influence of Coal Micro-Fineness and Volatiles Content

The flame stability data (test series MS) for a microfine grind of United Kingdom Gedling coal, and for a low-volatile char (BLVG) are discussed in this section. Since only small quantities of these fuels were supplied, only a few experiments could be conducted. The microfine coal was fired at three coal feed rates, 12.2, 16.3 and 20.4 kg/hr to produce gross heat inputs of 98,130 and 163 kW

respectively. The low-volatile char coded BLVG was fired with 15% excess air but only at 14kg/hr giving a gross input heat of 100 kW. The axial concentration profiles for one of the stable input conditons are also discussed in this section.

Note must be made of the higher ash and lower moisture contents of the microfine coal compared with the normally ground Gedling coal. The changes were doubtless due to the characteristics of the grinding mills used by their suppliers. It is assumed that these descrepancies will not be significantly affecting flame stability. The size distribution of the low-volatile char was much coarser and its ash content much higher than the normally ground Gedling coal. The discussion of the char stability results is in consequence subject to some uncertainity.

5.7.1.Effect of Microfineness of Coal

The stability data for the microfineness Gedling coal are illustrated in Figs. 5.11. These results are summarised in terms of $S_{s,min}$ and $R_{m,max}$ and are respectively presented in Figs. 5.12 and 5.13. Also shown on these two figures are the corresponding results for the normally pulverised Gedling coal, discussed in the previous section. In terms of $S_{s,min}$, see Fig. 5.12, the stability of microfine coal flame is insensitive to coal feed rates between 12 and 20 kg/hr. The magnitude of $S_{s,min}$ = 0.32 is much lower than the equivalent values for the normally ground pulverised Gedling coal. Since the tendency of fine particles to be retained in a weak inner recirculation zone should not be very different from the retention of coarser particles, the reason for the improved performance of the more finely ground coal must be due to faster rate of volatiles release. For such fine

particles, heterogeneous ignition is also possible, and their ignition time is of course shorter compared to the coarser particles. In fact the combustion of the microfine coal is probably limited by the chemical kinetics. Improved ignition characteristics of pulverised coals, although not as finely ground as the present microfine fuel, were also observed by Beer (1964) for anthracite coal and by Chedaille and Hemsath (1965) for bituminous coal.

The microfine coal supports larger values of $R_{m,max}$, see Fig. 5.13, without flame lifting at feed rates of 12 and 16kg/hr. At the highest feed rate of 20kg/hr there is however little to distinguish the performance of the microfine coal from the normal one. This is an unexpected and repeatable result which cannot be explained in the absence of more experimental data.

5.7.2. Effect of Volatiles Content

The performance of the low volatile fuel, BLVG, see Fig. 5.14 (a) is inferior to that of the bituminous coal, Fig. 5.14 (b). Compared with the Gedling coal, higher values of $S_{s,min}$ and lower values of $R_{m,max}$ are necessary to obtain lit back flames. This is in spite of much lower primary stream velocities as a consequence of using the larger central tube for firing the BLVG fuel. Visually, the flame root of this fuel was not as luminous as that of the Gedling coal. This is probably because of the small amount of soot formed with such a low volatile fuel. The influence of the lower volatility of the BLVG fuel is also reflected in the gas-species concentration profiles, see Fig. 5.15 on which the results for the normally pulverised Gedling coal are superimposed. A much lesser amount of CO was produced near the burner, a typical feature of the combustion of coals with little or

no volatiles. The reaction zone length indicated by the axial location at which the concentration of oxygen is a minimum, is longer by more than a factor of two than that for the bituminous coal. The longer reaction zone is due to the longer burning time necessary for heterogeneous combustion, Field et al (1967). Longer flame lengths with decreasing volatiles content of coal were also observed by Loison and Kissel (1962) who studied two coals containing 38% and 9.8% (daf) volatiles. Assuming that the combustion of char is diffusion controlled, then because of its larger particle size distribution, the low-volatile char will require a longer burning time ($t_b \propto d^2$, Nusselt (1924)).

5.8. Summary

Flame stability data for a fixed firing rate and excess air may be plotted in terms of the swirl number, S_s, and the momentum ratio, R_m. The stability plots reveal a minimum swirl number, $S_{s,min}$ below which a stable pulverised coal flame is not possible and a maximum value of the momentum ratio, $R_{m,max}$, beyond which a stable flame is not possible. Preliminary results show that flame stability is enhanced by lowering the inlet primary air velocity (longer residence times), by increasing the excess air level, and especially by increasing the fineness of grind. The performance of the three bituminous coals studied in section 5.5 depended on the volatiles content (daf) and the fineness of grind. The influence of the coal origin on flame stability can not be evaluated because of the large differences in their ultimate and proximate analyses as well as their size distributions. These preliminary results also indicate a dependency of the burner load.

Further experiments for gross coal heat inputs of between 65kW and 195kW show that the minimum swirl number, $S_{s,min}$, decreases as the heat input increases up to 130kW. Further heat inputs up to 195kW exhibit no influence on $S_{s,min}$. This trend is likely to be due to the increased ratio of heat lost to the walls to the heat release at low burner loads. The maximum momentum ratio, $R_{m,max}$ values are small for the lower burner loads (< 130 kW) but they increase dramatically with higher loads. An increase in excess air from 15% to 25% generally enhances only marginally the stability limits.

The firing of the microfine coal resulted in much enhanced flame stability in terms of $S_{s,min}$ and $R_{m,max}$ because of more rapid release of volatiles and also because of the increased tendency for heterogeneous ignition. However a drastic decline of $R_{m,max}$ was observed as the burner load was increased from 130 kW to 163 kW. This observed trend is probably connected with the complex interactions between the solid particles and the fluid flow near the burner zone.

The stability performance of a low-volatile char was poor even though it was fired at low inlet velocities. The axial concentration profiles show trace quantities of CO near the burner region, a typical characteristic of coals with little volatiles content. They also indicate a much longer reaction zone due to the slower heterogeneous combution and also due to its coarser particle size distribution.

Table 5.1: Run Conditions Test Series CT

	COALS							
	United Kingdom Grimethorpe (1)		United Kingdom Grimethorpe (2)		South African (A)		South African (B)	
	Feed rate* kg/hr	Nominal Excess air %	Feed rate* kg/hr	Nominal Excess air %	Feed rate* kg/hr	Nominal Excess air %	Feed rate* kg/hr	Nominal Excess air %
Primary tube	11.6	30	11.6	30	13.3	30	24.8	30
22 mm	8	30	8	30	9.2	30	24.8	23
ID	8	23	8	23	9.2	23	17.1	23
Primary tube								
31 mm							24.8	30
ID							17.1	23

* The low and high feed rates of coal maintain gross calorific inputs of 68 and 98 kW $\pm$ 6% respectively.

Table 5.2: Run Conditions Test Series BL

United Kingdom Gedling normally ground coal										
Coal feed rate kg/hr	8		12		16		20		24	
Excess air %	15	25	15	25	15	25	15	25	15	25
Gross heat input (kW)	65		98		130		163		195	
Primary tube 22 mm I.D.										

Table 5.3: Run Conditions Test Series MS

	Microfine-Gedling Coal			Low-Volatile char (BLVG)
Fuel feed rate kg/hr	12.2	16.3	20.4	14
Excess air %	15	15	15	15
Gross heat input (kW)	98	130	163	100
Primary tube I.D. (mm)	22	22	22	31

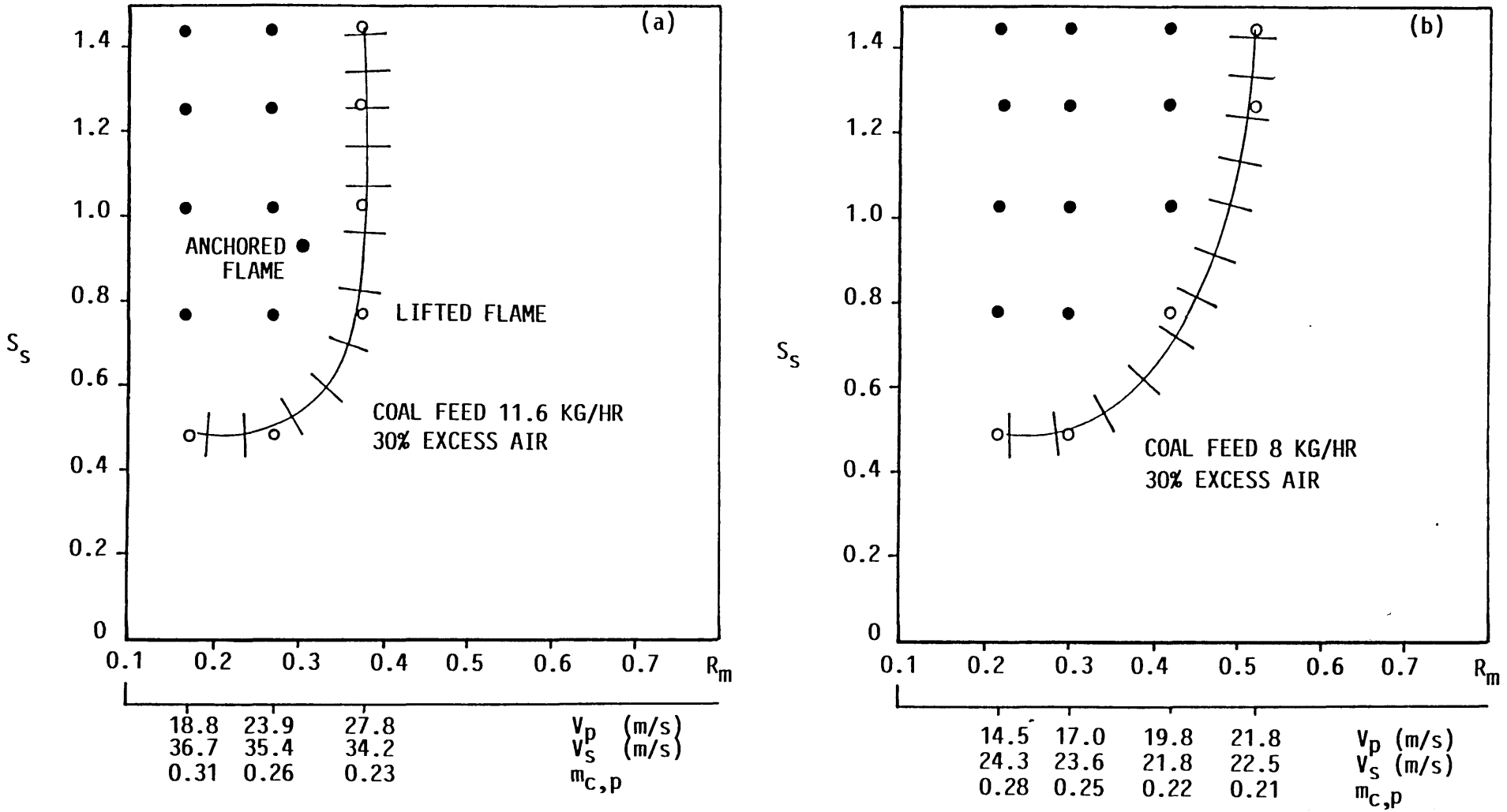


Fig. 5.1 Stability performance of United Kingdom Grimethorpe (1) coal.

(a) m_c = 11.6 kg/hr, 30% excess air
(b) m_c = 8.0 kg/hr, 30% excess air

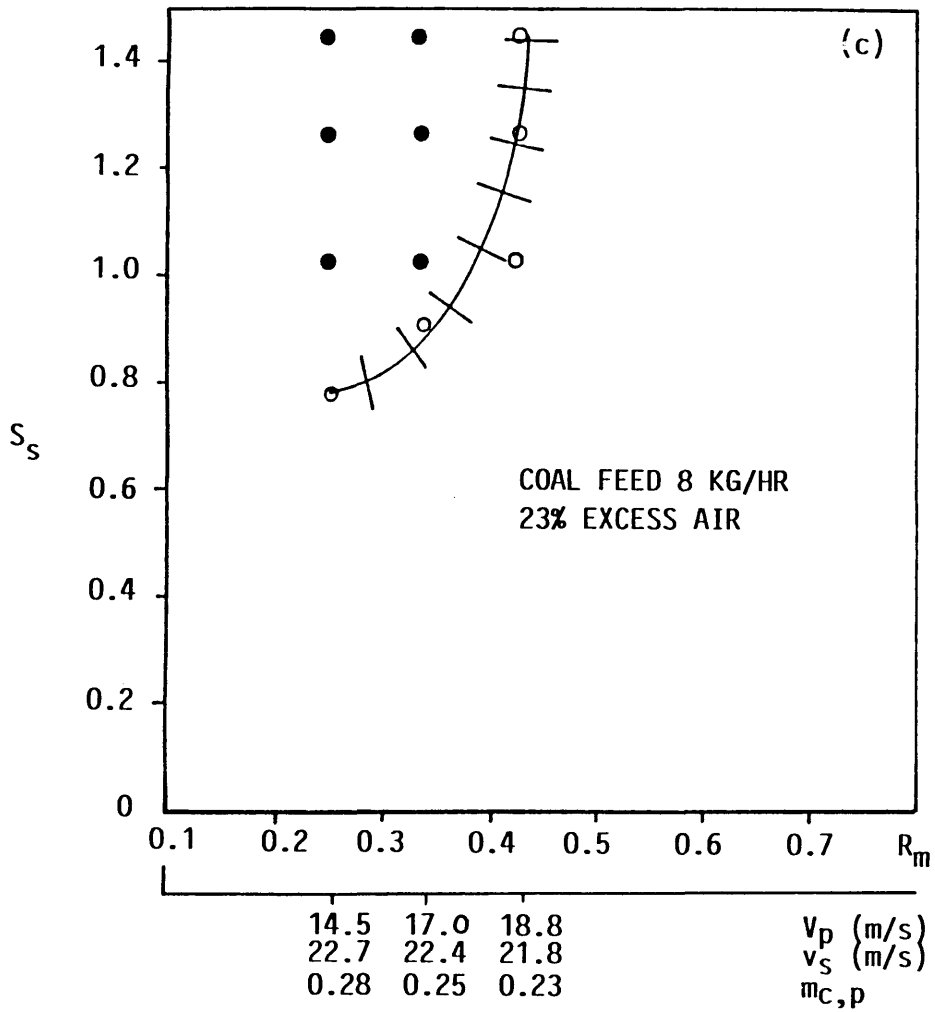


Fig. 5.1 Stability performance of United Kingdom Grimethorpe (1) coal.
(c) m_c = 8.0 kg/hr, 23% excess air

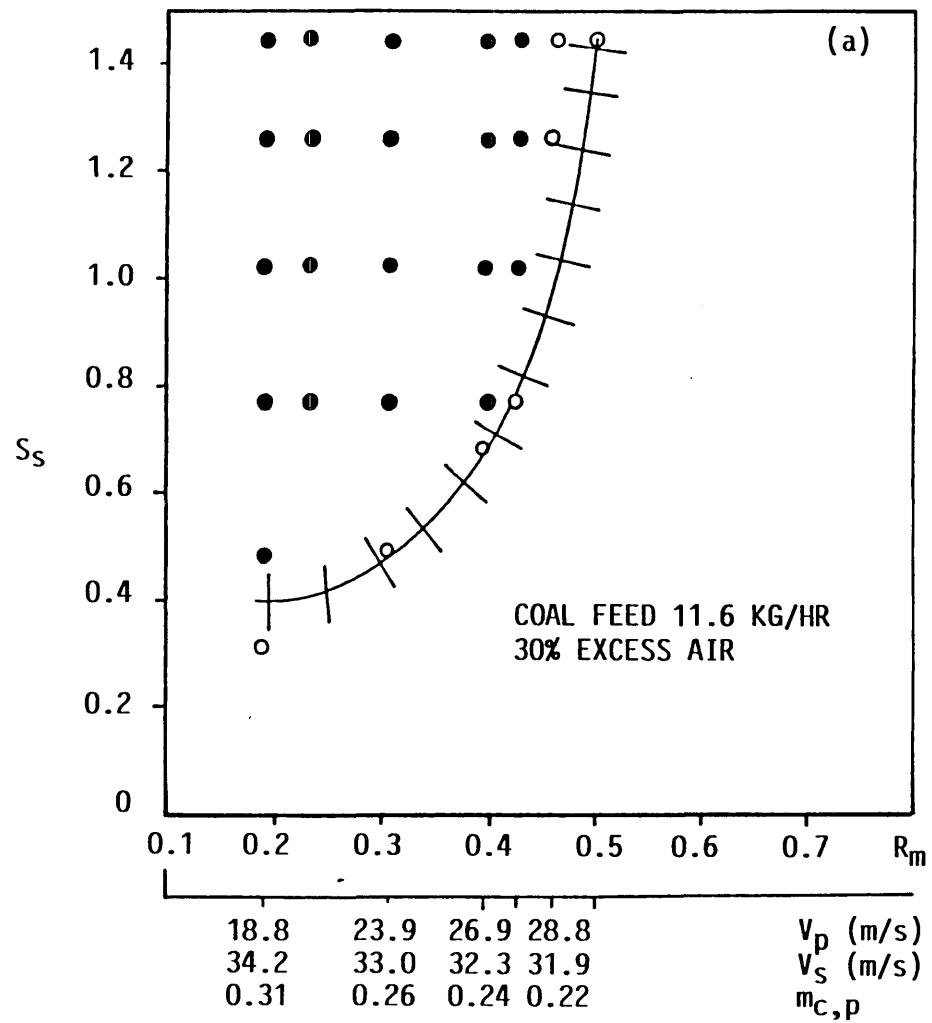


Fig. 5.2 Stability performance of United Kingdom Grimethorpe (2) coal.
(a) m_c = 11.6 kg/hr, 30% excess air

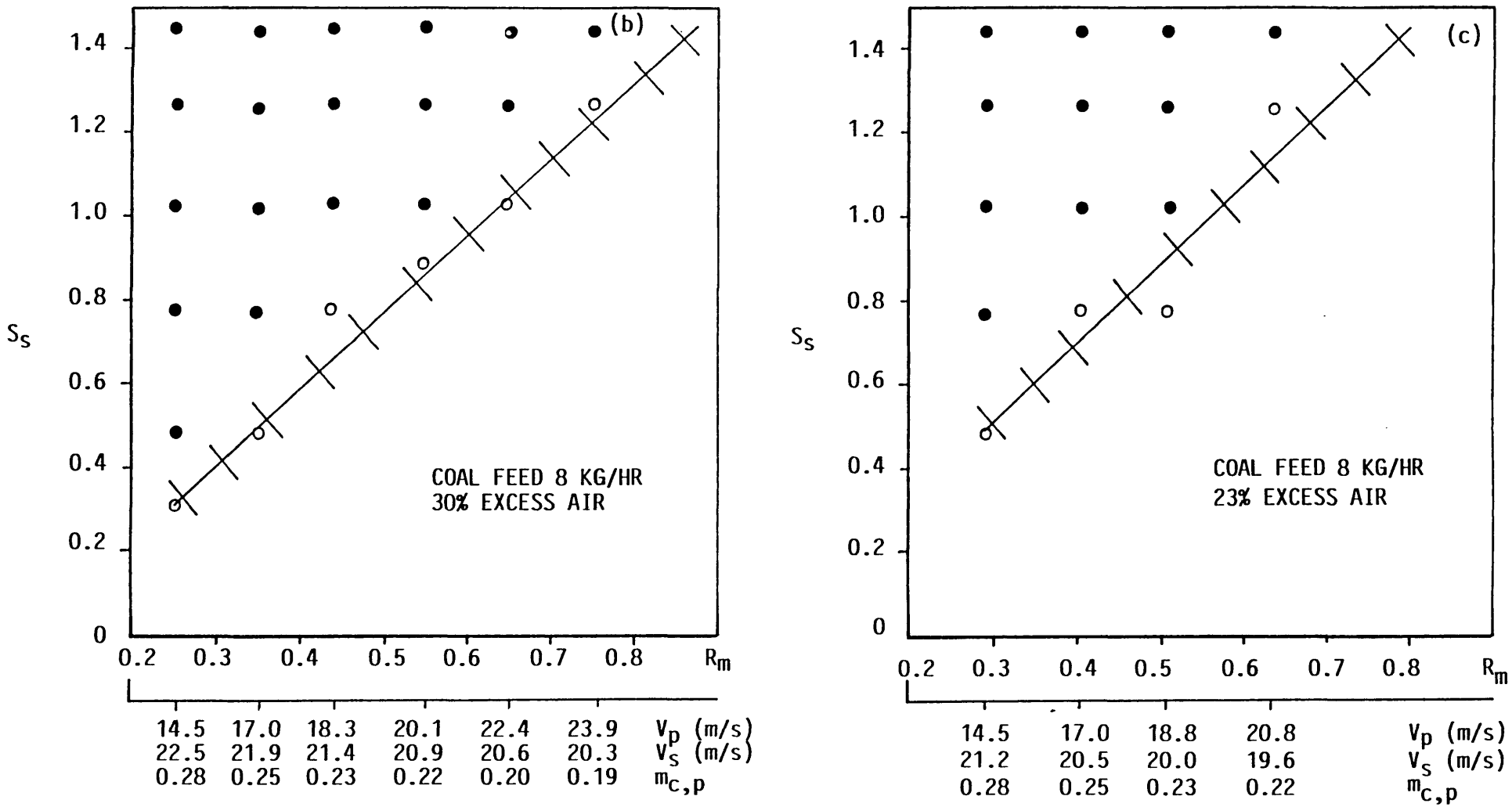


Fig. 5.2 Stability performance of United Kingdom Grimethorpe (2) coal.
(b) m_c = 8.0 kg/hr, 30% excess air
(c) m_c = 8.0 kg/hr, 23% excess air

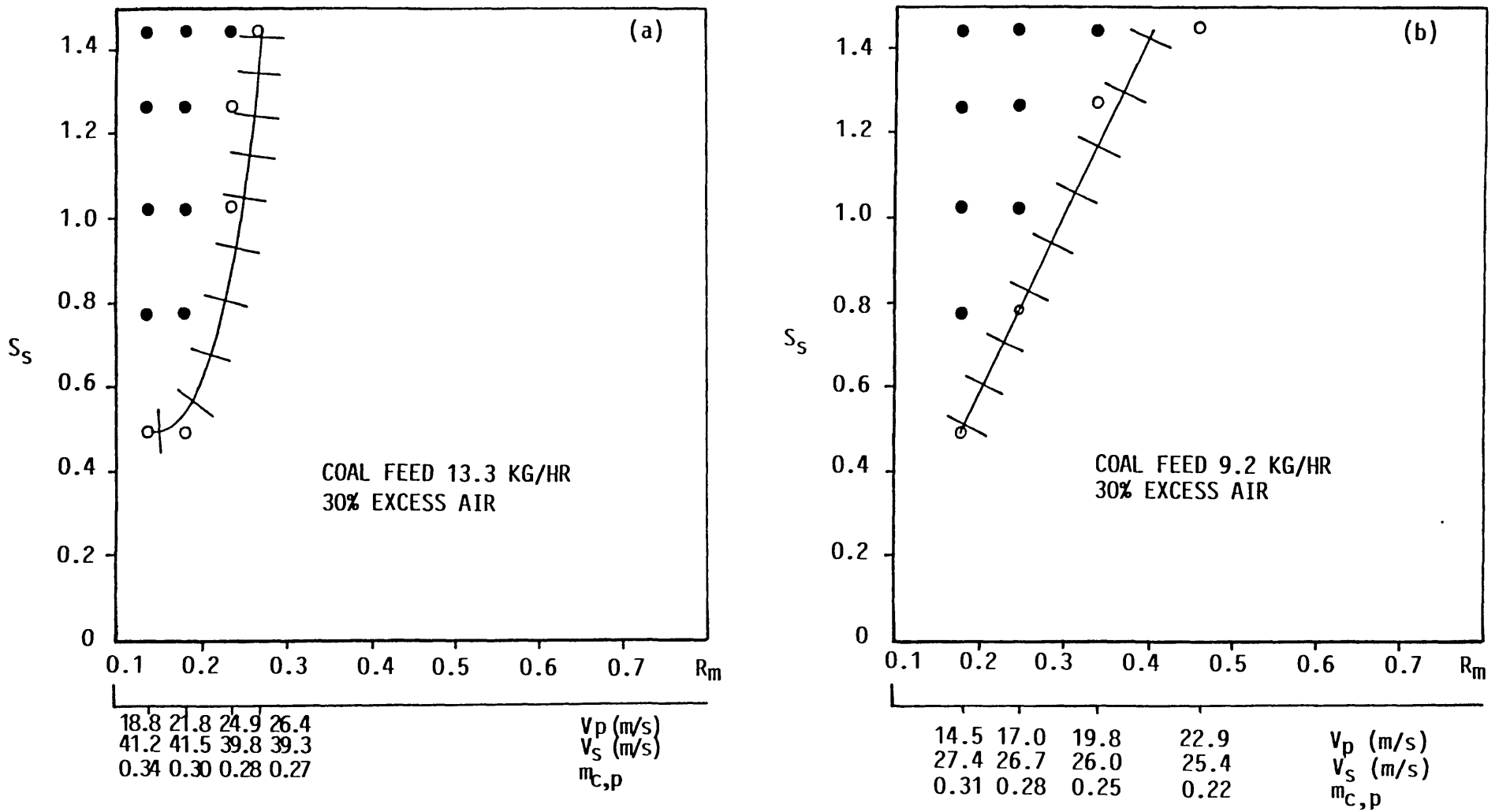


Fig. 5.3 Stability performance of South African (A) coal.

(a) m_c = 13.3 kg/hr, 30% excess air

(b) m_c = 9.2 kg/hr, 30% excess air

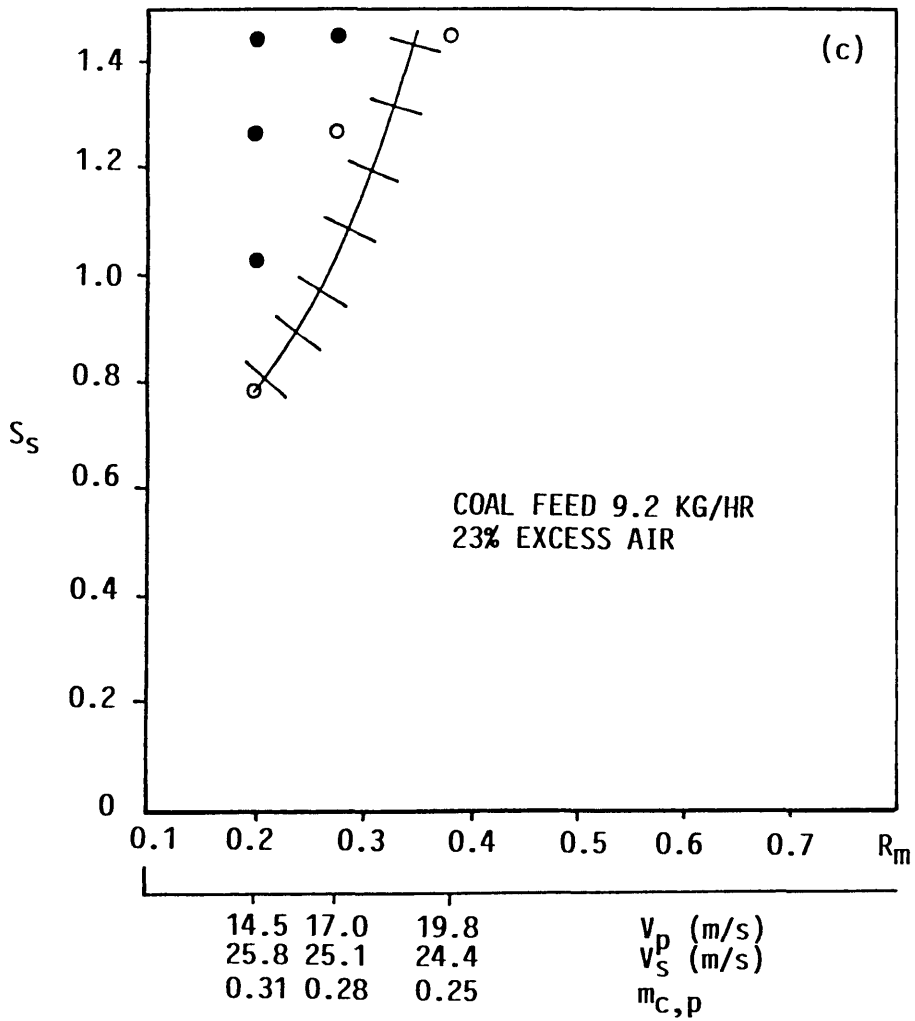


Fig. 5.3 Stability performance of South African (A) coal.

(c) m_c = 9.2 kg/hr, 23% excess air

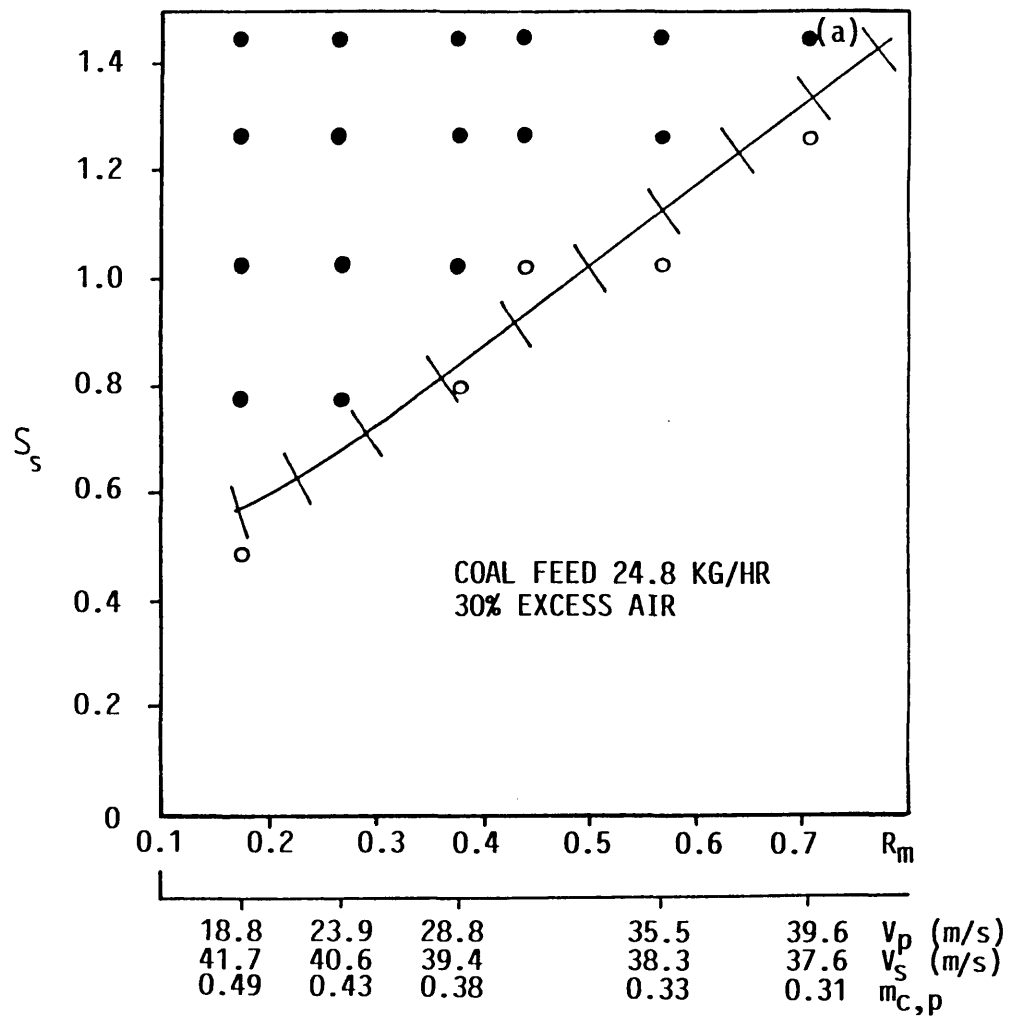
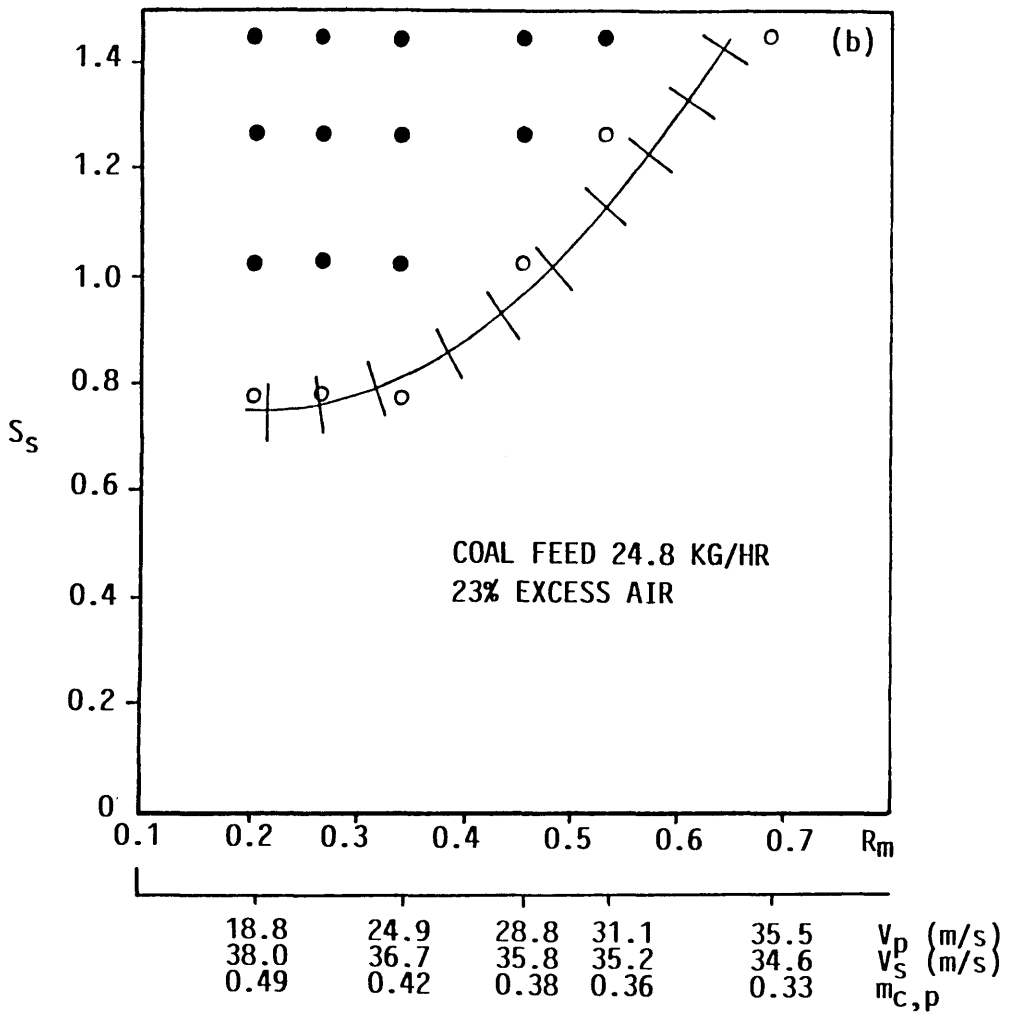


Fig. 5.4 Stability performance of South African (B) coal.

(a) m_c = 24.8 kg/hr, 30% excess air



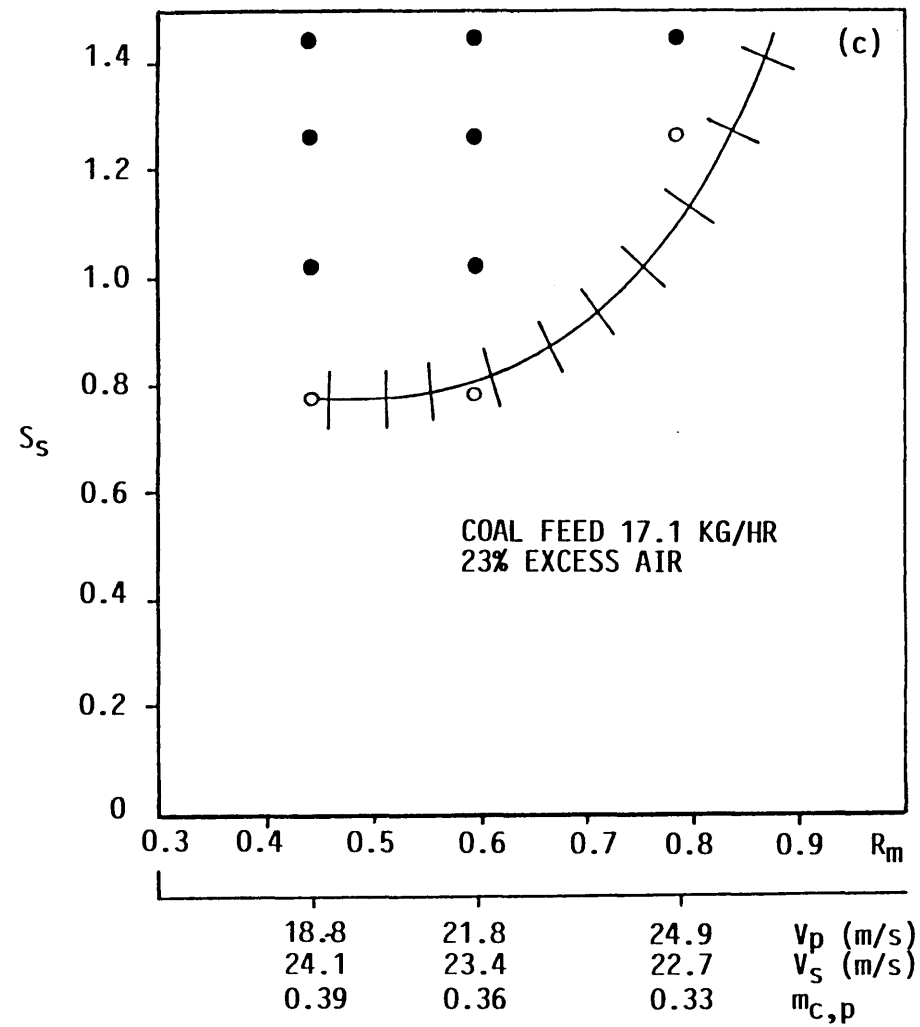


Fig. 5.4 Stability performance of South African (B) coal.

(b) m_c = 24.8 kg/hr, 23% excess air
(c) m_c = 17.1 kg/hr, 23% excess air.

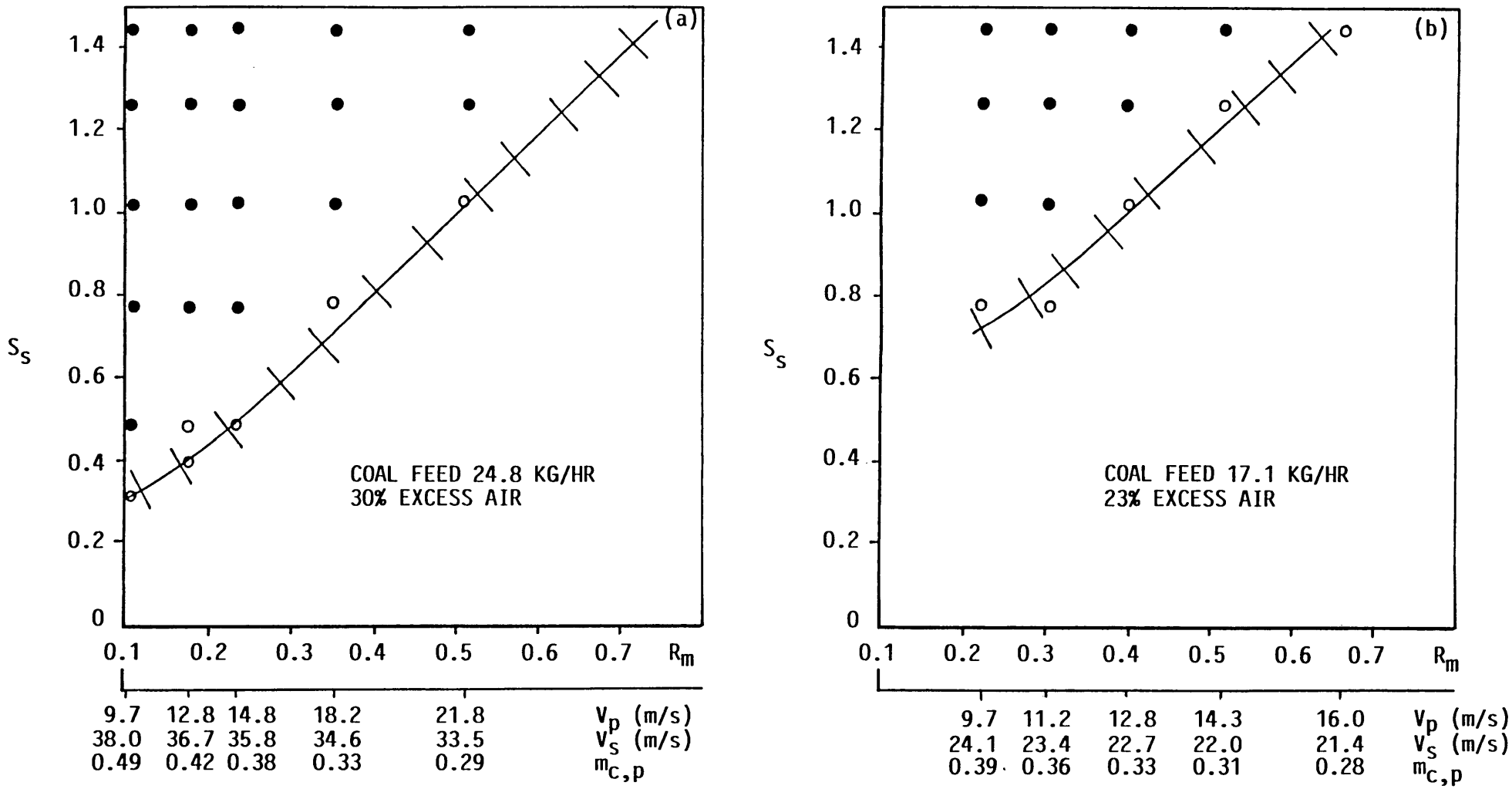


Fig. 5.5 Stability performance of South African (B) coal. 31mm I.D. primary tube.
(a) m_c = 24.8 kg/hr, 30% excess air
(b) m_c = 17.1 kg/hr, 23% excess air

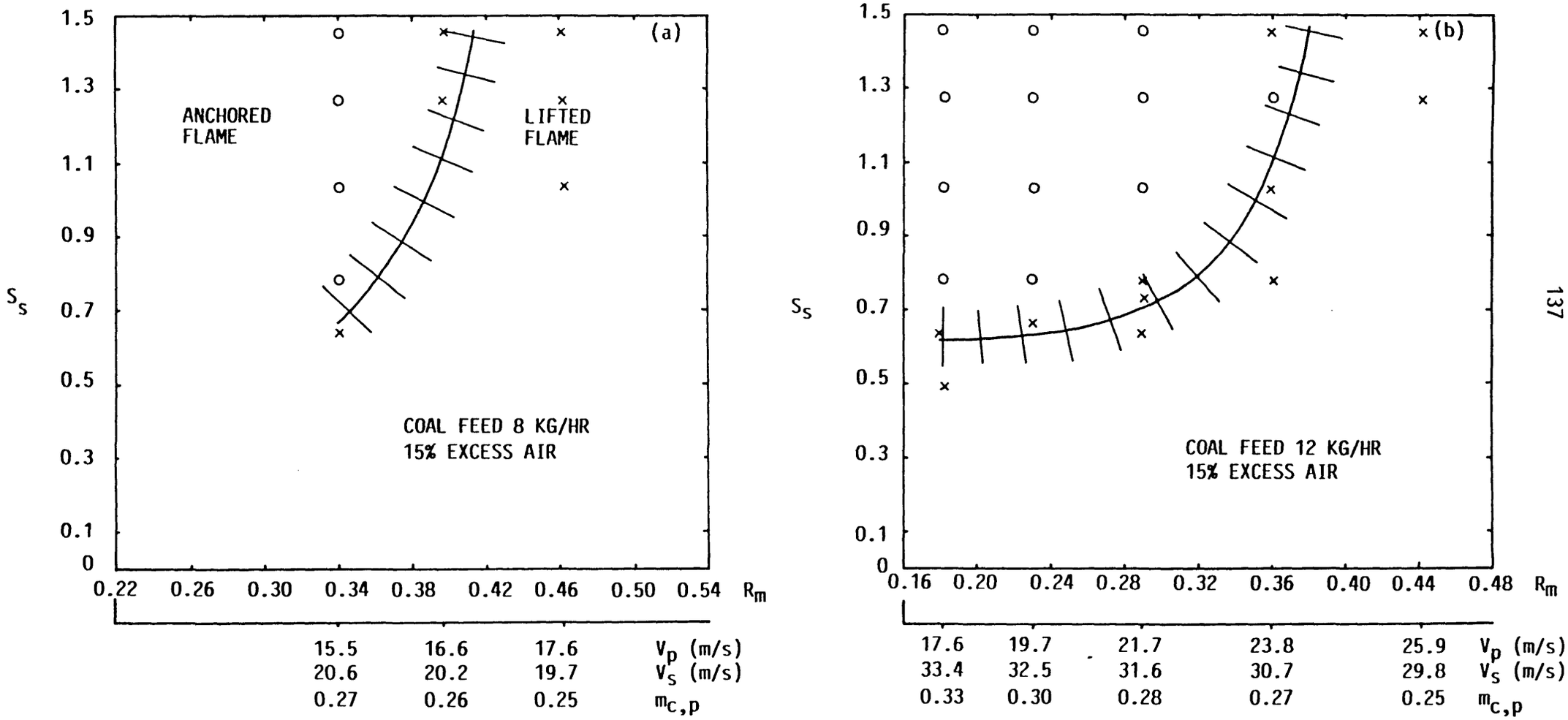
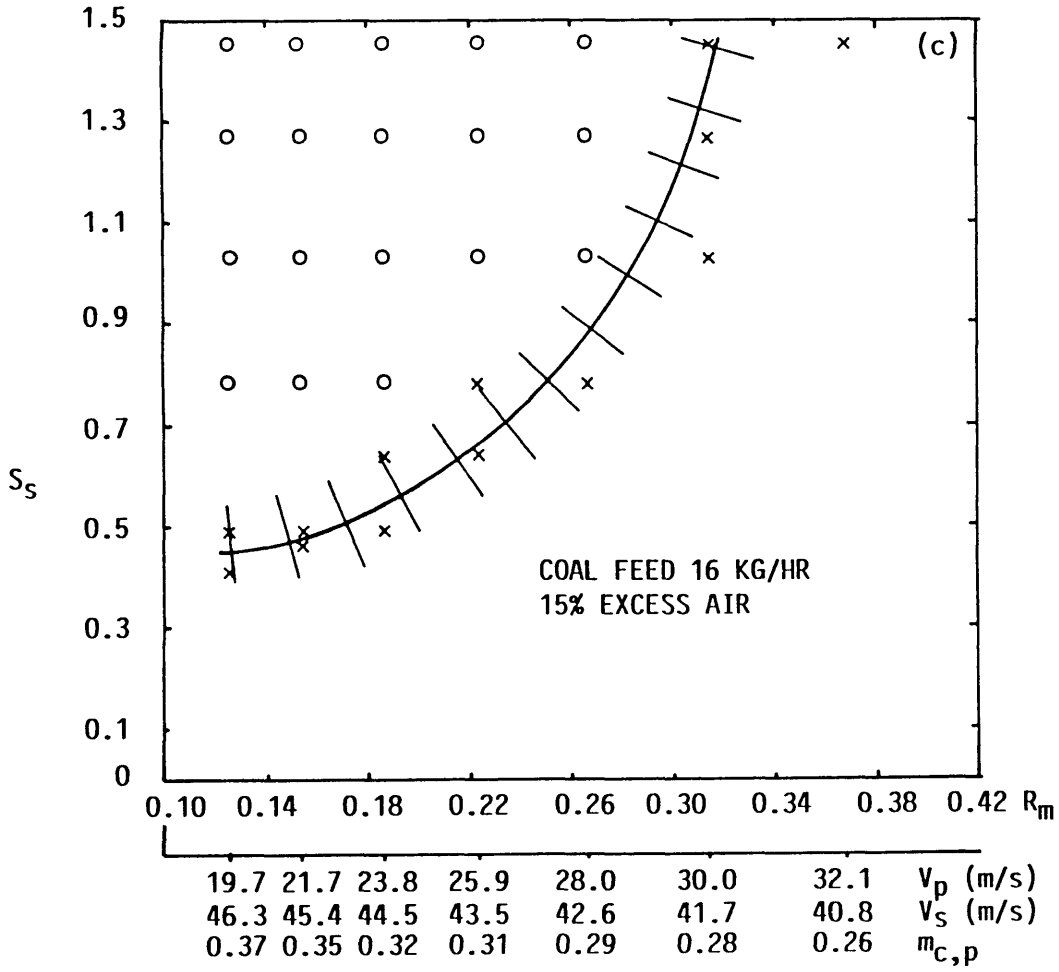


Fig. 5.6 Stability performance of United Kingdom Gedling coal, 15% excess air.

(a) m_c = 8.0 kg/hr
(b) m_c = 12.0 kg/hr



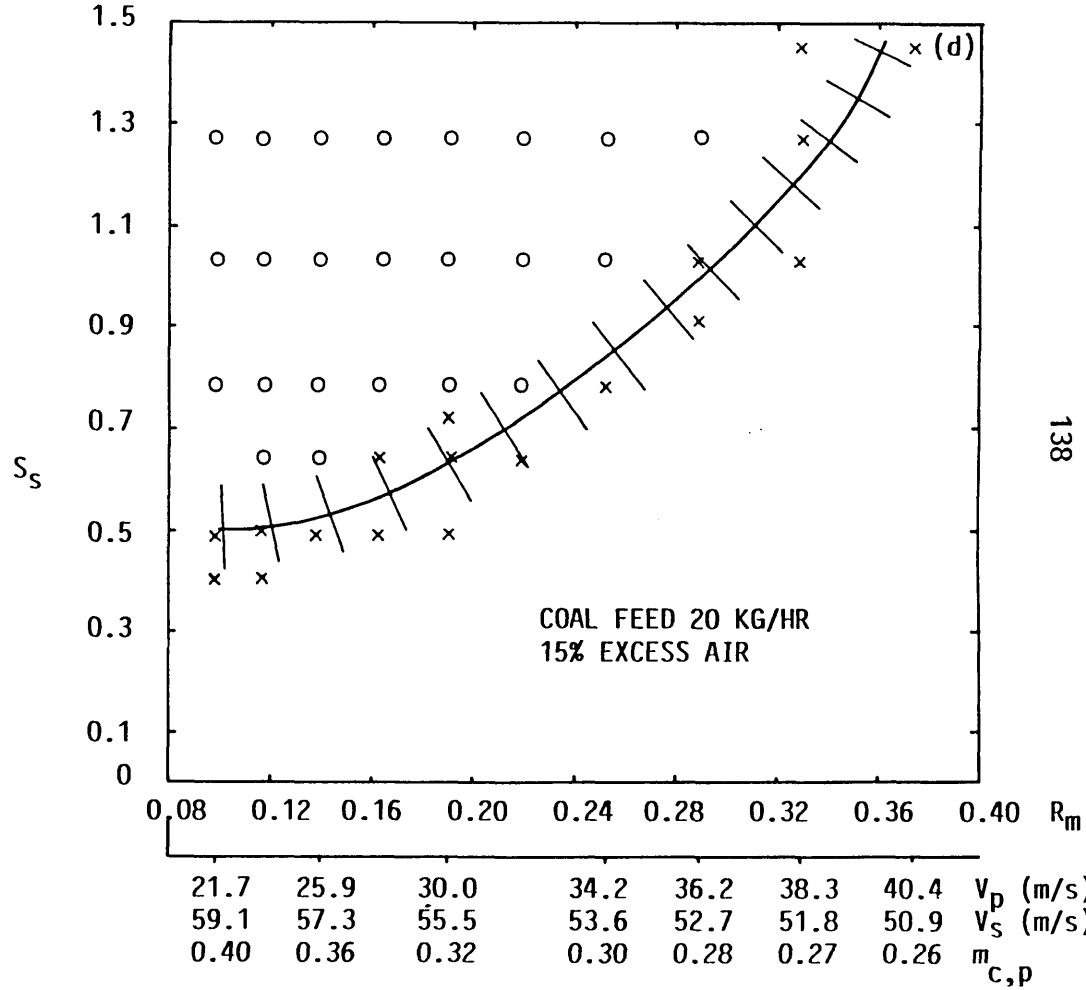


Fig. 5.6 Stability performacne of United Kingdom Gedling coal, 15% excess air.

(c) m_c = 16.0 kg/hr

(d) m_c = 20.0 kg/hr

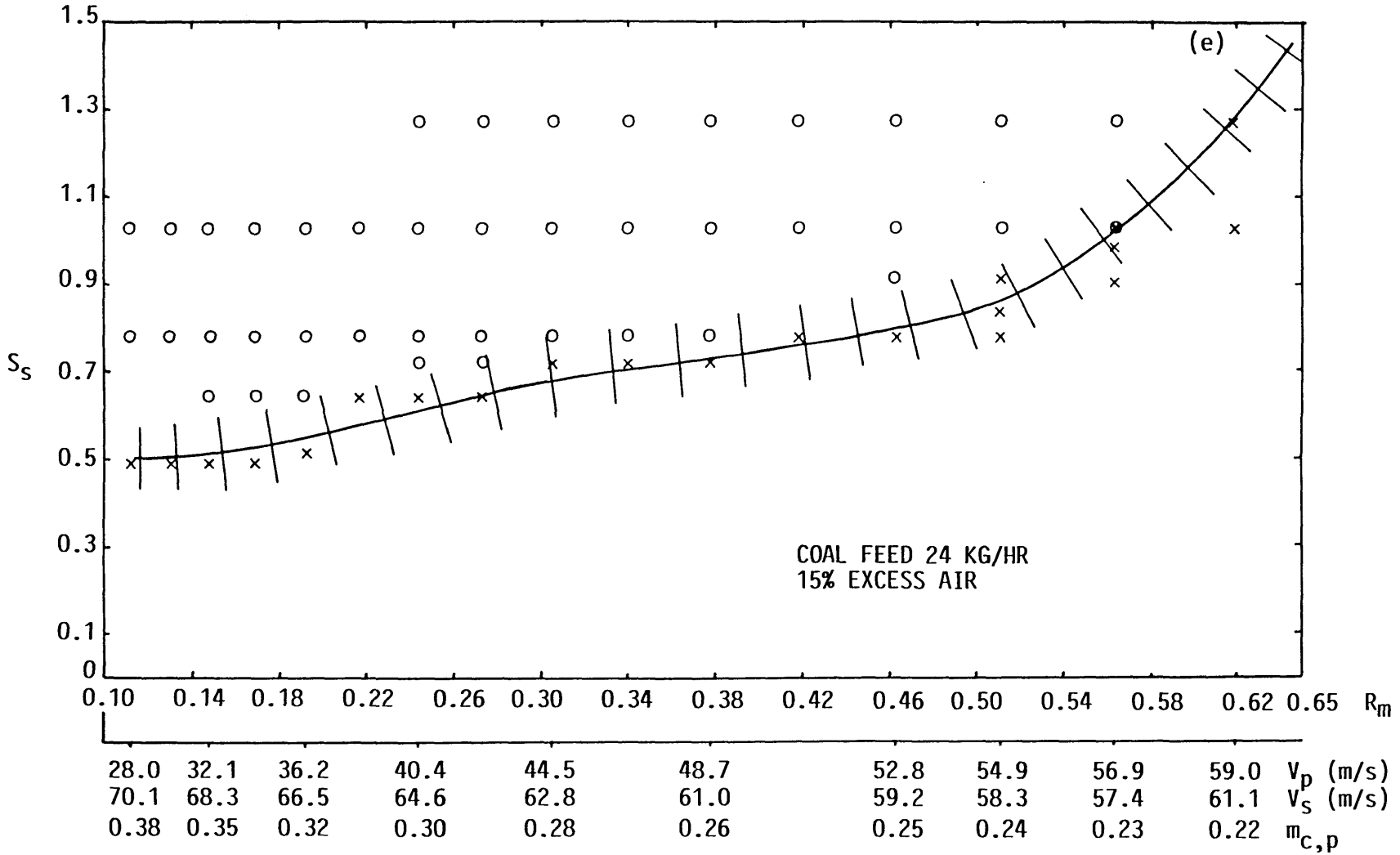


Fig.5.6 Stability performance of United Kingdom Gedling coal, 15% excess air.
(e) m_c = 24.0 kg/hr

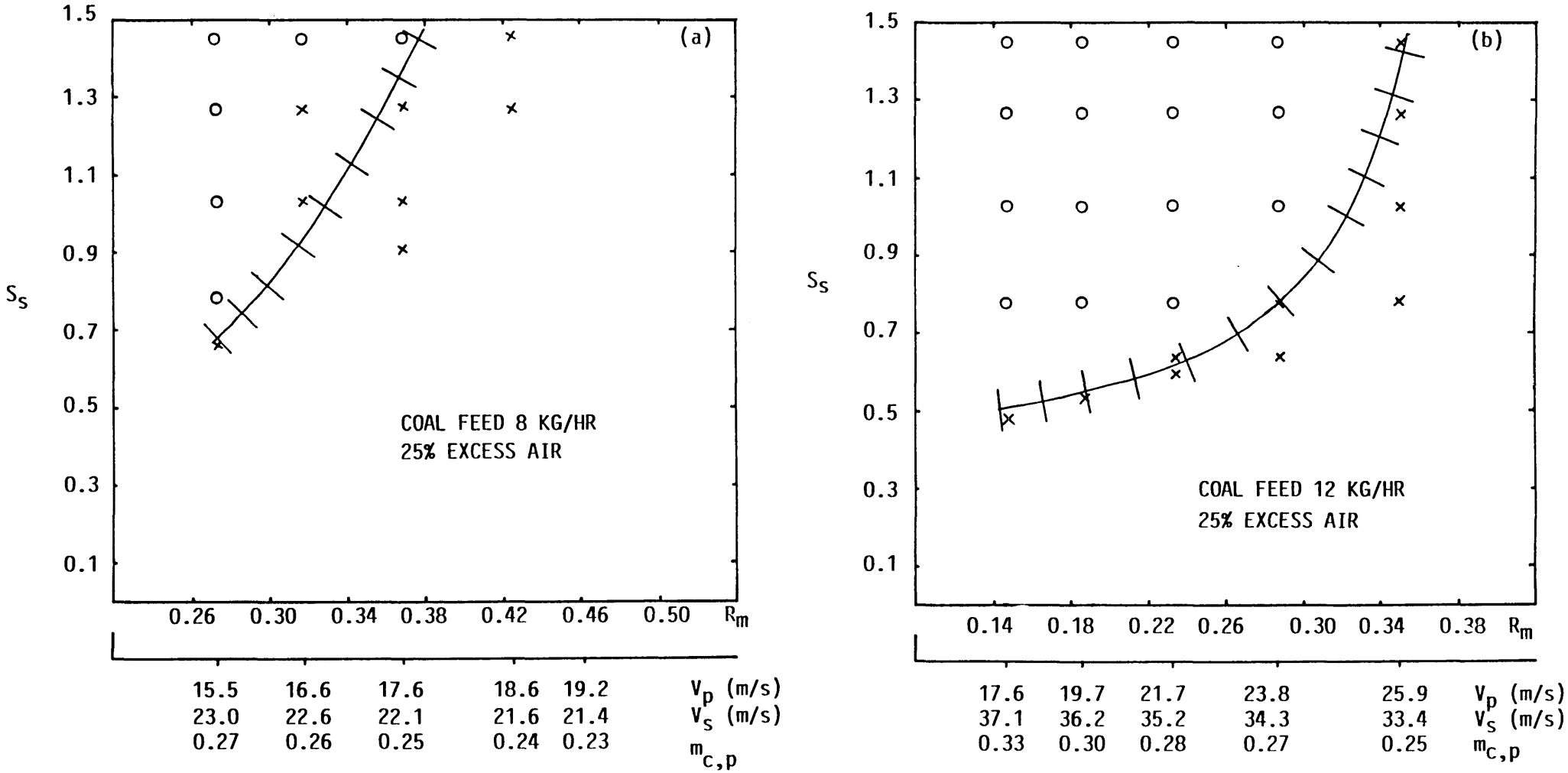


Fig. 5.7 Stability performance of United Kingdom Gedling coal, 25% excess air.

(a) m_c = 8.0 kg/hr
(b) m_c = 12.0 kg/hr

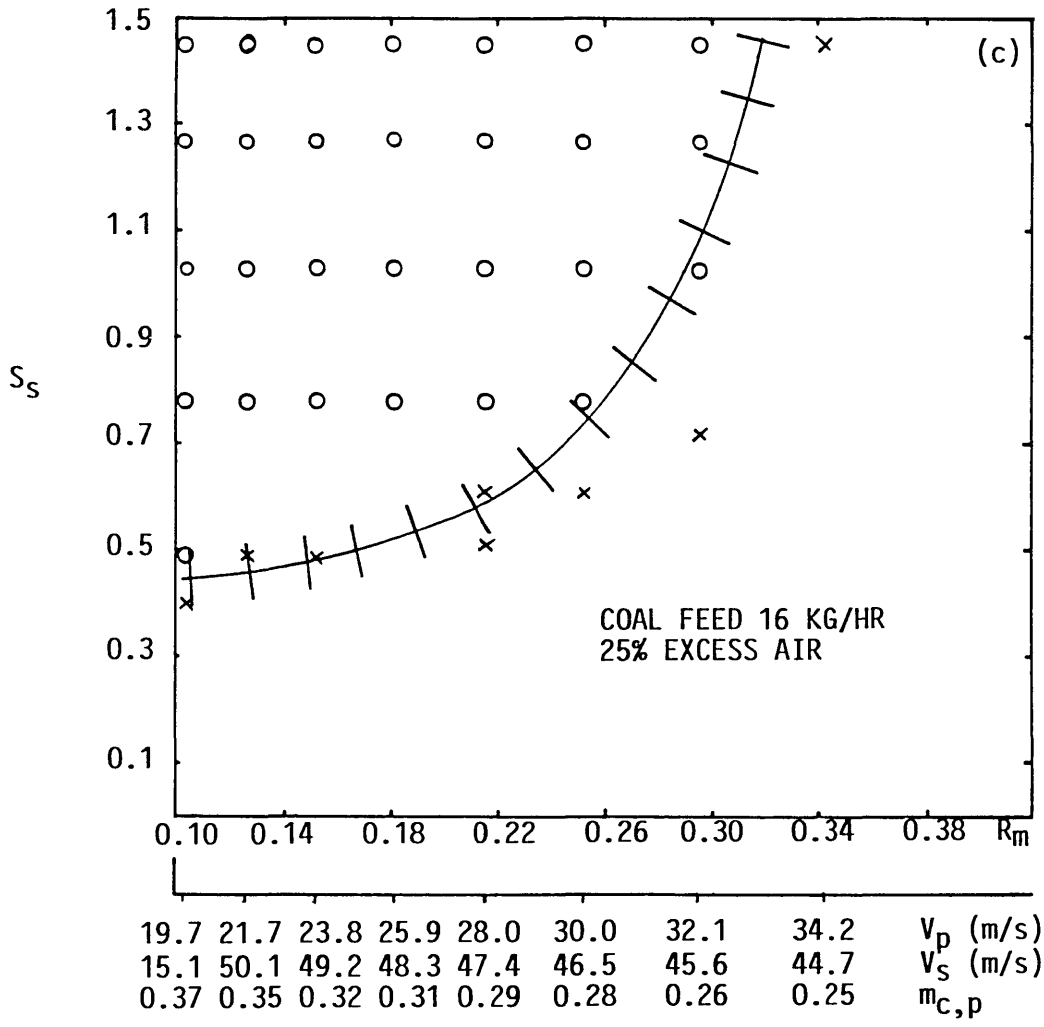


Fig. 5.7 Stability performance of United Kingdom Gedling coal, 25% excess air.

(c) m_c = 16.0 kg/hr

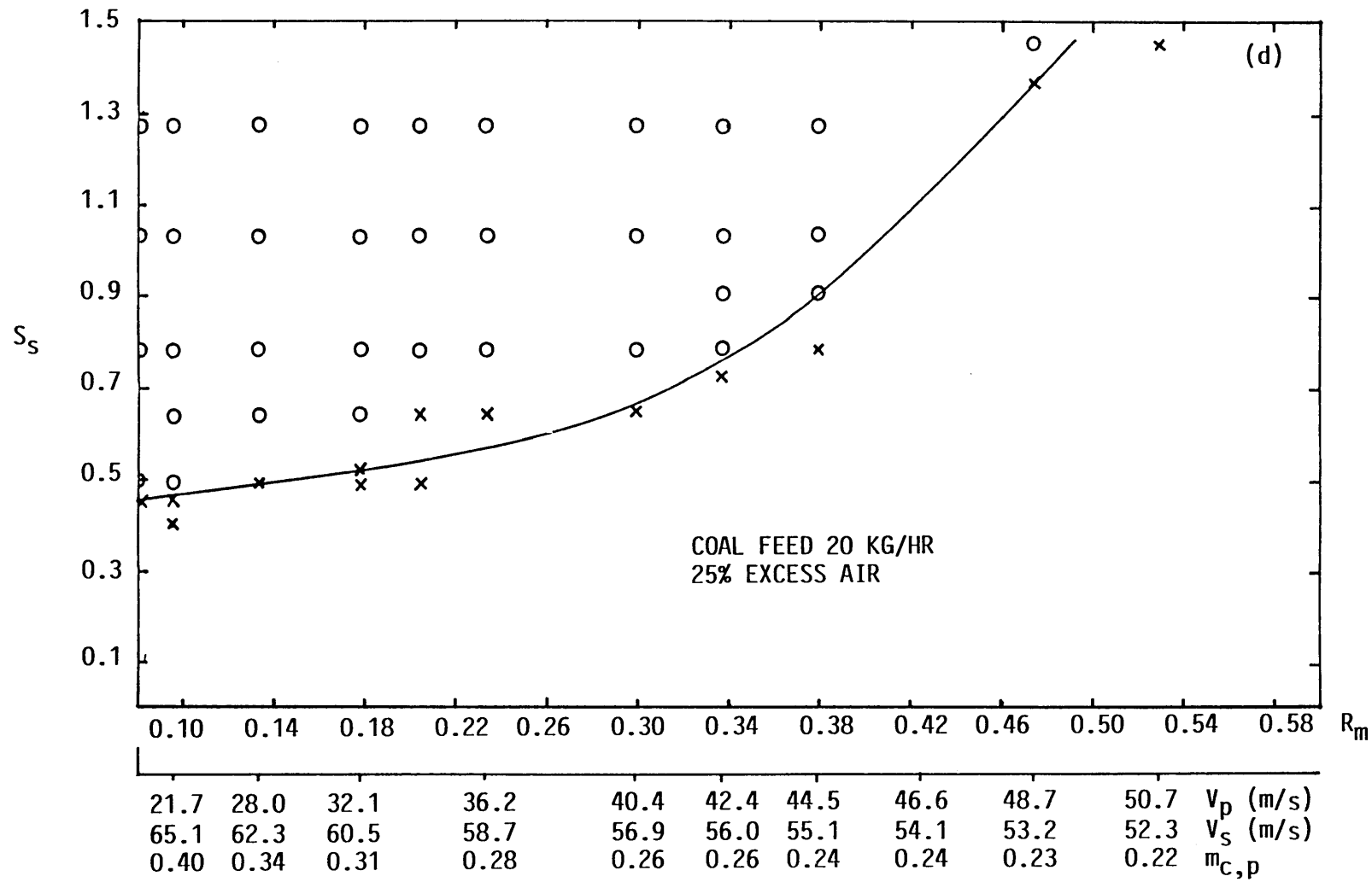


Fig. 5.7 Stability performance of United Kingdom Gedling coal, 25% excess air.
(d) m_c = 20.0 kg/hr

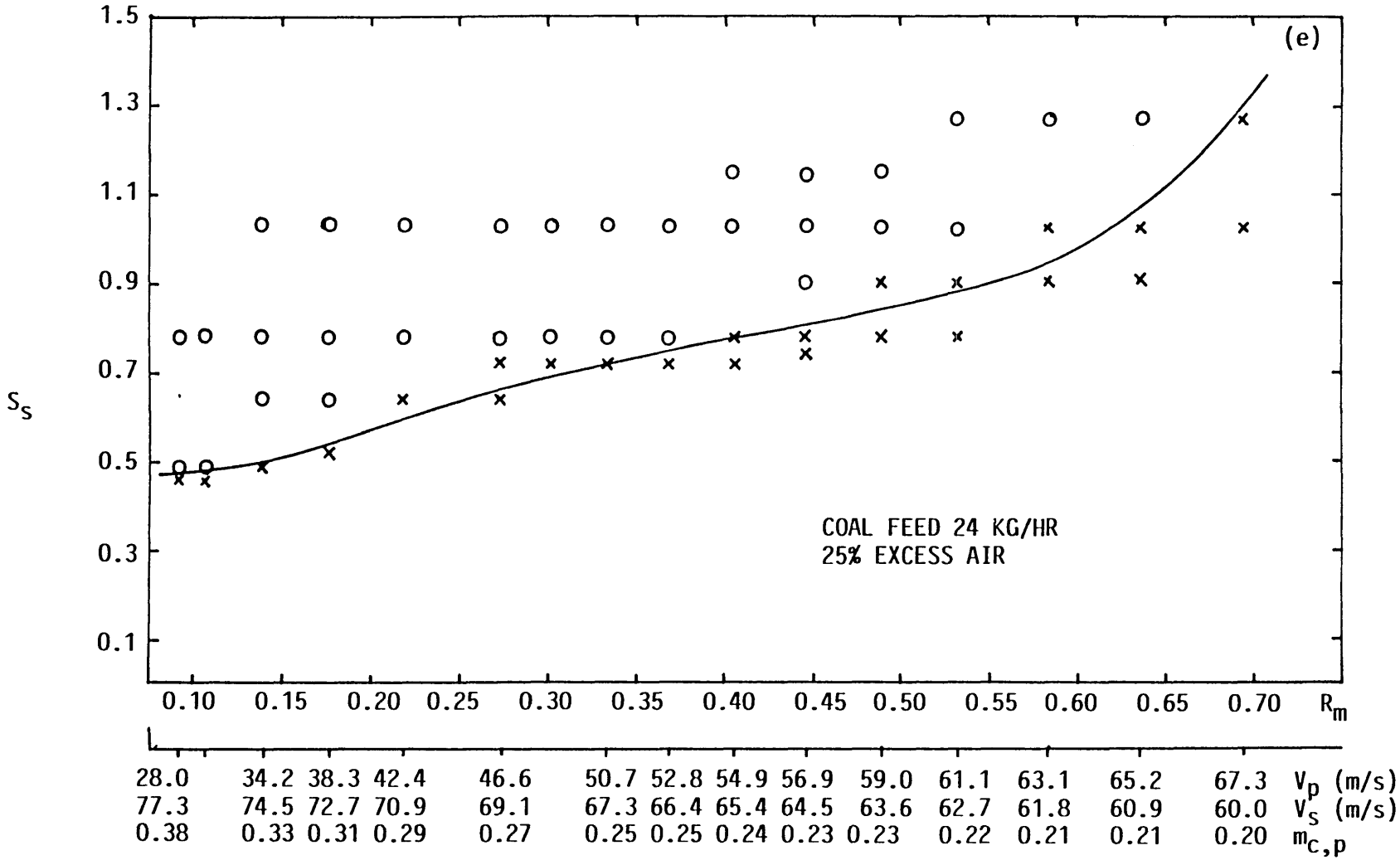


Fig. 5.7 Stability performance of United Kingdom Gedling coal, 25% excess air.
(e) m_c = 24.0 kg/hr

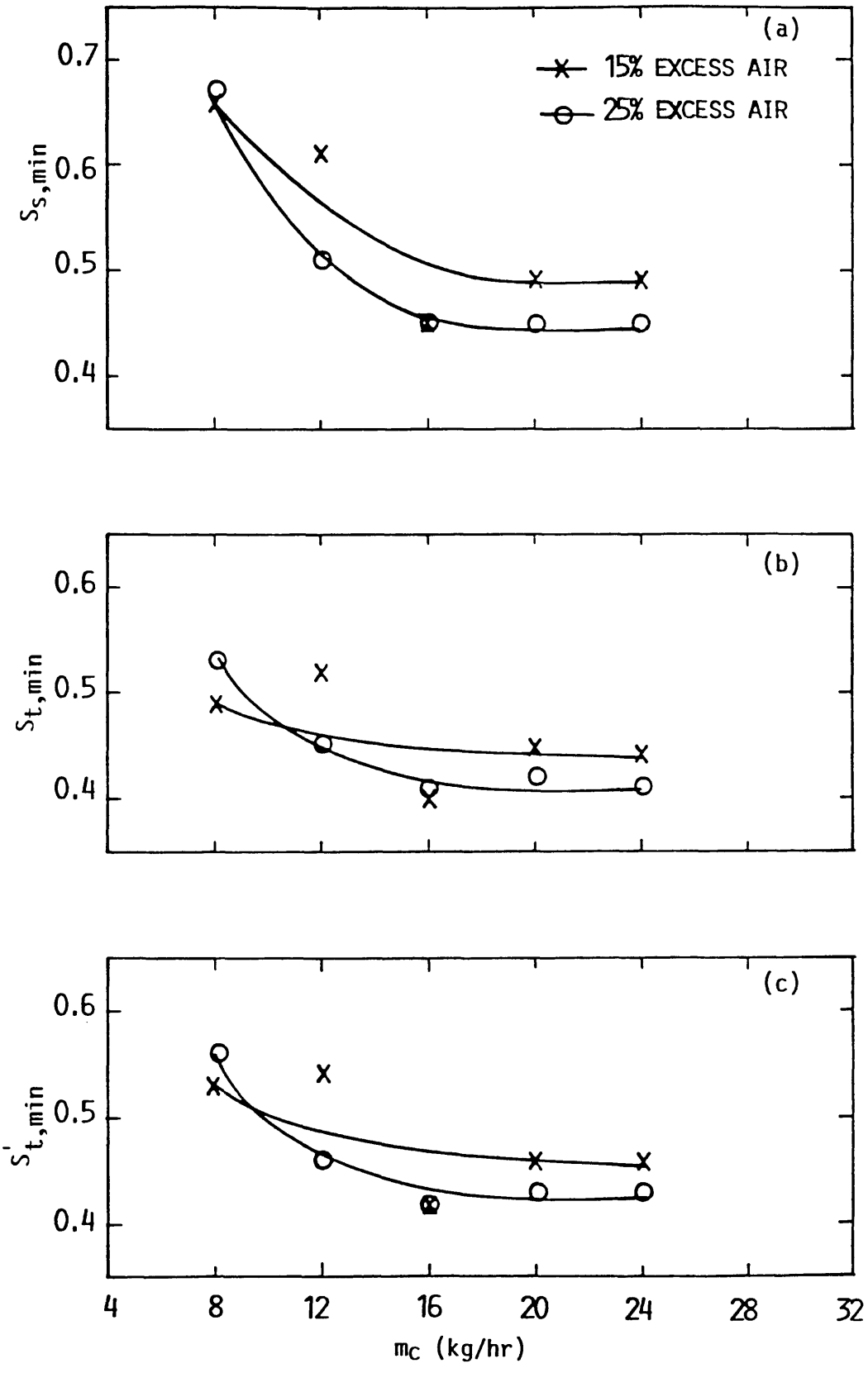


Fig. 5.8 Influence of burner load on minimum swirl number for stable flame. United Kingdom Gedling coal.

(a) $S_{s,min}$ vs m_c
(b) $S_{t,min}$ vs m_c
(c) $S'_{t,min}$ vs m_c

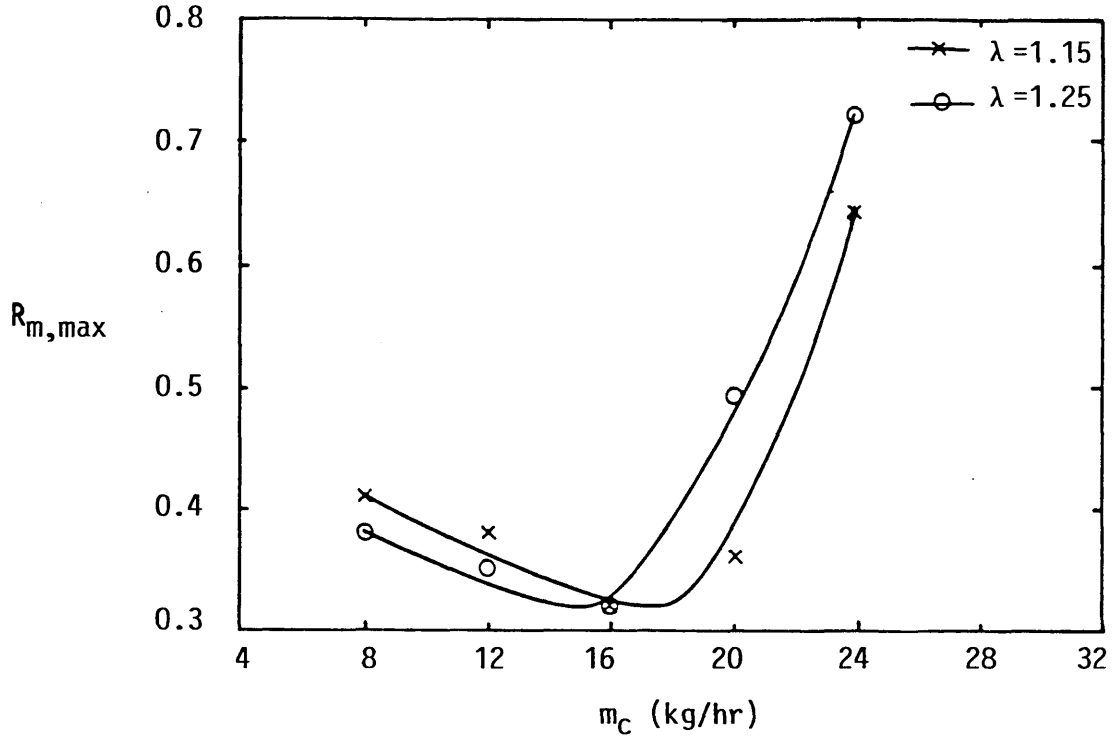


Fig. 5.9 Influence of burner load on maximum momentum ratio, $R_{m,max}$ for stable flame. United Kingdom Gedling coal.

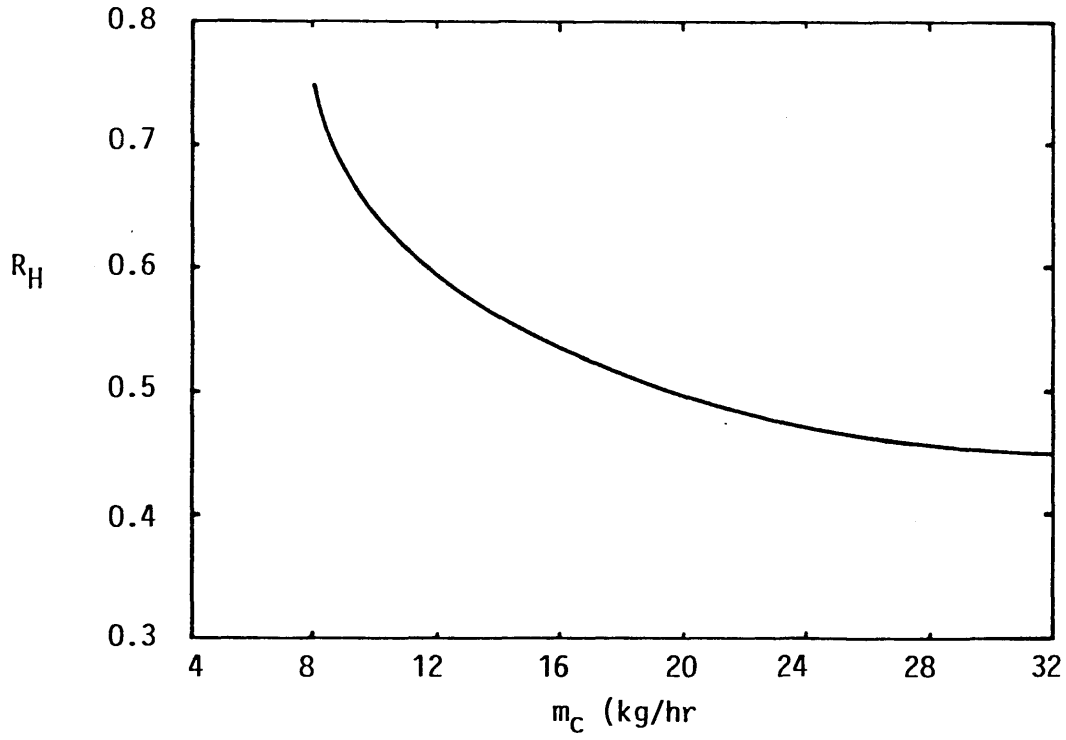


Fig. 5.10 Predicted Influence of burner load on ratio of radiation heat loss to furnace walls to flame zone heat release.

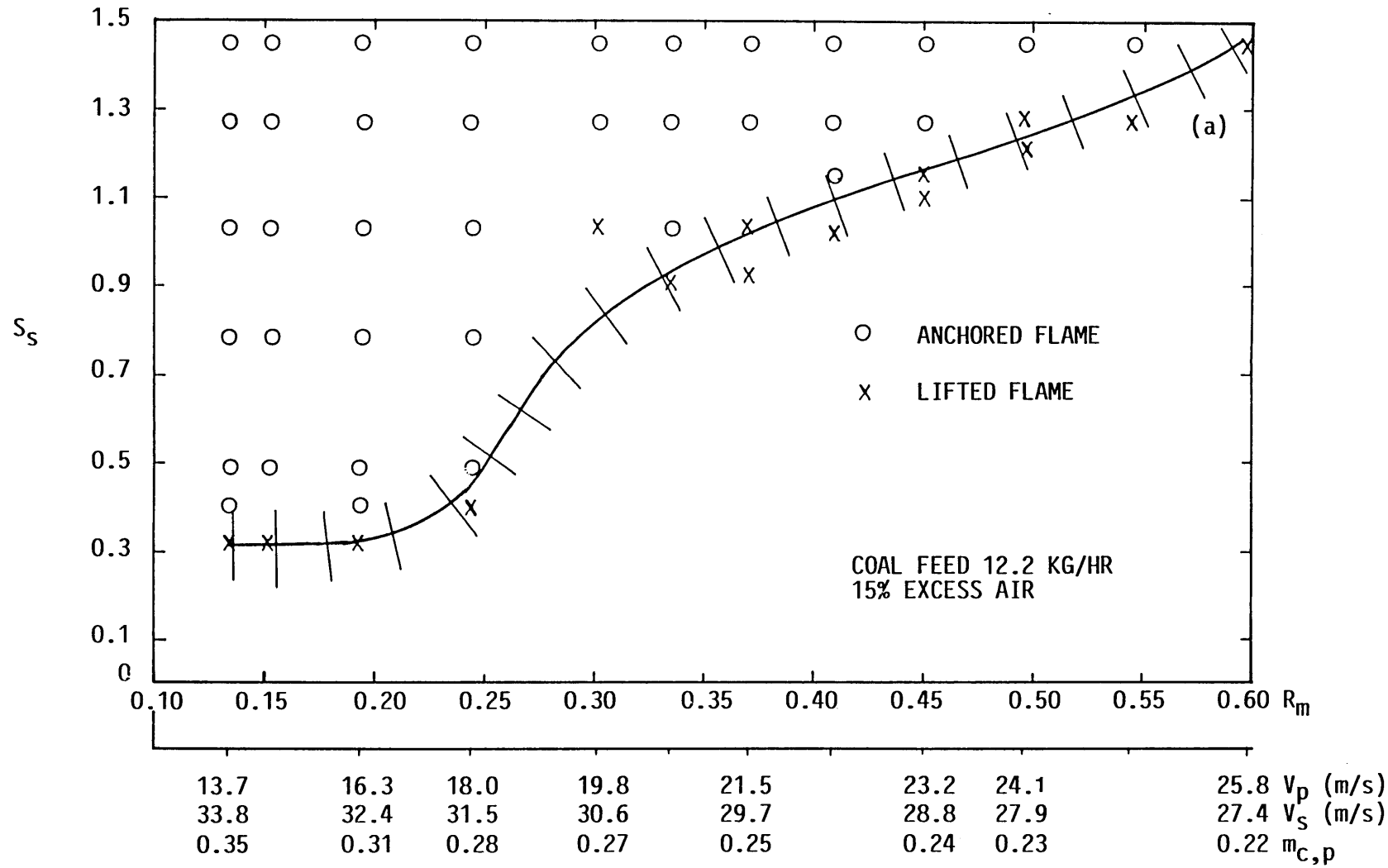


Fig. 5.11 Stability performance of United Kingdom Gedling-microfine coal,
15% excess air.
(a) m_c = 12.2 kg/hr

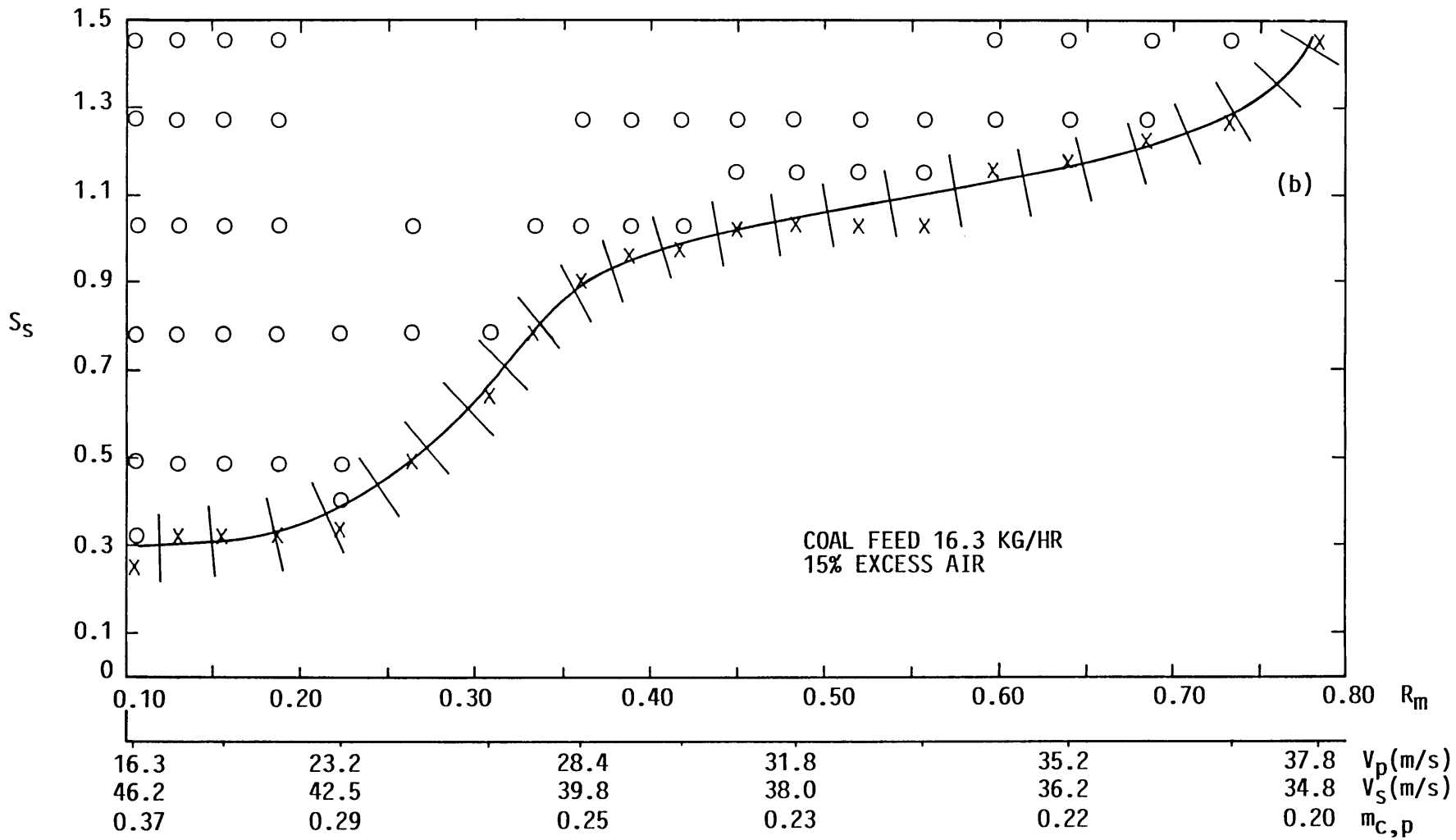


Fig. 5.11 Stability performance of United Kingdom Gedling-microfine coal, 15% excess air.
(b) m_c = 16.3 kg/hr

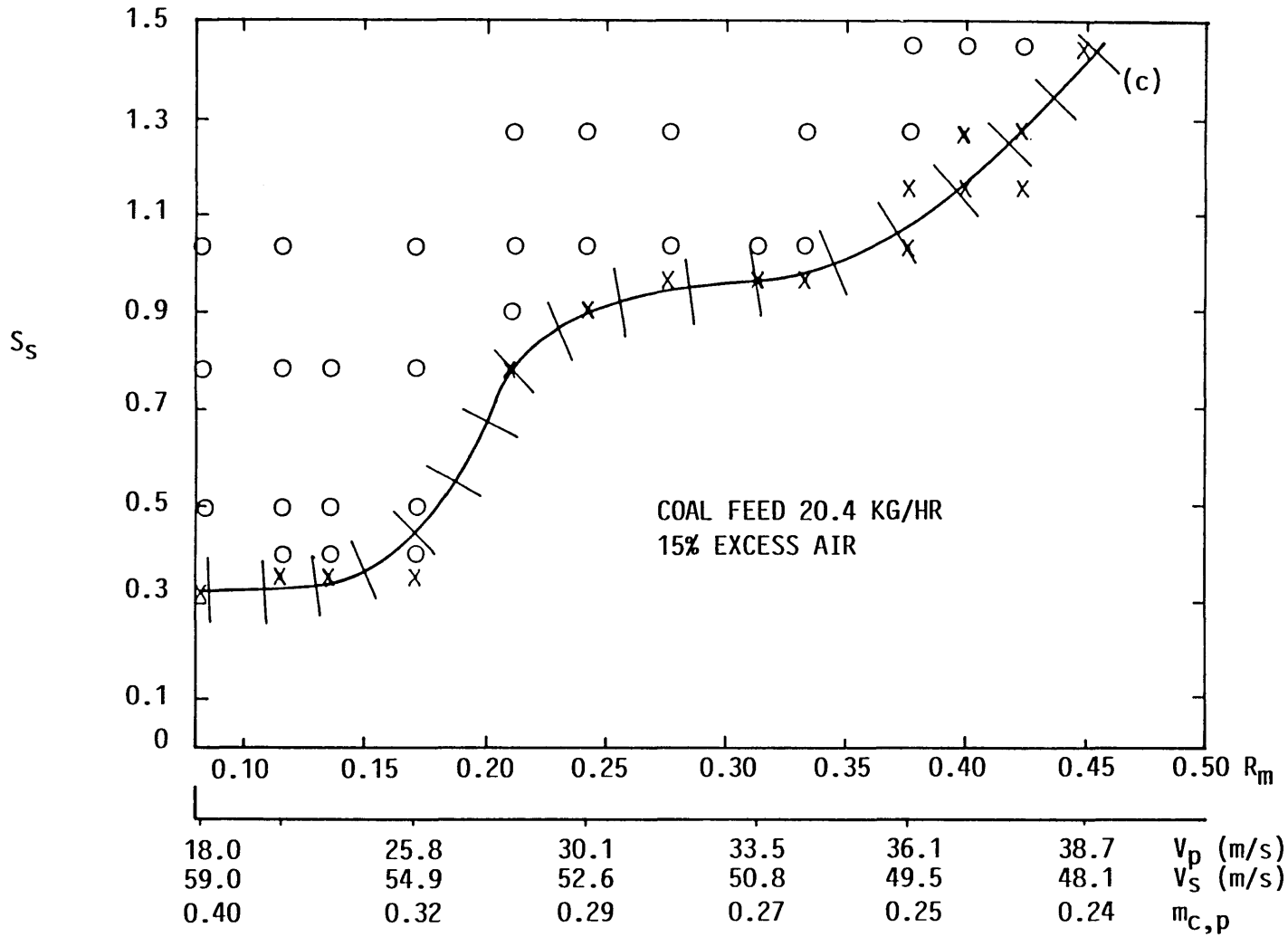


Fig. 5.11 Stability performance of United Kingdom Gedling-microfine coal, 15% excess air.
(c) m_c = 20.4 kg/hr

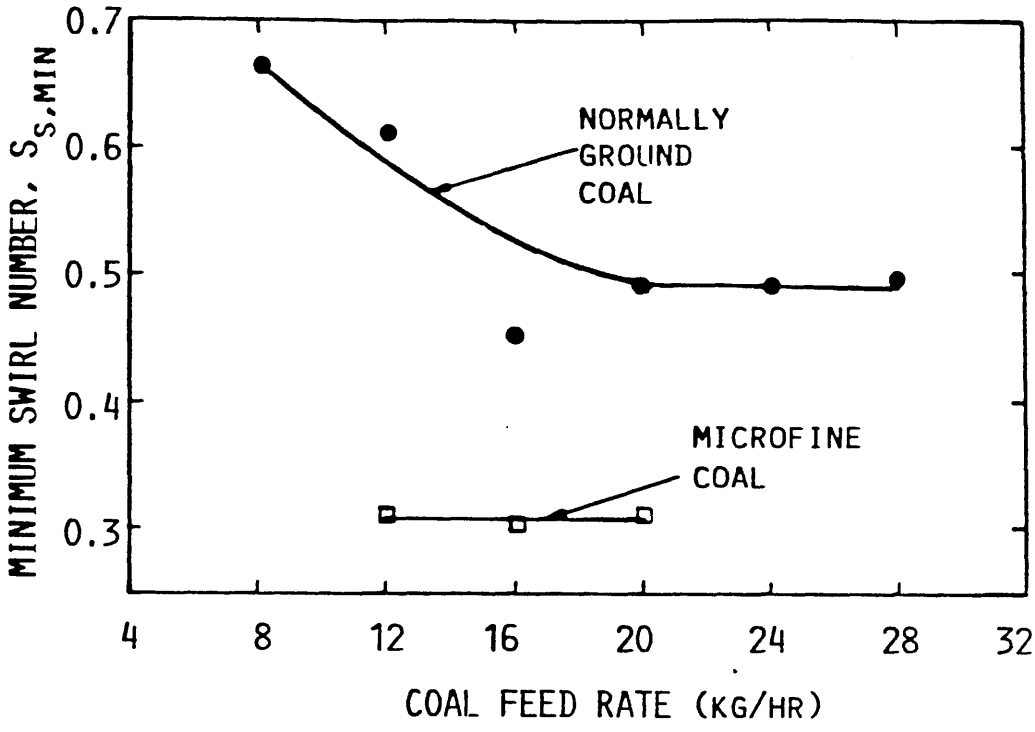


Fig. 5.12 Influence of burner load on minimum secondary air swirl number $S_{S,min}$ for stable flame. Normally ground and microfine Gedling coal, 15% excess air.

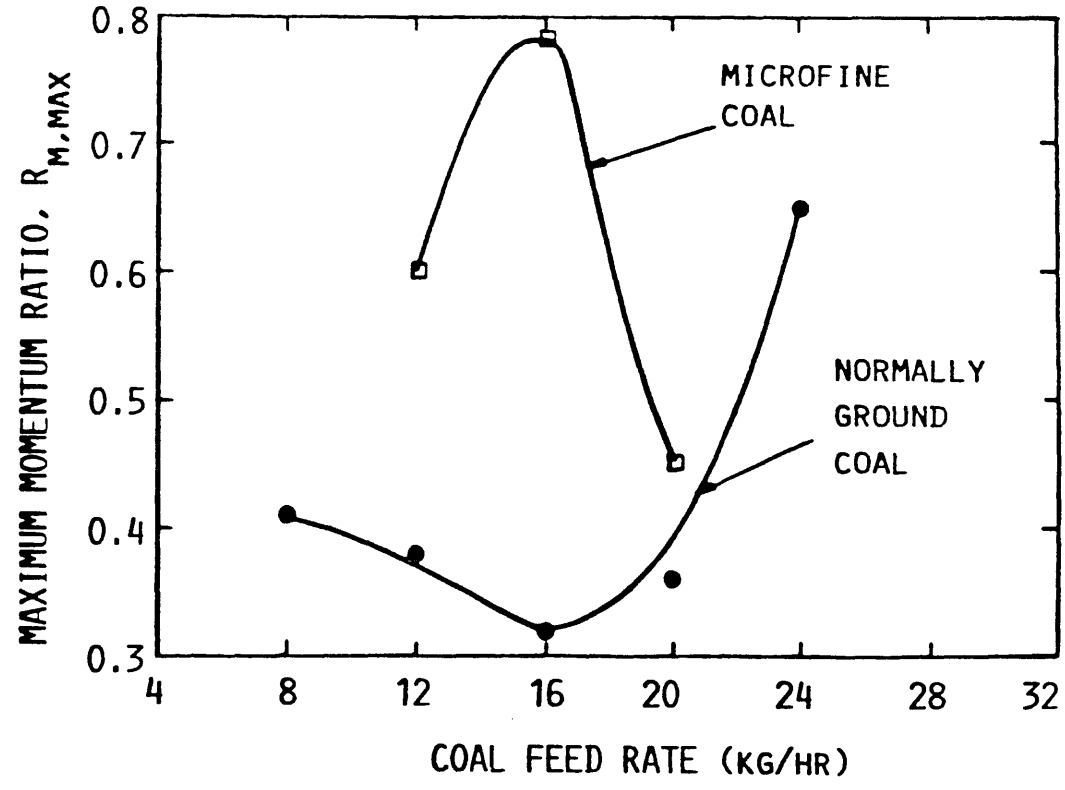
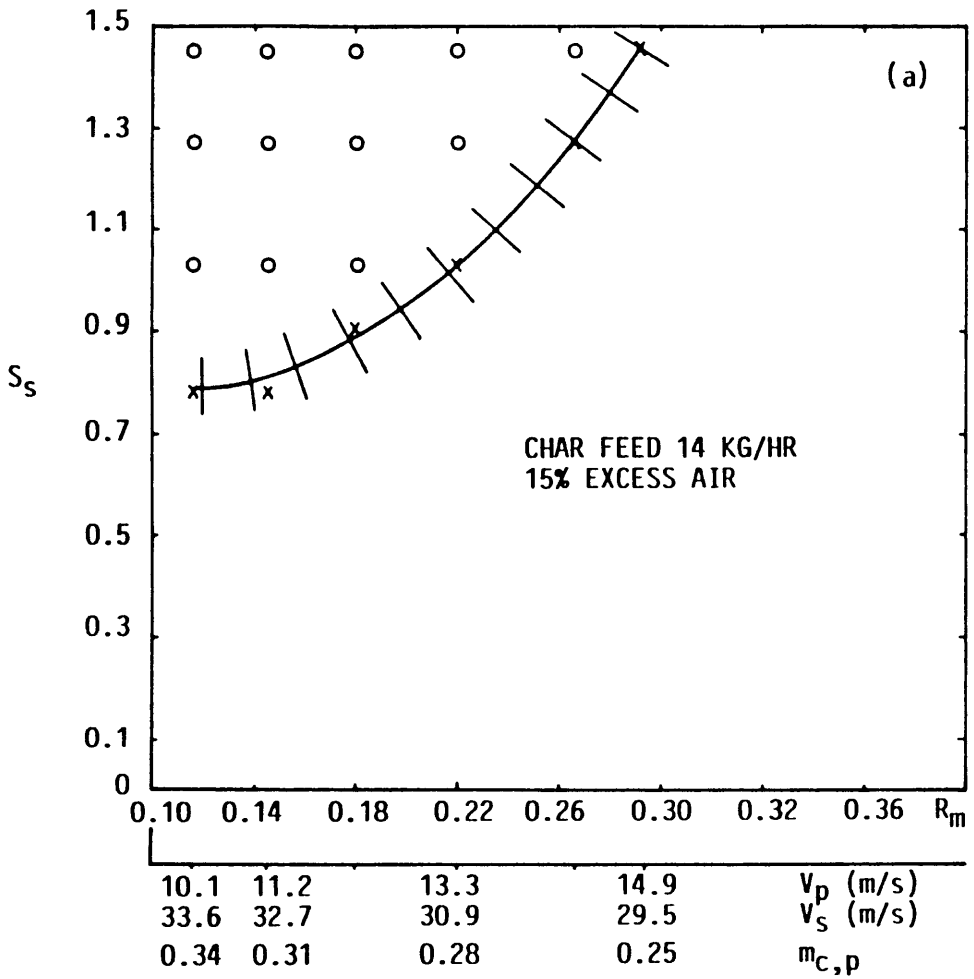


Fig. 5.13 Influence of burner load on maximum momentum ratio, $R_{m,max}$, for stable flame. Normally ground and microfine Gedling coal, 15% excess air.



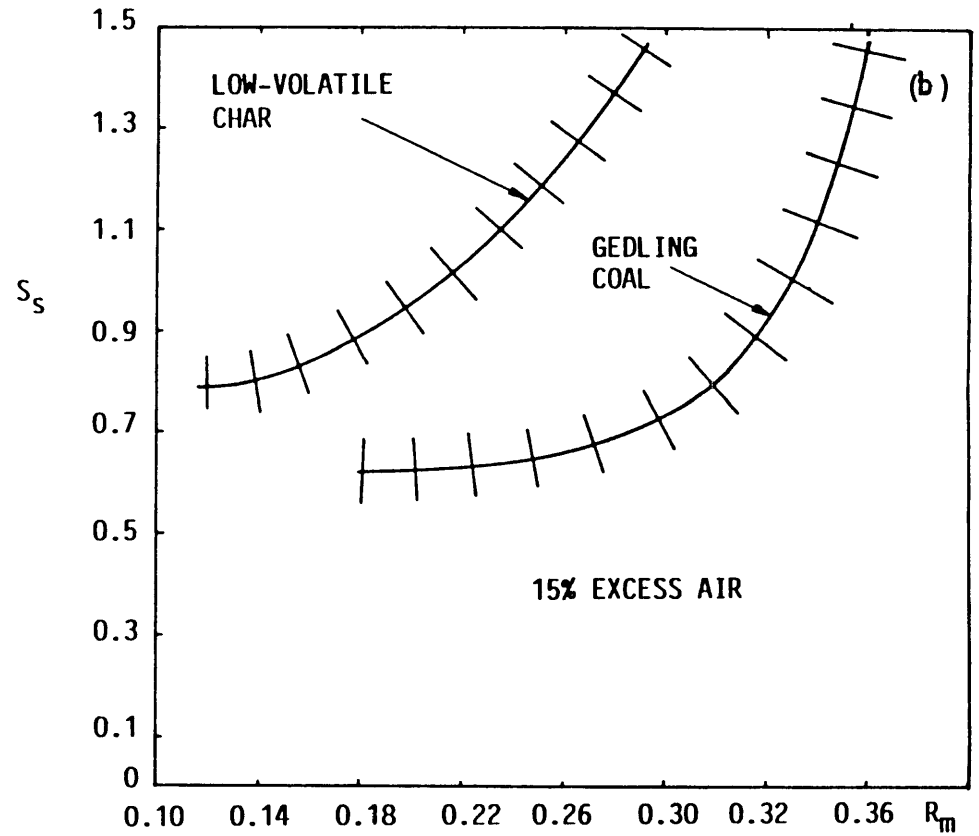


Fig. 5.14 Stability performance of low-volatile char (BLVG).

(a) m_c = 14.0 kg/hr, 15% excess air, 31mm I.D. primary tube.

(b) Comparison of stability performance of low-volatile char with normally ground Gedling coal. Gross input heating value 100kW, 15% excess air.
Low-volatile char - 31mm I.D. primary tube
Gedling coal - 22mm I.D. primary tube.

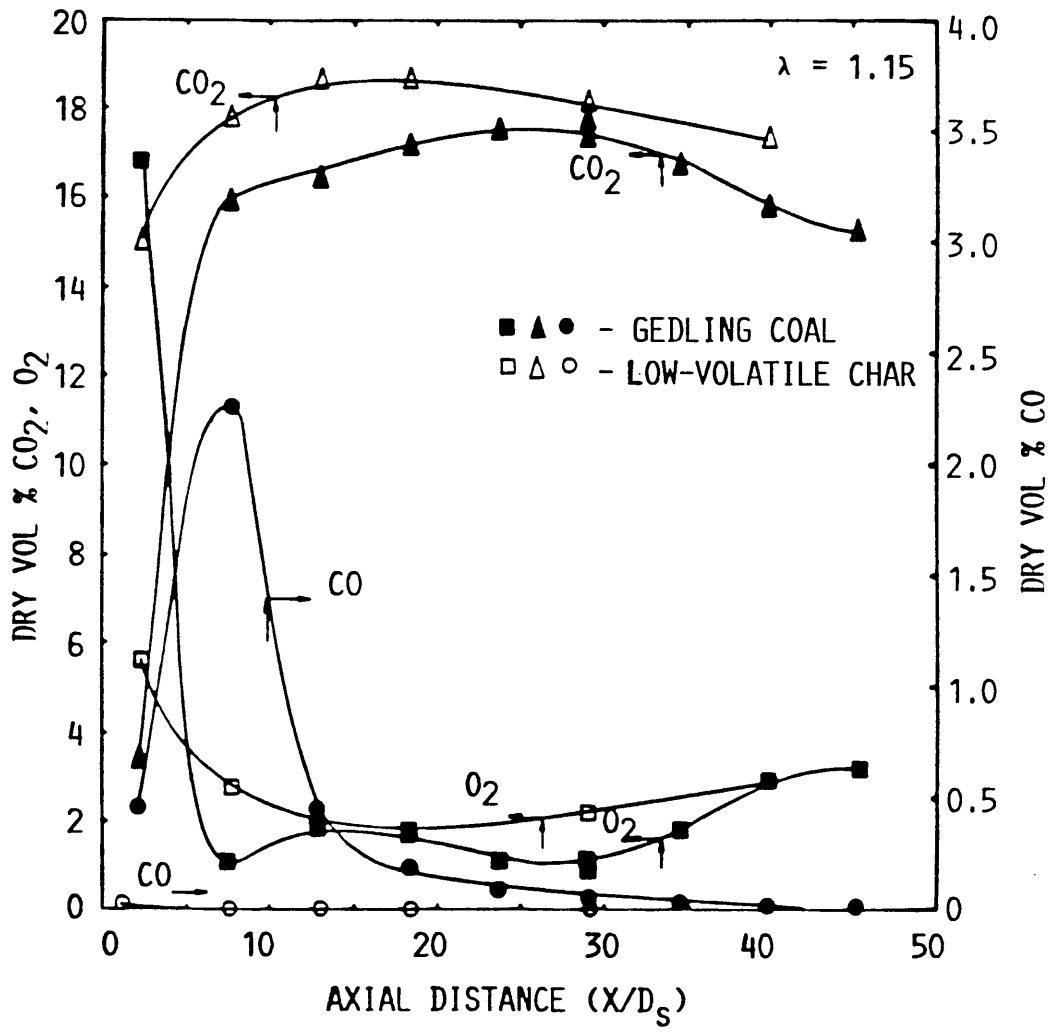


Fig. 5.15 On-axis gas species concentration profiles.
Gross input heating value 100kW, 15% excess air.
Low-volatile char: S_S = 1.45, R_m = 0.116, 31mm I.D. primary tube.
Gedling coal : S_S = 1.03, R_m = 0.231, 22mm I.D. primary tube.

APPENDIX 5.A

Prediction of Dependency of Heat Radiated to Furnace Walls on Burner Load

A zero dimensional time independent model was developed to evaluate the ratio, R_H, of the rate of heat absorbed by the walls to that of heat released in the flame region of the furnace. The purpose was to qualitatively demonstrate the effect on R_H of the burner load. The model is based on the equation for the heat balance, Hottel (1974).

$$q_{rel} = q_{rad} + m_g C_p((T_g - \Delta) - T_o) \qquad (5.8)$$

where q_{rel} = heat release rate,($q_{rel} = q_v + q_p$)

q_{rad} = radiation loss from the flame to the walls

m_g = net gas flow out of the flame zone

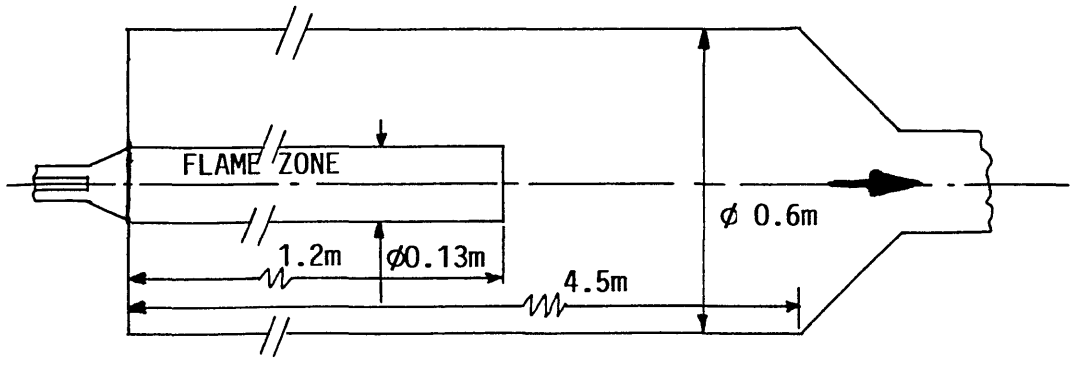
T_g = temperature in the flame zone

T_o = air inlet temperature

$(T_g - \Delta)$ = temperature of gas products exiting the flame zone.

Assumptions

1. The reactants are fully mixed in an assumed flame zone adjacent to the burner. The dimensions of the flame zone relative the heat sink surface are sketched below:



2. The heat transfer to the walls is by radiation only and the medium surrounding the flame zone is non-absorbing so that for $A_g << A_w$ the heat lost to the walls due to radiation is:

$$q_{rad} = \epsilon_g A_g \sigma (T_g^4 - T_w^4) \quad (5.9)$$

where A_g = flame zone surface area

A_w = surface area of furnace walls

T_w = wall temperature

ϵ_g = flame emissivity, and

σ = Stefan-Boltzmann constant.

The flame emissivity ϵ_g is assumed to be 0.8 for all the studied burner loads.

3. The volatile release rate is modelled by a single reaction model:

$$dV/dt = K (V^* - V) \quad (5.10)$$

where V = mass fraction of volatiles released in time t per unit mass of coal,

V^* = ultimate mass fraction volatiles release as $t \rightarrow \infty$ per unit mass of coal,

K = rate constant, $K = K_o \exp(-E/RT)$ (5.11)

The values of the rate constants were obtained from Badzioch and Hawksley (1970) as:

$E = 0.494 \times 10^8$ J/kg mol

$K_o = 706\ s^{-1}$, and

V^* = 1.25 x proximate volatiles content.

4. The residence time of coal particles is assumed to be constant (= 20ms) for all the cases. This assumption is justified on the basis

that the momentum ratios and the swirl numbers for the conditions in in Fig.5.8 (the case being studied) do not vary by a large magnitude.

5. The released volatiles mix with oxygen and burn instantaneously to produce heat at a rate:

$$q_v = m_F \times V \times H_v \qquad (5.12)$$

where m_F = coal mass feed rate,

H_v = net calorific value of volatiles.

For the present comparative analysis H_v was taken as the gross calorific value of the volatiles calculated from the expression of Jain and Sundararajan (1981). The volatiles were assumed to contain only carbon, hydrogen and oxygen. The amounts of these species were calculated from

$$C_{vol} = (C_{ult} - C_{fixed})$$

$$H_{vol} = (H_{ult} - H_{H2O})$$

$$O_{vol} = (O_{ult} - O_{H2O})$$

The calculated gross calorific value of the volatiles is equal to 10.0 MJ/kg coal.

6. The burning of the particles is modelled by the expression given by Field et al (1967) which includes both chemical and physical rate coefficients. The fractional mass loss of particles, M_p was solved from

$$\frac{dM_p}{dt} = \frac{6K_T\pi d_s^2 PP_{O2}}{\rho_C \pi d^3} \qquad (5.13)$$

where K_T = overall reaction rate coefficient,

d_s = particle diameter,

d = particle diameter at t = 0,

P = system pressure,

F_{O2} = molar fraction of oxygen in combustion gas, and

ρ_C = density of coal

For the present study, constant diameter of $d_s = d = 50\mu m$ is assumed. A constant stoichiometry is assumed for all the cases so that F_{O2} was assumed to be equal to 0.21. The density of coal, ρ_C, was taken as 1.2×10^3 kg/m^3 and $P = 1.013 \times 10^5$ Nm^{-2}. K_T is defined as:

$$K_T = \frac{1}{1/K_{CH} + 1/K_{pH}} \tag{5.14}$$

where

$$K_{CH} \equiv \text{chemical rate coefficient} \equiv A \exp(-E/RT) \tag{5.15}$$

$$K_{pH} \equiv \text{physical rate coefficient} \equiv \frac{4D_C M_C \Phi}{Rd_s(T_p + T_g)} \tag{5.16}$$

Here D_C is the diffusion coefficient and is defined as

$$D_C = D_o\left[\frac{P_o}{P}\right]\left[\frac{T_g}{T_o}\right]^{1.75} \tag{5.17}$$

where the subscript o designates the reference values of P and T. D_C is the binary diffusion coefficient for an $O_2 - N_2$ mixture, M_C is the atomic weight of carbon. Φ is the mechanism factor and its value is 2 if CO is the main product and 1 if CO_2 is the main product being driven away from the particle boundary layer. R is the universal gas constant and T_p is the particle temperature.

For the present calculations the rate constants $A = 0.86$kg/m^{2}s/(N/m^2) and $E = 1.052 \times 10^8$ J/kg mol for equation (5.15) were obtained from Baum and Street (1971). The values $D_o = 3.13 \times 10^{-4}$ m^2/s at the reference temperature and pressure of 1500K and 1.013×10^5 N/m^2 respectively and $\Phi = 2$, Rizvi (1985), are used for the calculations. The particle temperature is here assumed to be equal to the fluid

temperature. The heat released by the combustion of particles is defined as:

$$q_p = m_F \times M_p \times H_C \qquad (5.18)$$

where H_C = net calorific value of the residual coal.

The value of H_C = 20.0 MJ/Kg coal is here taken as the difference between the gross calorific values of the coal and that for the volatiles, see note (5) above.

8. The gas temperature exiting the defined zone, $(T_g - \Delta)$, is proportional to the coal feed rate and is defined by:

$$(T_g - \Delta) = (T_g - C/m_F) \qquad (5.19)$$

where C is a constant, here taken as C = 3600 K(kg/hr) and m_F is the coal feed rate in kg/hr.

9. The mass flow of gas products leaving the flame zone is equal to the sum of input mass flow rates (air plus (coal minus ash)). A constant level of 15% excess air is maintained for all coal feed rates. The inlet temperature of reactants is assumed to be 600K and the mean value of the specific heat of the gas products is taken as C_p = 1.12 kJ/kgK at 900K.

10. Constant wall temperature (T_w = 1200K) is assumed for all the burner loads.

Using the above assumptions, equation (5.8) was solved for T_g using the Newton Raphson's method for various coal feed rates. The ratio, $R_H = q_{rad}/q_{rel}$ was then evaluated and the results are presented in Fig. 5.10.

CHAPTER 6

EMISSIONS OF NITROGEN OXIDES

6.1. Introduction

Large reserves of coal make it an attractive major industrial fuel. However, one of the major constraints of its increased utility is due to the emission of pollutants such as the oxides of nitrogen, NO_x and sulphur, SO_x, into the environment. SO_x and NO_x released in stack plumes into the environment can travel a considerable distance. Subsequent deposition of the precipitations of SO_x and NO_x, commonly known as "acid rain" on forests and lakes results in the destruction of plant and aquatic life. Over 50% of the German forests, for example, exhibit damage which may be the result of acid rain, Heiting (1984). The harmful effects of NO_x may be more appreciated by illustrating its effects on human life. In sufficiently large concentrations, NO_2 affects the respiratory organs and NO reduces the capacity of blood to carry oxygen, Smith (1980).

The present chapter relates experimental data of NO_x emissions and a computer prediction procedure which has been coded so that the combined results should lead to a better understanding of NO formation mechanisms in a large scale laboratory furnace. Sections 6.2 and 6.3 provide the experimental conditions and the experimental methods and accuracy respectively. The NO prediction procedure with the aid of previous literature is described in seciton 6.4. The experimental results are presented in section 6.5 and a summary of the chapter in section 6.6.

6.2. Experimental Conditions

The furnace geometrical conditions and the input flow conditions have been described in section 4.2. United Kingdom Nottinghamshire Gedling coal was used as for the inflame measurements also for the present test programme. The analyses of the coal are provided in Tables 3.1 to 3.3.

The measurements were performed on the axis, near the exit of the furnace (X/D_S = 46.5). Trial radial traverses demonstrated uniformity of the gas species concentration at this station. Thirteen experimental runs were performed to determine the effects of the swirl number, S_s, the excess air and the primary stream to secondary air axial momenta ratio, R_m, on the emissions of NO_x. The run conditions are given in Table 6.1.

6.3. Experimental Methods and Accuracy

The experimental procedures have been described in section 3.6. The instrumental error did not exceed $\pm$3% of the measured value of the calibration gas over a number of hours. However the NO_x emissions were particularly sensitive to any flow asymmetries or to fluctuations in the input flow conditions. Indeed the NO_x emission measurements provided a reliable method of detecting changes of flow and combustion conditions in the near burner field. A detailed account of the consistency of data is provided in section 4.3.3. The NO_x measurements were repeatable to an accuracy of $\pm$5% of the measured ensemble mean.

Johnson et al (1978) showed experimentally that the NO_2 to NO ratio in the flame is small and that NO_2 is formed in the sampling probe. The amount of NO_2 so formed from NO depends on the rate at which the

sampled gas is quenched, the presence of oxygen, and also the availability of radicals, Cernansky and Sawyer (1974). Provided the gas sample is quenched rapidly, the amount of NO_x measured is invariant. The measured fraction of NO_2 in NO was generally less than 1%. Since the measuring time was longer for the separate measurements of NO_2 and NO, only the total NO_x was measured.

The NO is also subjected to heterogeneous reduction to N_2 by char particles especially in the presence of CO, De Soete (1985). The sampling probe was designed so that the sample was quenched near the probe tip to 150°C, well below the temperatures at which the heterogeneous reactions are important, Heap et al (1973).

6.4. Prediction Procedure For NO Formation

Since the major constituent of NO_x was NO, only the formation of NO is considered here. The small concentration of NO (≈0.05% by volume) permits the prior solution of the velocity, density and temperature fields using a generalised coal combustion prediction procedure described in detail by Lockwood et al (1984) and Rizvi (1985). The formation of NO depends on the concentration of other gas species, for example, OH and H_2O derived from the solution procedure of the combustion of coal. The equations governing the rate of formation of NO are solved after the solutions of the velocity, density and temperature have been converged.

6.4.1. NO Formation Mechanisms

NO may be formed by three processes:

(i) By the reaction of atmospheric nitrogen with oxygen (thermal NO),

(ii) By the reactions of the fuel derived hydrocarbon radicals with the molecular nitrogen and subsequent oxidation to NO (prompt NO), and

(iii) By the oxidation of chemically bound nitrogen in the fuel (fuel NO).

The formation of thermal NO is extremely dependent on temperature and residence time, Zeldovich (1985). The thermal NO formation in a typical coal fired combustor is substantially reduced at temperatures less than 1800K, Morrison (1980). The formation of prompt NO requires hydrocarbon radicals to react with the molecular nitrogen hence the mechanism is more prevalent in fuel-rich hydrocarbon flames. Smith et al (1982) have estimated that prompt NO in coal flames is less than 5% of the total NO formed. The fuel NO on the other hand amounts to over 80% of the total NO formed, Pershing and Wendt (1976). This NO yield is mainly controlled by the local stoichiometry and depends only weakly on temperature, De Soete (1985). Considering then only the formation of fuel NO, the reaction scheme used here is given in Fig 6.1.

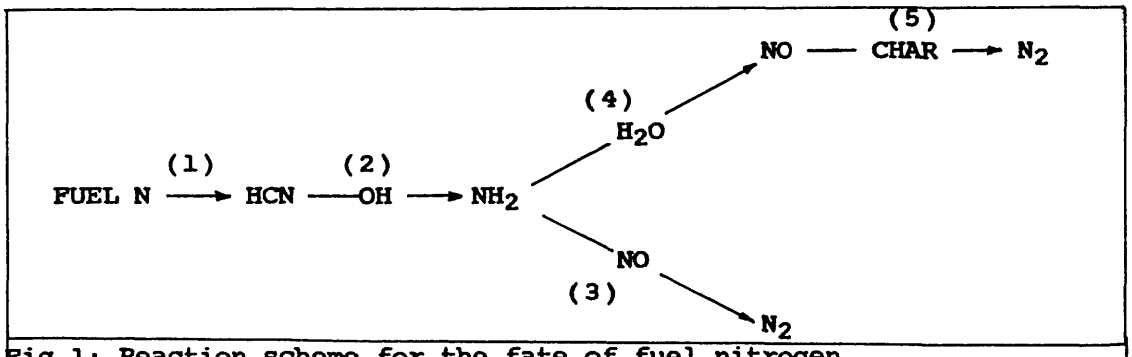


Fig.1: Reaction scheme for the fate of fuel nitrogen.

As coal enters the flame, the fuel bound nitrogen is either transformed very rapidly into HCN or it remains in the char. Fenimore (1976) observed experimentally that HCN did not form or destroy NO directly and recommended that HCN hydrolyzes entirely with OH to form NH_i + CO. This approach has been successfully used by Glass and Wendt (1982) to correlate their experimental measurements of HCN, NH_3 and NO in pulverised coal flames and is presently used here in preference to De Soete's (1974) model which excludes the reaction (2), see Fig 6.1.

The NH_i produced is subjected to two competitive reaction paths, one that results into the formation of NO (reaction (4)) by the attack of oxygen-containing species, OX, the other leading to N_2 formation on reacting with NO, reaction (3), Fenimore (1976). The correlation of the available reaction rate constants data with his experimental data resulted in Fenimore's (1976) choice of $NH_i = NH_2$, and $OX = H_2O$, Fenimore (1978). The NO formed may be subsequently reduced by char to form N_2. This occurs by means of dissociation of the adsorbed NO on the solid bound carbon atoms. Rapid surface diffusion and desorbtion leads to the formation of N_2 whereas the oxygen is strongly chemisorbed resulting in the formation of oxygen-carbon surface complexes which may desorb again as CO or as CO_2, Levy et al (1981). Reducing gases like CO and H_2 enhance the NO reduction rate by scavenging the inhibiting chemisorbed oxygen on the char particle surface, De Soete (1985). The reduction of NO by char in pulverised coal flames is less than 15% of the fuel NO formed earlier in the flames, Song et al (1982).

The yield of devolatilized nitrogen from coal increases with increasing temperature, but the conversion to NO decreases with

increasing nitrogen content in the homgeneous phase resulting in a weak temperature dependence of NO formation in pulverised coal flames, Wendt (1980). The fuel NO formed from the oxidation of the devolatilized nitrogen amounts to, depending on the stoichiometry, 60% to 80% of the total NO formed, Wendt (1980).

The fuel bound nitrogen that remains after devolatilization in the char is assumed to evolve at a rate proportional to the mean particle burnout. The evolved char nitrogen then follows the same reaction scheme as that for the homogeneous phase, see Fig. 6.1.

6.4.2. Modelling of Fuel NO Formation

The rate of nitrogen evovled (as HCN) from the coal is assumed to be directly proportional to S_m, the total mass of the material entering the gas phase from the coal due to pyrolysis and char burnout, per unit volume,

$$w_1 \equiv \frac{d(HCN)}{dt} = m_{n,c} S_m \qquad kg/cm^3 s \qquad (R1)$$

where $m_{n,c}$ is the mass fraction of nitrogen in the coal. S_m is evaluated in the main coal combustion computer programme. The concentrations of OH and NH_2 radicals are obtained by making partial equilibrum assumptions, Glass and Wendt (1982).

$$2H_2O \overset{K_{OH}}{\rightleftharpoons} H_2 + 2OH \qquad (6.1)$$

where $$K_{OH} = 2.841 \times 10^7 \exp(-\frac{137.7\ kCal}{RT}) \qquad (6.2)$$

and $$OH + NH_3 \overset{K_{NH3}}{\rightleftharpoons} NH_2 + H_2O \qquad (6.3)$$

where $$K_{NH3} = 1.661\exp(+\frac{12.1\ kCal}{RT}) \qquad (6.4)$$

Using the reaction rate data of Glass and Wendt (1982), the destruction rates of HCN and NO are given by

$$w_2 \equiv \frac{d[HCN]}{dt} = 5.5x10^{17}\exp\left(-\frac{83.3\ kCal}{RT}\right)\frac{[HCN][H_2O]}{[H_2]^{0.5}} \qquad \frac{mole}{cm^3 s} \qquad (R2)$$

and

$$w_3 \equiv \frac{d[NO]}{dt} = 2.2x10^{16}\exp\left(-\frac{54.4\ kCal}{RT}\right)\frac{[NO][NH_3]}{[H_2]^{0.5}} \qquad \frac{mole}{cm^3 s} \qquad (R3)$$

The rate of formation of NO, reaction (4) is given, Fenimore (1978), as

$$w_4 \equiv \frac{d[NO]}{dt} = w_3\ 700\exp\left(-\frac{50\ kCal}{RT}\right)\frac{[H_2O]}{[NO]} \qquad \frac{mole}{cm^3 s} \qquad (R4)$$

The heterogeneous reduction of NO is given by the correlation of Levy et al (1981)

$$w_5 \equiv \frac{d[NO]}{dt} = 4.18x10^{4}\exp\left(-\frac{34.7\ kCal}{RT}\right) A_E\ P_{NO} \qquad \frac{mole}{s} \qquad (R5)$$

where A_E is the external surface area of the char in m^2/gm and P_{NO} is in atmospheres.

The net overall production of the species HCN, NH_2 and NO are given as:

$$w_{HCN} = (w_1 - (w_2\ M_{HCN}))V \qquad kg/s \qquad (6.5)$$

$$w_{NH_2} = (w_2 - w_3 - w_4)V\ M_{NH_2} \qquad kg/s \qquad (6.6)$$

$$w_{NO} = ((w_4 - w_3)V - w_5)M_{NO} \qquad kg/s \qquad (6.7)$$

where M's are the molecular weights and V is the volume.

The effects of the turbulent fluctuations on the chemical reactions requires the knowledge of multi-dimensional probability density functions for the systems variables. Since the aim of the present study is to predict only the trends of NO, the complex interaction of turbulence on chemical kinetics is not included in this NO model. The

numerical solution procedure has been provided in the author's department by Offergeld (1986). At the time of writing, the coding of this NO subroutine had been completed and preliminary results obtained.

6.5 Discussion of Results

The formation of NO in pulverised coal flames will primarily depend on the rate of release of the fuel-bound nitrogen, on the availability of an oxidant, and their rate of reaction. Since most of the NO is produced from the devolatilized N, Wendt (1980), the formation of NO is in the main, a near burner field phenomenon. The rates of formation and destruction of NO by char are slow and hence not easily controllable. For a particular pulverised coal, the near field phenomena relevant to the NO formation are the overall flow patterns, the rate of mixing of the fuel and air, the local stoichiometry and the spatial location and residence time of coal particles near the burner zone. These phenomena are used to discuss the effects of swirl, excess air and the momentum ratio, R_m on NO_x. The measured values of NO_x were corrected for the dilution effect of the excess air, thus

$$NO_{x,stoich} = NO_{x,meas} \times \lambda \qquad (6.8)$$

where $$\lambda = \frac{(\ A/F\ )_{input}}{(\ A/F\ )_{stoich}} \qquad (6.9)$$

6.5.1. The Influence of Swirl Number, S_g

The swirl number was varied between $S_g = 0.77$ and $S_g = 1.45$. Fig. 6.2. shows that on increasing the swirl number whilst maintaining the momentum ratio and the excess air constant, the NO_x emission

decreases at first and reaches a minimum when S_g = 1.27 but then it increases again. The decline in emissions between S_g = 0.77 and 1.27 may be explained with reference to the associated predicted flow profiles, Fig. 6.3. With increasing swirl the forward stagnation point moves further upstream towards the burner resulting in a shorter length of the penetration of the primary stream into the inner recirculation zone (IRZ). For the case when S_g = 1.27, because the coal particles are turned around (reverse axial flow) their residence time in this central fuel rich zone increases. This leads to the preference of reaction (3), the destruction of NO. Furthermore the longer residence of particles in this region means more nitrogen being devolatilized, but a lower conversion rate to NO, as observed also by Wendt (1980) and Song (1982). This results also in a smaller amount of fuel-bound nitrogen remaining in the char, leading to a smaller subsequent amount of NO produced from the char-N.

At lower swirl numbers, the central primary stream rapidly transgresses the fuel rich central zone, whilst at the higher swirl numbers, there is an increased tendency for the primary stream to be radially deflected away from the central IRZ, towards the fuel lean secondary air stream. Both of these flow changes result in higher NO_x. These flow patterns for progressively increasing swirl numbers are known in the IFRF terms, Bortz (1983) as: the type III whereby there is no IRZ, type I with partial penetration and type II with no penetration into the IRZ, see Fig. 2.1.

The observed trend of NO_x versus swirl number is in qualitative agreement with the results presented by Hill et al (1984), for a smaller scale laboratory furnace and exceptionally high swirl numbers $0 < S_g < 7.0$. Higher swirl numbers were probably necessary to

establish an IRZ for the smaller geometry, Claypole and Syred (1981), Escudier and Zehnder (1982). Experimental data obtained from a 2m x 2m IFRF furnace, Phelan and Flament (1983), show the tendency of increasing NO_x emissions with the increase in swirl in the range 0.3 < S_s < 2.1, the rate of change of NO_x being dependent upon the coal type.

The present data show an increase of NO_x for the range of swirl numbers 1.27 < S_s < 1.45. From the comparison with the referred literature, it is apparent that the difference in the NO trend may be due to the changes in flow patterns which depend on the burner and furnace geometries as well as the input flow conditions.

The exit O_2 concentrations, also shown in Fig. 6.2 illustrate the effect of increasing swirl on the improved burnout, hence lower O_2.

6.5.2. The Influence of Excess Air

Increasing the input excess air for constant swirl number and the momentum ratio results in increasing NO_x emissions, see Fig. 6.4. Since the formation of NO , reaction (4) depends strongly on the availability of an oxidant, the NO increase would be expected with increasing excess air, despite some reduction of temperature due to the dilution effect of the excess air. Theoretically, the NO should reach a maximum constant value when all the coal bound nitrogen has been depleted. This stage is rarely reached because of the economical requirement of operating boilers at as low an excess air as possible. Of course at stoichiometric or low excess air conditions, there is an increased susceptibility of incomplete combustion and increased CO emissions. The observed NO_x versus excess air trend is universal for the conventional furnaces and has also been observed amongst others

by Wendt (1980), Asay et al (1983), Phelan and Flament (1983) and Okazaki et al (1984).

6.5.3. The Influence of Primary Stream to Secondary Air Axial Momentum Ratio, R_m

The effects of R_m on the NO_x emissions has not been previously studied. Fig. 6.5 illustrates the present experimental data of NO_x showing the effect of R_m. The flue NO_x declines rapidly from 625ppm when R_m = 0.12 to 540ppm when R_m = 0.16. The NO_x emission is insensitive to R_m for $0.16 < R_m < 0.28$. A transformation of the flow pattern from the type II at low R_m, to type I is likely to have occurred between R_m = 0.12 and 0.16. At low R_m the central fuel-laden jet is deflected outwards to the oxygen-rich secondary air stream, hence high NO_x.

As R_m increases, the flow partially penetrates the IRZ resulting in the release of fuel-N under oxygen lean region hence a decline in NO_x. This type I flow persists and gradually transforms to the type III flow for the high values of R_m and the insensitivity of NO_x emissions is due to two self cancelling effects. On the one hand the mixing between the primary and secondary streams declines with increasing R_m due to the diminishing difference in their velocities resulting in localised fuel-rich pockets, hence low NO_x. On the other hand, the requirement that all other input conditions be held constant results in the increase of the ratio of the primary air to coal mass flow rates with increasing R_m, thus providing oxygen to the otherwise oxygen lean central region. This means an increase in NO emissions. There results no net influence of high value of R_m on NO_x.

6.6. Summary

It cannot be over-emphasised as to the care that was taken to obtain the repeatable NO_x data to within $\pm 5\%$ of the ensemble mean. The experimental data show that there exists an optimum value of the swirl number when the NO_x emission is a minimum for constant momentum ratio and excess air. Although better burnout is obtained at higher swirl numbers, the NO_x emissions increase. In agreement with other workers, increasing the excess air results in the increase of NO_x emissions. The NO_x emission decreases rapidly with increasing R_m for $0.12 < R_m < 0.16$ but it is insensitive to higher values of R_m up to $R_m = 0.28$. This is an important parameter for the design of burners since it is a function of the flow velocities, hence its importance for the calculation of pressure drop amongst other parameters.

The experimental data reported here will be very useful for the validation of the proposed computational code for the prediction of NO.

Table 6.1: Run Conditions: NO_x Emission Measurments

Flame Index	m_c kg/hr	m_p kg/hr	m_s kg/hr	λ	R_m	S_s
A1	12	26.8	108.7	1.15	0.20	1.27
A2/C3	16	35.7	145.0	1.15	0.20	1.27
B1	12	27.6	102.0	1.10	0.24	1.00
B2/D2	12	29.0	106.5	1.15	0.24	1.00
B3	12	30.5	110.9	1.20	0.24	1.00
B4	12	31.9	115.4	1.25	0.24	1.00
C1	16	27.9	152.7	1.15	0.12	1.27
C2	16	32.1	148.5	1.15	0.16	1.27
C4	16	38.7	141.9	1.15	0.24	1.27
C5	16	41.4	139.2	1.15	0.28	1.27
D1	12	29.0	106.5	1.15	0.24	0.77
D3	12	29.0	106.5	1.15	0.24	1.27
D4	12	29.0	106.5	1.15	0.24	1.45

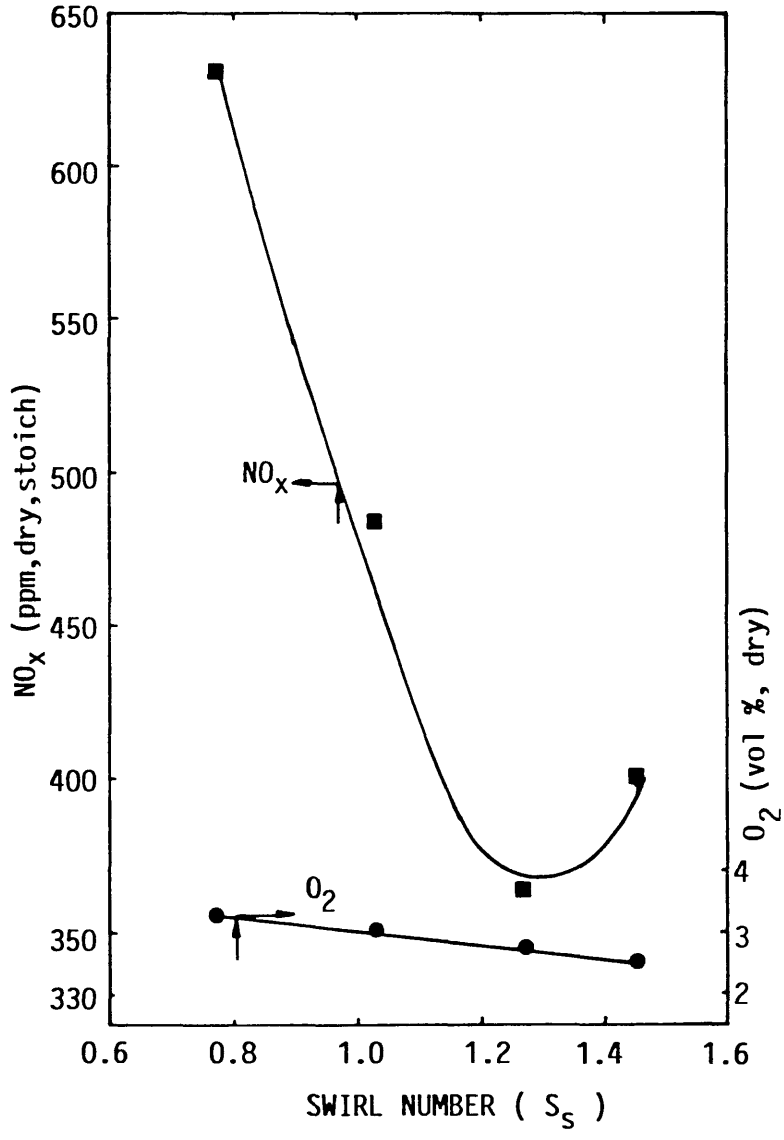


Fig. 6.2 Effect of swirl on emission of NO_x.

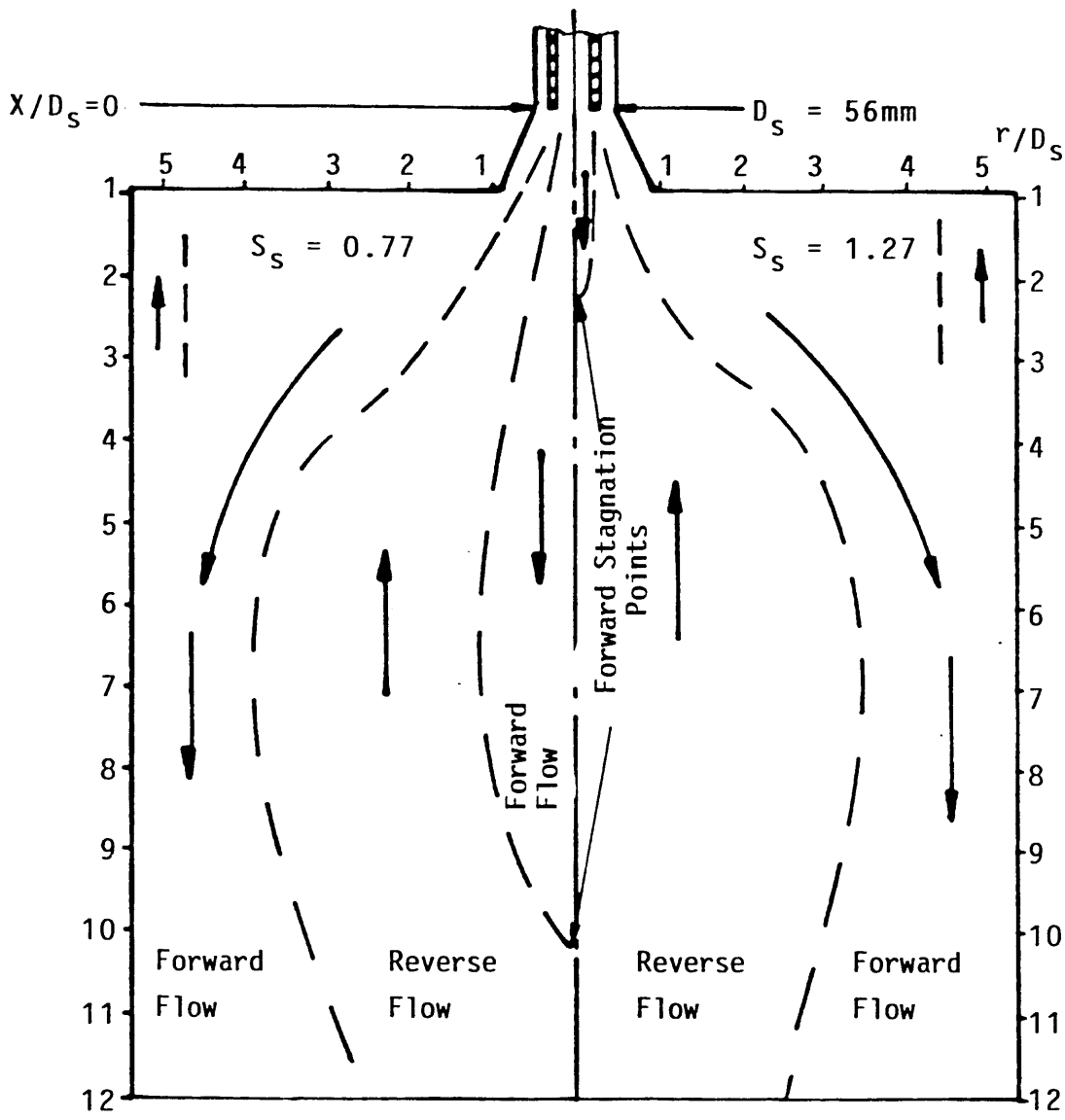


Fig. 6.3 Predicted near field flow patterns for S_s = 0.77 and S_s = 1.27.

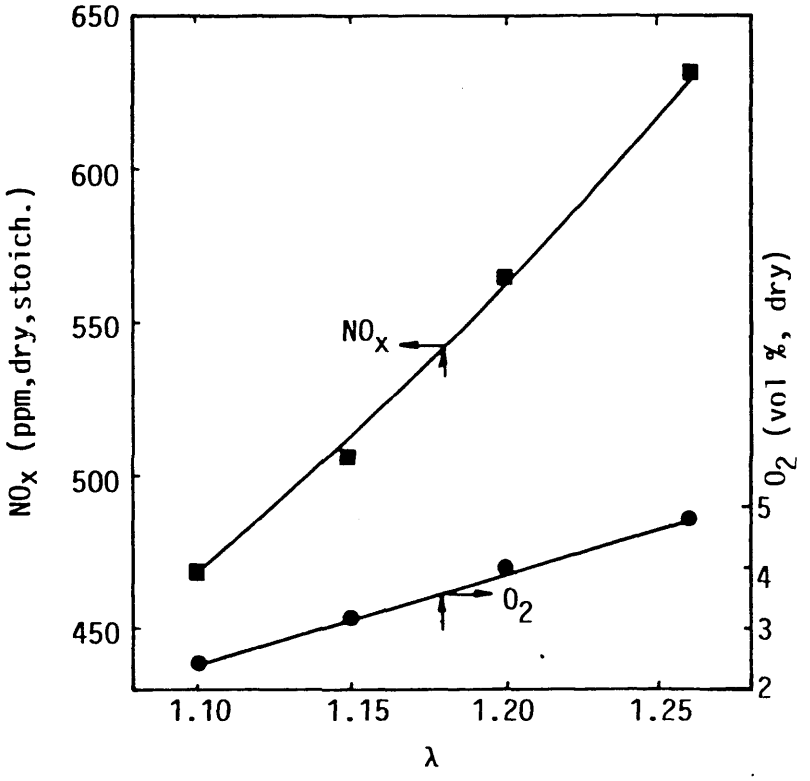


Fig. 6.4 Effect of excess air on emission of NO_x.

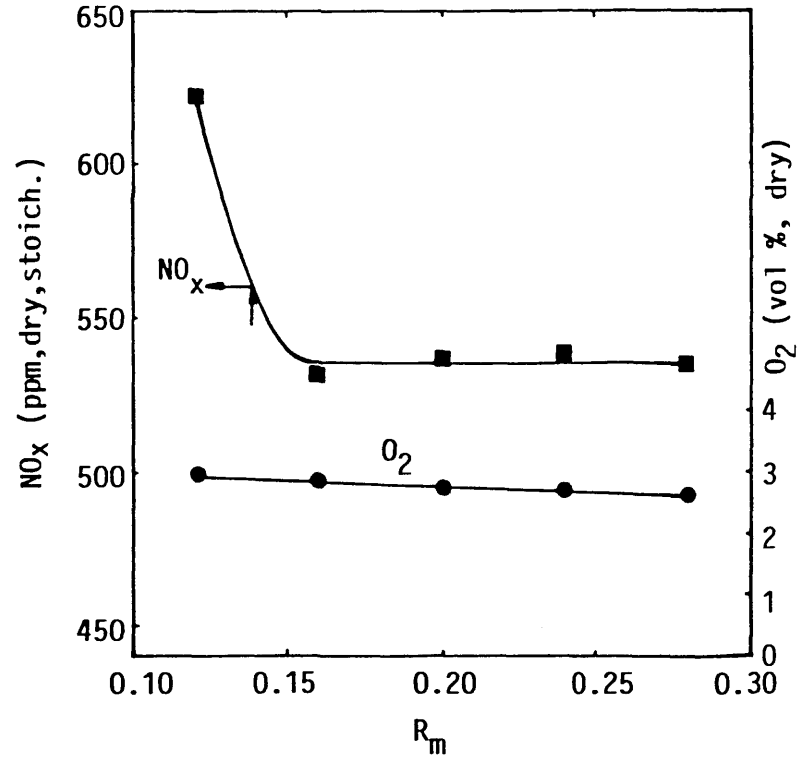


Fig. 6.5 Influence of momentum ratio, R_m, on emission of NO_x.

CHAPTER 7

CLOSURE

The main findings of the thesis are summarised in the first sub-section of this chapter and recommendations for further research are made in the second sub-section.

7.1. Conclusions

Experimental data of (a) inflame gas species concentration and temperature, (b) flame stability and (c) nitrogen oxides (NO_x) emissions have been presented and discussed. Considerable difficulties were encountered especially those connected with the inflame and NO_x measurements. The majority of the difficulties were associated with flow asymmetries which occurred due to slight burner misalignments and slag deposition on the quarl surface. Monitoring of consistency of the presented data was by means of frequent repetitions of inflame measurements on a few locations. The inflame results presented here were repeatable to less than $\pm$10% of their mean values.

The on-axis inflame data illustrate that increasing the swirl results in more rapid evolution of the volatiles and more rapid combustion. The effect of increasing the excess air from 15% to 25% is to promote the rates of both production and decay of CO. The radial data for swirl numbers S_g = 0.78 and S_g = 1.03 show that for both these conditions the central primary jet penetrates at least two burner diameters into the central region of the furnace. Significant concentrations (> 50ppm) of unburnt hydrocarbons were measured up to X/D_g = 13 for both the swirl numbers, but much higher concentrations were measured when operating at the lower swirl number, S_g = 0.78. The reaction zone shifted away from the axis when the swirl number

was increased and also resulted in a more rapid decay of the species concentrations. The temperature profiles near the burner indicate the existence of an annular inner recirculation zone. Further downstream the temperature profiles quickly flattened due to strong radiation exchange between the particles and the walls.

Flame stability data have been presented in terms of the secondary air swirl number, S_s and the ratio of the axial momentum of the primary stream (coal plus air) to that of the secondary air, R_m. The data exhibit a minimum swirl number, $S_{s,min}$, below which a stable flame is not possible and a maximum value of the momentum ratio, $R_{m,max}$, beyond which a stable flame is not possible. The results show that for the fixed burner and furnace geometries, and for a given coal, the flame stability is enhanced by lowering the inlet primary air velocity, by increasing the excess air level and especially by increasing the fineness of grind of the coal.

The stability performance of the various bituminous coals is characterised by their volatiles (daf) content. The data show that the limiting values $S_{s,min}$ and $R_{m,max}$ depend on the burner load. At low heat inputs the limits are inferior because of the increased relative heat lost to the walls. $R_{m,max}$ increases rapidly with increasing burner loads. For Gedling coal feed rates m_c > 16 kg/hr, $S_{s,min}$ remains insensitive to the burner load. The firing of the Gedling microfine coal resulted in much enhanced flame stability. A decline of $R_{m,max}$ was however observed as the burner load was increased from 130kW to 163kW. The stability performance of a low-volatile char was poor even though it was fired at low inlet velocities.

The NO_x emissions data show that the emissions increase with excess air. For a given value of excess air and the momenta ratio, R_m, there exists an optimum value of the swirl number at which the NO_x emission is a minimum. The NO_x emission decreases rapidly with increasing R_m for $0.12 < R_m < 0.16$ but it is insensitive to higher values of R_m up to $R_m = 0.28$. A model has been proposed for the prediction of NO formation.

The presented experimental data are believed to be as accurate as practically possible for measurements carried out in pulverised coal flames. They are well defined and consistent, and because of the axial symmetry of the flow, they render themselves particularly suitable for the validation of the computer prediction models.

7.2. Recommendations for Future Work

The inflame measurements may be extended to evaluate the influences of the momentum ratio, the burner load and the coal type.Measurements in lifted flames are also desirable. The flame stability experiments should be extended to cover the effects of burner geometry, for example the quarl half-angle. Inflame measurements of NO_x should be attempted and various burner configurations should be experimentally explored in order to optimise a low-NO_x burner configuration.

The axial location nearest to the burner throat at which inflame measurements were made was two burner diameters downstream. Measurements even closer to the burner are desirable but difficult mainly because of blockage of the sampling probe. Also, in the near burner region, the aerodynamic blockage due to the sampling probe itself may strongly affect the flow. It is recommended therefore that optical systems be developed for the measurements of the

concentration of the gas species, the particle size, the temperature of the particles and the gas, and the velocities of both the particles and the gas. The near burner data will extend understanding of the flame stabilisation and NO_x formation mechanisms.

The measurement of the velocities of the fluid and solid particles though difficult, are particularly desirable. Currently an LDA system for the measurement of isothermal gas-solid flows is being developed at the author's department. Such a system needs much further development in order to be able to measure the two phase velocities in a large furnace firing poly-disperse, non-spherical coal particles.

REFERENCES

A.S. ABBAS and F.C. LOCKWOOD (1986).
Prediction of power station combustors. To be presented at the 21st Symposium (Int) on Combustion, The Combustion Institute.

V.N. AFROSIMOVA (1967).
Study of the aerodynamics of a furnace space. Thermal Engineering, Vol. 14, p.10.

R.A. ALTENKIRCH and A.M. MELLOR (1974).
Emissions and performance of continuous flow combustors. 15th Symposium (Int) on combustion, The Combustion Institute, p. 1181.

H. ALTGELD, W.P. JONES and J. WILHEMI (1983).
Velocity measurements in a confined swirl driven recirculating flow. Exp in fluids, 1, p.73.

K. ANNAMALAI and P. DURBETAKI (1977).
A theory on transition of ignition phase of coal particles. Comb. and Flame, 29, p.193.

D.B. ANTHONY, J.B. HOWARD, H.C. HOTTEL and H.P. MEISSNER (1974).
Rapid devolatilization of pulverised coal. 15th Symposium (Int) on Combustion, The Combustion Institute, p.1303.

B.W. ASAY, L.D. SMOOT and P.O. HEDMAN (1983)
Effect of coal moisture on burnout and nitrogen oxide formation. Comb. Sci. and Tech., 35, p.15.

A.M. ATTYA and J.H. WHITELAW (1981).
Velocity, temperature and species concentrations in unconfined kerosene spray flames. ASME paper 81-WA/HT-47.

S. BADZIOCH and P.G.W. HAWKSLEY (1970).
Kinetics of thermal decomposition of pulverised coal particles. Ind. Eng. Chem. Process Des. Develop., Vol 9, No. 4.

P.C. BAKER, M.H. BARKER, D.J. LOVERIDGE, G.G. THURLOW and G.J. WINGFIELD (1969).
A furnace for research into the combustion of pulverised coal. J. Inst. Fuel, 42, p.371.

R.J. BAKER, P. HUTCHINSON, E.E. KHALIL and J.H. WHITELAW (1974).
Measurements of three velocity components in a model furnace with and without combustion. 15th Symposium (Int) on combustion, The Combustion Institute, p-553.

S. BANDYOPADHYAY and D. BHADURI (1972).
Prediction of ignition temperature of a single coal particle. Comb. and flame, 18, p.411.

M.M. BAUM and P.J. STREET (1971)
Predicting the combustion behaviour of coal particles. Comb. Science and Tech., 3, p.231.

J.M. BEER (1962).
Combustion of pulverised coal. Proc. 2nd symposium on Flames and Industry, Inst. of Fuel, London, June 1962.

J.M. BEER, N.A. CHIGIER and K.B. LEE (1963).
Modelling of double concentric burning jets. 9th Symposium (Int) on Combustion Institute, p.892.

J.M. BEER (1964).
The effect of fineness and recirculation on the combustion of low volatile pulverised coal. J. Inst. Fuel, 37, p.286.

J.M. BEER and N.A. CHIGIER (1969).
Stability and combustion intensity of pulverised-coal flames - effect of swirl and impingement, J. Inst. Fuel, 42, p443.

J.M. BEER and N.A. CHIGIER (1972)
Combustion Aerodynamics. Applied Science Pulbishers Ltd, London.

J.M. BEER (1986)
Clean combustion of coal, research and applications. An overview of recent developmenmts in the USA. J. Inst. Energy, 59, p.3.

C.L. BEYLER and F.C. GOULDIN (1981).
Flame structure in a swirl stabilised combustion inferred by radiant emission measurements. 18th Symposium (Int) on Combustion. The Combustion Institute, p.1011.

R.W. BILGER (1977).
Probe measurements in turbulent combustion. Progress in Aeronautics and Astronautics, 53, p.49.

S. BORTZ (1983).
Background and programme outline for the IFRF burner near field aerodynamics project. IFRF Doc. nr G14/a/2.

H.M. BOWERS and J.G. WRIGHT (1978).
An investigation of pulverised fuel deposition in a long horizontal pipeline following a 90 degrees horizontal bend. Pneumotransport 4, paper A2.

D. BRADLEY, G.DIXON-LEWIS, S. EL-DIN HABIK and E.M.J. MUSHI (1984).
The oxidation of graphite powder in flame reaction zones. 20th Symposium (Int) on Combustion, The Combustion Institute, p. 931.

D. BRADLEY and A.G. ENTWISTLE (1961).
Determination of the emissivity, for total radiation, of small diameter platinium - 10% rhodium wires in the temperature range 600-1450°C. British Journal of Applied Physics, 12, p. 708.

D. BRADLEY and K.J. MATHEWS (1968).
Measurement of high gas temperatures with fine wire thermocouples. J. Mech. Eng. Science, 10, p.299.

BRITISH STANDARDS (1977).
BS1016: Methods for analysis and testing of coal and coke. The British Standards Institution.

J.E. BROADWELL, W.J.A. DAHM and M.G. MUNGAL (1984).
Blowout of turbulent diffusion flames. 20th Symposium (Int) on Combustion, The Combustion Institute, P. 303.

R.S. BROKAW (1961).
Alignment charts for transport properties viscosity, thermal conductivity and diffusion coefficeints for nonpolar gases and gas mixtures at low density. NASA TR R-81.

H.M. CASSEL and I. LIEBMAN (1959).
The cooperative mechanism in the ignition of dust dispersions. Comb. Sci. and Tecnology, 3, p.467.

N.P. CERNANSKY and R.F. SAWYER (1974).
NO and NO_2 formation in a turbulent hydrocarbon/air diffusion flame. 15th Symposium (Int) on Combustion, The Combustion Institute, p. 1039.

A. CHAKRAVARTY, F.C.LOCKWOOD and G. SINICROPI (1984).
The prediction of burner stability limits. Comb. Sci. and Tech., 42, p.67.

J. CHEDAILLE and Y. BRAUD (1972).
Industrial Flames, J.M. BEER and M.W. THRING (Eds.), Vol 1: Measurements in Flames, Edward Arnold, ISBN 0-731-3265-5.

J. CHEDAILLE and K. HEMSATH (1965).
C-10 trials: influence of burner type, coal fineness, the proportion of primary air and temperature on the combustion of pulverised coal. IFRF Doc. nr. F 32/ac/32.

J. CHEDAILLE, W. LEUCKEL and A.K. CHESTERS (1966).
Aerodynamic studies carried out on turbulent jets by the International Flame Research Foundation. J. Inst. Fuel, 39, p.506.

M. CHEN, L. FAN and R.H. ESSENHIGH (1984).
Prediction and measurement of ignition temperatures of coal particles. 20th Symposium (Int) on Combustion, The Combustion Institute, p. 1513.

S.L. CHEN, M.P. HEAP, D.W. PERSHING and G.B. MARTIN (1982).
Influence of coal composition on the fate of volatile and char nitrogen during combustion. 19th Sumposium (Int) on Combustion, The Combustion Institute, p. 1271.

T.C. CLAYPOLE and N. SYRED (1981).
The effect of swirl burner aerodynamics on NO_x formation. 18th Symposium (Int) on Combustion, The Combustion Institute, p.81.

T.C. CLAYPOLE and N. SYRED (1982).
The stabilization of flames in swirl combustors. J. Inst Energy, 55, p.14.

J.G. COGOLI, D. GRAY and R.H. ESSENHIGH (1977).
Flame stabilization of low volatile fuels. Comb. Sci. and Tech., 16, p 165.

D. COOK and N.R. HURWORTH (1980).
Recent research on pulverised fuel settlement in power station pipelines, and the significance of "roping". Pneumotransport 5, paper F2.

G.G. DESOETE (1974).
Overall reaction rates of NO and N_2 formation from fuel nitrogen. 15th Symposium (Int) on Combustion. The Combustion Institute, p. 1093.

G.G. DESOETE (1985).
Environmental aspects of coal combustion: NO_x and SO_x. Pulverised coal combustion - intensive course organised by F.C. Lockwood, held at Imperial College, London.

T.F. DIXON, J.S. TRUELOVE and T.F. WALL (1983).
Aerodynamic studies on swirled coaxial jets from nozzles with divergent quarls. Trans. ASME, J. Fluids Eng., 105, p. 197.

V.M. DOMKUNDWAR, V. SRIRAMULA and M.C. GUPTA (1979).
Factors controlling stability of swirling flames at diffusers in gas turbines. J. Inst. Energy, 52, p.17.

E.R.G. ECKERT and R.M. DRAKE (1959).
Heat and Mass Transfer. McGraw-Hill book co., New York.

H. EICKHOFF, B. LENZE and W. LEUCKEL (1984).
Experimental investigation on the stabilization mechanism of jet diffusion flames. 20th Symposium (Int) on Combustion, The Combustion Institute, p. 311.

ELECTRICITY COUNCIL (1984-85).
The electricity council annual report, U.K. ISBN 0 85188 0991.

M.A. ELLIOT (1981).
Chemistry of Coal Utilization, M.A. Elliot, ed., Wiley Publ.

M.P. ESCUDIER and N. ZEHENDER (1982).
Vortex-flow regimes. J. Fluid Mech., 115, p. 105.

M.P. ESCUDIER and J.J. KELLER (1983).
Vortex breakdown: a two-stage transition. AGARD, CP342, paper 25.

M.P. ESCUDIER and J.J. KELLER (1985).
Recirculation in swirling flow: A manifestation of vortex breakdown, AIAA, 23, p.111.

R.H. ESSENHIGH (1957).
Burning times of coal particles in a P.F. furnace. 2nd Conference on Pulverised Fuel (CPF), Inst of Fuel, paper 2.

R.H. ESSENHIGH (1961).
A Short history of pulverised-fuel firing. J. Inst. Fuel, 34,p.16.

R.H. ESSENHIGH and J. CSABA (1963).
The thermal radiation theory for plane flame propogation in coal dust clouds. 9th Symposium (Int) on Combustion, The Combustion Institute, p. 111.

R.H. ESSENHIGH (1976).
Combustion and flame propogation in coal systems.: A review. 16th Symposium (Int) on Combustion. The Combustion Institute, p. 353.

R.H. ESSENHIGH (1981).
Fundamentals of Coal Combustion. Chemistry of coal utilization, M.A. ELLIOT, Ed., Wiley Publ., chapter 19.

J.H. FALER and S. LEIBOVICH (1977).
Disrupted states of vortex flow and vortex breakdown. The Physics of Fluids, 20, p. 1385.

M. FARADAY and C. LYELL (1845).
Explosions in coal mines. Phil. Mag., 26, p.16.

C.P. FENIMORE (1970).
Formation of nitric oxide in premixed hydrocarbon flames. 13th Symposium (int) on Combustion, The Combustion Institute, p. 373.

C.P. FENIMORE (1976).
Reactions of fuel-nitrogen in rich flame gases. Comb. and Flame, 26, p. 249.

C.P. FENIMORE (1978).
Studies of fuel-nitrogen species in rich flame gases. 17th Symposium (Int) on Combustion, The Combustion Institute, p. 661.

M.A. FIELD, D.W. GILL, B.B. MORGAN and P.G.W. HAWKSLEY (1967)
Combustion of pulverised coal. The British Coal Utilization Research Association, Leatherhead, U.K. (reprinted in 1983 by the Institute of Energy).

D.A. FRANK-KAMENETSKII (1955).
Diffusion and heat exchange in chemical kinetics, translated by N. Thon. Princeton University Press.

N. FRICKER and W. LEUCKEL (1976).
The characteristics of swirl-stabilized natural gas flames. Part 3: The effect of swirl and burner mouth geometry on flame stability. J. Inst. Fuel, 49, p. 152.

R.M. FRISTROM and A.A. WESTENBERG (1965).
Flame Structure. McGraw-Hill Book Co.

R.W. FROBERG and R. ESSENGHIGH (1978).
Reaction order and activation energy of carbon oxidation during internal burning. 17th Symposium (Int) on Combustion, The Combustion Institute, p. 179.

A.G. GAYDON and H.G. WOLFHARD (1979).
Flames, their structure, radiation and temperature. 4th ed., Chap and Hall-London.

D.W. GILL (1975).
Pulverised-coal firing. A review of J. Inst. Fuel literature. Energy World, 14, p.4.

J.W. GLASS and J.O.L. WENDT (1982).
Mechanisms governing the destruction of nitrogeneous species during the fuel rich combustion of pulverised coal. 19th Symposium (Int) on Combustion, The Combustion Institute. p. 1243.

I. GLASSMAN (1977)
Combustion, Academic Press.

S. GODOY (1982).
Turbulent diffusion flames. Ph.D. Thesis, University of London.

P.M. GOLDBERG and R.H. ESSENHIGH (1978).
Coal Combustion in a jet-mix stirred reactor. 17th Symposium (Int) on Combustion, The Combustion Institute, p. 145.

A.D. GOSMAN, F.C. LOCKWOOD and A.P. SALOOJA (1978).
The prediction of cylindrical furnaces gaseous fuelled with premixed and diffusion burners. 17th Synposium (Int) on Combustion, The Combustion Institute, p. 747.

A.K. GUPTA, D.G. LILLEY and N. SYRED (1984).
Swirl flows. Abacus Press. ISBN 085626 1750.

K. GURUZ and C. ILICALI (1981).
An invetigation of isothermal confined double concentric jet system. Comb. Sci. and Tech., 25, p. 193.

A. HAGIWARA and S. BORTZ (1984)
Studies on the near field aerodynamics of swirl burners. IFRF Doc. nr. F. 259/a/1.

I. HARDALUPAS, A.M.K.P. TAYLOR and J.H. WHITELAW (1986).
Measurements of velocity in two-phase recirculating flows (in preparation), Imperial College, London.

J.K. HARVEY (1962).
Some observations of the vortex breakdown phenomenon. J. Fluid Mech., 14, p.585.

M.M.A. HASSAN (1983)
A study of natural gas and pulverised coal diffusion flames. Ph.D Thesis, University of London.

M.M.A. HASSAN, F.C. LOCKWOOD and H.A. MONEIB (1983).
Measurements in a gas-fired cylindrical furance. Comb. and Flame, 51, p. 249.

M.A. HASSAN, K.A. HIRJI, F.C.LOCKWOOD and H.A. MONEIB (1985).
Measurements in a pulverised coal-fired cylindrical furnace. Exp. in Fluids, 3, p. 153.

H. HATTORI (1956).
Flame propogation in pulverised coal-air mixtures. 6th Symposium (Int) on Combustion, The Combustion Institute, p. 590.

M.P. HEAP, T.M. LOWES and R. WALMSLEY (1973).
Emission of nitric oxide from large turbulent diffusion flames. 14th Symposium (Int) on Combustion, The Combustion Institute, p. 883.

A.B. HEDLEY and E.W. JACKSON (1966).
A simplified mathematical model of a pulverised coal flame showing the effect of recirculation on combustion rate. J. Inst. Fuel, 39, p. 208.

K. HEIN and W. LEUCKEL (1969).
Trials C-14. Further studies on the effect of swirl on pulverised coal flames. IFRF Doc. No. F32/a/40^2.

B. HEITING (1984).
Abscheidung von NO_x and SO_2 Aus Rauchgasen, BWK 36, Nr. 10, S.411.

M.V. HEITOR (1985).
Experiments in turbulent reacting flows. Ph.D. Thesis, University of London.

M. HERTZBERG, K.L. CASHDOLLAR, D.L. NG and R.S. CONTI (1982).
Domains of flammability and thermal ignitability for pulvrised coals and other dusts: particle size dependencies and microscopic residue analyses. 19th Symposium (Int) on Combustion, The Combustion Institute, p. 1169.

R.S. HIGGINS AND W.J. MORLEY (1984).
International register of experimental furnaces associated with combustion and combustion related processes. Herman Research Laboratory, State Electricity Commission of Victoria, Australia.

S.C. HILL, L.D. SMOOT and P.J. SMITH (1984).
Prediction of nitrogen oxide formation in turbulent coal flames. 20th Symposium (Int) on Combustion. The Combustion Institute, p. 1391.

K. A. HIRJI, M. ISMAIL, F.C. LOCKWOOD and J. MILLER (1986).
Burner stability limits of some pulverised fuels. Imperial College, Mech. Eng. Dept., report FS/86/13.

G. HORN, J. CSABA and P.J. STREET (1966).
Combustion experiments using a pulverised-coal fired superheater. J. Inst. Fuel, 39, p. 521.

H.C. HOTTEL (1974).
First estimates of industrial furnace performance - the one-gas-zone model re-examined. Heat Transfer in Flames, N.H. AFGAN and J.M. BEER, Eds. Wiley Pubs, ISBN 0-470-00931-4, chapter 1.

J.B. HOWARD and R.H. ESSENHIGH (1965).
The mechanism of ignition of pulverised coal. Comb. and Flame, 9, p. 337.

J.B. HOWARD and R.H. ESSENHIGH (1966 (a)).
Combustion mechanism in pulverised coal flames. Comb. and Flame, 10, p. 92.

J.B. HOWARD and R.H. ESSENHIGH (1966 (b)).
Mechanism of solid-partical combustion with simultaneous gas-phase volatiles combustion. 11th Symposium (Int) on Combustion, The Combustion Institute, p.399.

J.B. HOWARD (1981)
Fundamentals of coal pyrolysis and hydropyrolysis. Chemistry of Coal utilization, M.A. ELLIOT, Ed., Wiley Publ., chapter 12.

E.H. HUBBARD (1960)
The first performance trial and first combustion mechanism trial with pulverised coal. J. Inst. Fuel, 33, p.386.

M. ISMAIL (1986)
Private Communication. Imperial College, Mech. Eng. Dept.

S.R. JAIN and R. SUNDARARAJAN (1981).
New method of calculating calorific values from elemental compositions of fossil fuels. FUEL 60, p. 1079.

A.S. JAMALUDDIN, J.S. TRUELOVE and T.F. WALL (1986).
Devolatilization of bituminous coals at medium to high heating rates. Comb. and Flame, 63, p.329.

G.M. JOHNSON, M.Y. SMITH and M.F.R. MULCAHY (1978).
The presence of NO_2 in premixed flames. 17th Symposium (Int) on Combustion, The Combustion Institute, p. 647.

W.P. JONES and J.H. WHITELAW (1984).
Modelling and measurements in turbulent combustion. 20th Symposium (Int) on combustion, The Combustion Institute, p.233.

M.JOST, I. LESLIE and C. KRUGER (1984).
Flow-tube reactor studies of devolatilization of pulverised coal in an oxidising environment. 20th Symposium (Int) on Combustion, The Combustion Institute, p. 1531.

H. JUNTGEN AND K.H. VAN HEEK (1968).
Gas release from coal as a function of the rate of heating. FUEL, 47, P. 103.

A.M. KANURY (1975).
Introduction to Combustion Phenomena. Gordon and Beach Sci. Publ. ISBN 0-677-02690-0.

I.M. KENNEDY AND J.H. KENT (1981).
Scalar measurements in a co-flowing turbulent diffusion flame. Comb. Sci. and Tech., 25, p109.

K. KIMOTO, I. SHIRAISHI and R. MATSUMOTO (1981).
Structure of turbulent jet flames in annular air jet. Comb. Sci. and Tech., 25, p.31.

G.E. KLINZING (1981)
Gas-solid transport. McGraw-Hill. ISBN 007035047 7.

H. KOBAYASHI, J.B. HOWARD and A.F. SAROFIM (1976).
Coal devolatilization at high temperatures. 16th Symposium (Int) on Combustion, The Combustion Insttitute, p. 411.

A.A. LEFT (1983)
Particle size dependence of the evolution and yield of products from coals under rapid heating conditions. Proc. IEA Conference (Int) on Coal Science, p. 499.

S. LEIBOVICH (1978).
The structure of vortex breakdown. Ann. Rev. Fluid Mech., 10, p. 221.

G. LENGELLE and C. VERDIER (1973).
Gas sampling and analysis in combustion phenomena. AGARDOGRAPH No. 168.

B. LENZE (1982)
The influence of recirculation and excess air on enclosed turbulent diffusion flames. 19th Symposium (Int) on Combustion. The Combustion Institute, p. 565.

W. LEUCKEL and N. FRICKER (1976).
The characteristics of swirl-stabiliszed natural gas flames. PART 1: Different flame types and their relation to flow and mixing patterns. J. Inst. Fuel, 49, p.103.

J.M. LEVY, L.K. CHAN, A.F. SAROFIM and J.M. BEER (1981).
NO/CHAR reactions at pulverised coal flame conditions. 18th Symposium (Int) on Combustion. The Combustion Institute, p.111.

B. LEWIS and G. VON ELBE (1961).
Combustion, Flames and Explosions of Gases. 2nd ed., Academic Press, New York.

M.H. LEWIS and L.D. SMOOT (1981)
Turbulent gaseous combustion. Part I: local species concentration measurements. Comb. and Flame, 42, p. 183.

F.C. LOCKWOOD, A.P. SALOOJA and S.A. SYED (1980).
A prediction method for coal fired furnaces. Comb. and Flame, 38, p.1.

F.C. LOCKWOOD, S.M.A. RIZVI, G.K. LEE and H. WHALEY (1984).
Coal combustion model validation using cylindrical furnace data. 20th symposium (Int) on Combustion, The Combustion Institute, p. 513.

F.C. LOCKWOOD,(1986)
Private Communication, Mech Eng. Dept., Imperial College, London.

F.C. LOCKWOOD, S.M.A. RIZVI and N.G. SHAH (1986).
Comparative predictive experience of coal firing. Proc. Instn. Mech. Engrs., Vol. 200, No. C2, p. 79.

R. LOISON and R.R. KISSEL (1962).
International Flame Research Foundation: observations on experiments carried out on the combustion on pulversied coal. J. Inst. Fuel, 35, p. 60.

J.P. LONGWELL (1955).
Flame stabilization and flame propogation in ramjet combustors. Combustion Researches and Reviews 1955, AGARDograph No. 9, p. 58.

J.P. LONGWELL, E.E. FROST and M.A. WEISS (1953).
Flame stability in bluff body recirculation zones. Ind. Eng. Chem, 45, p.1629.

H.H. LOWRY (1963).
Chemistry of Coal Utilization, supplementary volume. H.H. Lowry, Ed., John Wiley and Sons, New York.

A. MACEK (1978)
Coal combustion in boilers: a mature technology facing new constraints. 17th Symposium (Int) on Combustion, The Combustion Institute, p.65.

W.J. MCLEAN, D.R. HARDESTY and J.H. POHL (1981).
Direct observations of devolatilizing pulverised coal particles in a combustion environment. 18th Symposium (Int) on Combustion, The Combustion Institute, p. 1239.

J.B. MICHEL AND R. PAYNE (1980).
Detailed measurement of long pulverised coal flames for the characterization of pollutant formation. IFRF Doc. nr. F09/a/23.

D. MILLS (1980).
The operational velocity range in pneumatic conveying and its influence on product flow rate. Pneumotransport 5, paper C1.

T.A. MILNE and J.E. BEACHEY (1977).
The microstructure of pulverised coal-air flames. I. Stabilization on small burners and direct sampling techniques. Comb. Sci. and Tech. 16, p.123. II. Gaseous species, particulate and temperature profiles, p. 139.

R.E. MITCHELL AND W.J. MCLEAN (1982)
On the temperature and reaction rate of burning pulverised fuels. 19th Symposium (Int) on Combustion, The Combustion Institute, p. 1113.

D. MODARRESS, J. WUERER and S. ELGOBASHI (1982).
An experimental study of a turbulent round two-phase jet. AIAA paper 82-0964, St. Louis, Mo.

D. MODARRESS, H. TAN and S. ELGOBASHI (1984).
Two-component LDA measurement in a two-phase turbulent jet. AIAA, 22, p.624.

H.A. MONEIB (1980)
Experimental study of the fluctuation temperature in inert and reacting turbulent jets. Ph.D. Thesis, University of London.

G.F. MORRISON (1980).
Nitrogen from coal combustion - abatement and control. IEA report number ICTIS/TR II, IEA coal research, London.

S.P. MUSARRA, T.H. FLETCHER, S. NIKSA and H.A. DWYER (1986).
Heat and mass transfer in the vicinity of a devolatilizing coal particle. Comb. Sci. and Tech., 45, p. 289.

B.N. NANDI, T.D. BROWN and G.K. LEE (1977).
Inert coal macerals in combustion. Fuel, 56, p. 125.

R.C. NEAVEL (1981).
Origin, petrography, and classification of coal. Chemistry of coal utilization, M.A. ELLIOT, Ed., Wiley Publ. chapter 3.

W. NUSSELT (1924).
The process of combustion in powdered-coal firing (translation), VDI 68, 124.

H. OFFERGELD (1986).
Prediction of NO (in German). Dissertation for Dipolarbeit, Institut fur Technische Thermodynamik, Aachen.

K. OKAZAKI, H. SHISHIDO, T.NISHIKAWA and K. OHTAKE (1984).
Separaton of the basic factors affecting NO formation in pulverised coal combustion. 20th Symposium (Int) on Combustion, The Combustion Institute, p. 1381.

R.C. PATTERSON (1959).
Pulverised coal transport through pipes. Trans. ASME. J. Eng. Power, 81, p43.

D.W. PERSHING and J.O.L. WENDT (1976).
Pulverised coal combustion: the influence of flame temperature and coal composition on thermal and fuel NO_x. 16th Symposium (Int) on Combustion Institute, p.389.

N. PETERS and F.A. WILLIAMS (1983).
Liftoff characteristics of turbulent jet diffusion flames. AIAA J.21 (3), p. 423.

W. PHELAN and G. FLAMENT (1983).
The reduction of NO_x emissions by staged combustion for a range of diverse coals fired under boiler simulated conditions. IFRF Doc. nr. F037/a/12.

W.J. PHELAN and S. BORTZ (1984).
Studies on the influence of burner design parameters on NO_x reduction when staging the combusion air for four diverse coals. IFRF Doc. nr. F137/a/14.

S.L. PLEE and A.M. MELLOR (1979).
Characteristic time correlation for lean blowoff of bluff-body-stabilized flames. Comb. and Flame, 35, p.61.

C. PRESSER, J.B. GREENBERG, Y. GOLDMAN and Y.M. TIMNAT (1982).
A numerical study of furnace flame root stabilization using conical burner tunnels. 19th Symposium (Int) on Combustion. The Combustion Institute, p. 519.

A.N. RAO, V. GANESAN, K.V. GOPALAKRISHNAN and R. NATARAJAN (1983).
Experimental and theoretical investigations of vane-generated swirling flows in a circular chamber. J. Inst. Energy, 56, p.137.

R. RAWE and H. KREMER (1981).
Stability limits of natural gas diffusion flames with swirl. 18th Symposium (Int) on Combustion, The Combustion Institute, p. 667.

S.M.A. RIZVI (1985).
Prediction of flow, combustion and heat transfer in pulverised coal flames. Ph.D. Thesis, University of London.

M. SADAKATA, A. YOSHINO, T. SAKAI and H. MATSUOKA (1984).
Formation of submicron unburnt carbon and NO_x from pulverised coal combustion system. 20th Symposium (Int) on Combustion, The Combustion Institute, p.913.

T.SARPKAYA (1971 (a)).
On stationery and travelling vortex breakdowns. J. Fluid Mech., 45, p.545.

T. SARPKAYA (1971 (b)).
Vortex breakdown in swirling conical flows. AIAA, 9, p. 1792.

A. SATO, K. HASHIBA, M. HASATANI, S. SUGIYAMA and J. KIMURA (1975).
A correctional calculation method for themocouple measurements of temperatures in flames. Comb. and Flame, 24, p.35.

W.R. SEEKER, D.C. WEGENER, T.W. LESTER and J.F. MERKLIN (1978).
Single pulse shock-tube studies of pulverised coal ignition. 17th Symposium (Int) on Combustion. The Combustion Institute, p. 155.

C.W. SEITZ (1986)
Measurement of NO_x (in German). Dissertation for Diplomarbeit, Institut fur Technische Thermodynamik, Aachen.

I. SMITH (1980).
Nitrogen oxides from coal combustion - environmental effects. IEA report number ICTIS/TR 10, IEA coal research, London.

I.W. SMITH (1982).
The combustion rates of coal chars: a review. 19th Symposium (Int) on Combustion, The Combustion Institute, p.1045.

P.J. SMITH, S.C. HILL and L.D. SMOOT (1982).
Theory for NO formation in turbulent coal flames. 19th Symposium (Int) on Combustion, The Combustion Institute, p. 1263.

L.D. SMOOT, M.D. HORTON and G.A. WILLIAMS (1976).
Propqgation of laminar pulverised coal-air flames. 16th Symposium (Int) on Combustion, The Combustion Institute, p.375.

L.D. SMOOT and D.T. PRATT (1979).
Pulverised-Coal Combustion and Gasification. Plenum Press. ISBN 0-306-40084-7.

L.D. SMOOT (1981)
Pulverised coal diffusion flames: a perspective through modelling. 18th Symposium (Int) on Combustion, The Combustion Institute, p. 1185.

L.D. SMOOT and P.J. SMITH (1985).
Coal Combustion and qasification, Plenum, New York.

P.R. SOLOMON and M.B. COLKET (1978).
Coal devolatilization. 17th Symposium (Int) on Combustion, The Combustion Institution, p.131.

P.R. SOLOMON, D.G. HAMBLEN, R.M. CARANGELO and J.KL. KRAUSE (1982).
Coal thermal decomposition in an entrained flow reactor: experiments and theory. 19th Symposium (Int) on Combustion, The Combustion Institute, p. 1139.

Y.H. SONG, J.H. POHL, J.M. BEER and A.F.SAROFIM (1982).
Nitric oxide formation during pulverised coal combustion. Comb. Sci. and Tech., 28, p.31.

D.B. SPALDING (1979).
Combustion and mass transfer, Pergamon Press ISBN 0 080221068.

E. STACH (1982).
Textbook of coal petrology, E. Stach, Ed., Gebruder Borntraeger, Berlin and Stuttgart.

F.R. STEWARD and K.N. TENNANKORE (1976)
Similarity criterion for a confined swirling jet system. 16th Symposium (Int) on Combustion, The Combustion Institute, p. 1593.

E.M. SUUBERG, W.A. PETERS and J.B. HOWARD (1978).
Product compositions and formation kinetics in rapid pyrolysis of pulverised coal - implications for combustion. 17th Symposium (Int) on Combustion, The Combustion Institute, p. 117.

R.A. SVEHLA (1962).
Estimated viscosities and thermal conductivities of gases at high temperature. NASA TR R-132.

N. SYRED, N.A. CHIGIER and J.M. BEER (1970).
Flame stabilization in recirculation zones of jets with swirl. 13th Symposium (1970) on Combustion. The Combustion Institute, p. 617.

N. SYRED and J.M. BEER (1972).
The damping of precessing vortex cores by combustion in swirl generators. Astronautica Acta, 17, p.783.

N. SYRED and J.M. BEER (1974).
Combustion in Swirling Flows: a review. Comb. and Flame, 23, p. 143.

N. SYRED, A.K. GUPTA and J.M. BEER (1974).
Temperature and density changes arising with the precessing vortex core and vortex breakdown in swirl burners. 15th Symposium (Int) on Combustion, The Combustion Institute, p. 587.

N. SYRED (1985).
Private Communication.

M.W. THRING (1962).
The science of flames and furnaces. 2ndEd., John Wiley, New York.

M.W. THRING and M.P. NEWBY (1952).
Combustion length of enclosed turbulent jet flames. 4th Symposium (Int) on Combustion, The Combustion Institute, p. 789.

J.R. THURGOOD, L.D. SMOOT and P.O. HEDMAN (1980).
Rate measurements in a laboratory-scale pulverised coal combustor. Comb. Sci. and Tech. 21, p. 213.

D.A. TICHENOR, R.E. MITCHELL, K.R. HENCHEN and S. NIKSA (1984).
Simultaneous in situ measurement of the size, temperature and velocity of particles in a combustion environment. 20th Symposium (Int) on Combustion, The Combustion Institute, p. 1213.

L.D. TIMOTHY, A.F. SAROFIM and J.M. BEER (1982).
Characteristics of single particle coal combustion. 19th Symposium (Int) on Combustion, The Combustion Institute, p. 1123.

G. TINE (1961).
Gas sampling and chemical analysis in combustion processes. Pergamcon Press, London.

L. TOGNOTTI, A. MALOTTI, L. PETARCA and S. ZANELLI (1985).
Measurement of ignition temperature of coal particles using a thermogravimetric technique. Comb. Sci. and Tech., 44, p.15.

J.S. TRUELOVE, T.F. WALL, T.F. DIXON and I.M. STEWART (1982).
Flow, mixing and combustion within the quarl of a swirled, pulverised-coal burner. 19th Symposium (Int) on Combustion, The Combustion Institute, p. 1181.

A. VRANOS and B.A. KNIGHT (1984).
A gas sampling probe for particulate laden streams. Comb. and Flame, 55, p. 121.

L.A. VULIS (1961).
Thermal regimes of combustion, translation by M.D. Friedman, McGraw-Hill.

T.F. WALL (1984).
Coal properties and classification. Pulverised coal combustion - intensive course organised by F. C. Lockwood, held at Imperial College, London.

J.O.L. WENDT, D.W. PERSHING, J.W. LEE and J.W. GLASS (1978).
Pulverised coal combustion: NO_x formation mechanisms under fuel rich and staged combustion conditions. 17th Symposium (Int) on Combustion, The Combustion Institute, p. 77.

J.O.L. WENDT (1980).
Fundamental coal combustion mechanisms and pollutant formation in furnaces. Prog. Energy Comb. Sci., 6, p.201.

F.A. WILLIAMS (1965).
Combustion Theory, Addison-Wesley, Massachusetts, U.S.A.

P. WOLANSKI and S. WOJCICKI (1974)
Stabilization of coal dust-air mixture by bluff bodies. 15th Symposium (Int) on Combustion, The Combustion Institute, p. 1295.

V. WROBLEWSKA, J. ZELKOWSKI and S. WOJCICKI (1976).
The optimum conditions for the combustion of low-calorific coal dust in swirl burners. 16th Symposium (Int) on Combustion, The Combustion Institute, p. 401.

H.L. WU and N. FRICKER (1976).
The characteristics of swirl-stabilized natural gas flames. Part 2: The behaviour of swirling jet flames in a narrow cylindrical furnace. J. Inst Fuel, 49, p. 144.

W. YANG, D.A. ECKHARDT and M.C. SKRIBA (1980)
Dilute phase pneumatic transport of fine nuclear fuel powders. Pneumotransport 5, paper F3.

Y.B. ZELDOVICH, G.I. BARENBLATT, V.B. LIBROVICH and G.M. MAKHVILADZE (1985).
The mathematical theory of combustion and explosions. Translated from Russian by D.H. MCNEILL, Plenum Publ., ISBN -306-10974-3.

E.E. ZUKOSKI and F.E. MARBLE (1955).
Experiments concerning the mechanism of flame blow-off from bluff bodies. Proc. of Gas Dynamics Symposium on Aerothermochemistry, Northwestern Univ. Aug 1955, p. 205.